Experimental study on effective width through openings using Kinect.

Juan Manuel Chaves Posada

Fire Safety Engineering
Lund University
Sweden

Report 5573, Lund 2018

Master Thesis in Fire Safety Engineering

Experimental study on effective width through openings using Kinect.

Juan Manuel Chaves Posada

Report 5573
ISRN: XXX
Number of pages: 74
Illustrations: 17
Keywords: Kinect, Effective Width, Effective Width Through Openings, Boundary Layer, Flow Through Openings, Pedestrian Tracking, Low-Density Flows.

Abstract

The effective width model was introduced to show how the flow was linearly proportional to the effective width on stairwells accounting for the edge effect as well as lateral body sway. In this sense, small increments on the width of the stairwell were proven to increment the flow through it in a linear manner. This same principle is currently applied as part of the background for the hydraulic calculations for engineering evacuation such as the one developed by Nelson and Mowrer in the SFPE Handbook of Fire Protection Engineering. Therefore, a fundamental part of this model is the use of effective width for each specific section of the evacuation route being analysed.
Consequently, the SFPE handbook suggests values for the dimension of the boundary layer that should be used for each specific element.

However, in the case of openings, such as doors and archways, there is limited experimental research on the effective width that can justify the values suggested by the SFPE handbook. Therefore, this project uses novel pedestrian tracking techniques using the Kinect v2 sensor as a tool to measure the dimensions of the boundary layer on three simple scenarios considering low-density flows.

The results obtained from this project show how the values suggested by the SFPE are very close to the obtained values from experimental data collection considering low-density flows with reference density values between 0.38 to 0.56 occupants per square meter. These values are not entirely conservative in the case of low-density flows since this does not account of the possible impact of doors. Additionally, this experimental study showed how the dimensions of the boundary layer, considering low-density flows, are not static. These findings indicate that the boundary layer changes its dimensions depending on the width of the opening, as there is a dependence on the number of lanes that can be observed on openings of different sizes.

Lund 2018.

Division of Fire Safety Engineering Lund University
P.O. Box 118
SE-221 00 Lund
Sweden
http://www.brand.lth.se
Telephone: +46 46 222 73

HOST UNIVERSITY: Lund University

FACULTY: Faculty of Engineering

DEPARTMENT: Division of Fire Safety Engineering

Academic Year 2017-2018

Experimental study on effective width through openings using Kinect.

Juan Manuel Chaves

Promoter: Senior Lecturer Prof. Enrico Ronchi

Master thesis submitted in the Erasmus Mundus Study Programme

International Master of Science in Fire Safety Engineering

Disclaimer

This thesis is submitted in partial fulfilment of the requirements for the degree of ***The International Master of Science in Fire Safety Engineering (IMFSE)***. This thesis has never been submitted for any degree or examination to any other University/programme. The author(s) declare(s) that this thesis is original work except where stated. This declaration constitutes an assertion that full and accurate references and citations have been included for all material, directly included and indirectly contributing to the thesis. The author(s) gives (give) permission to make this master thesis available for consultation and to copy parts of this master thesis for personal use. In the case of any other use, the limitations of the copyright have to be respected, in particular with regard to the obligation to state expressly the source when quoting results from this master thesis. The thesis supervisor must be informed when data or results are used.

Read and approved.

Juan Manuel Chaves
April 30, 2018

Abstract (English)

The effective width model was introduced to show how the flow was linearly proportional to the effective width on stairwells accounting for the edge effect as well as lateral body sway. In this sense, small increments on the width of the stairwell were proven to increment the flow through it in a linear manner. This same principle is currently applied as part of the background for the hydraulic calculations for engineering evacuation such as the one developed by Nelson and Mowrer in the SFPE Handbook of Fire Protection Engineering. Therefore, a fundamental part of this model is the use of effective width for each specific section of the evacuation route being analysed. Consequently, the SFPE handbook suggests values for the dimension of the boundary layer that should be used for each specific element.

However, in the case of openings, such as doors and archways, there is limited experimental research on the effective width that can justify the values suggested by the SFPE handbook. Therefore, this project uses novel pedestrian tracking techniques using the Kinect v2 sensor as a tool to measure the dimensions of the boundary layer on three simple scenarios considering low-density flows.

The results obtained from this project show how the values suggested by the SFPE are very close to the obtained values from experimental data collection considering low-density flows with reference density values between 0.38 to 0.56 occupants per square meter. These values are not entirely conservative in the case of low-density flows since this does not account of the possible impact of doors. Additionally, this experimental study showed how the dimensions of the boundary layer, considering low-density flows, are not static. These findings indicate that the boundary layer changes its dimensions depending on the width of the opening, as there is a dependence on the number of lanes that can be observed on openings of different sizes.

Abstract (Español)

El modelo del ancho efectivo fue desarrollado para mostrar como el flujo de personas es linealmente proporcional al ancho efectivo en escaleras, teniendo en cuenta el efecto del borde y el movimiento lateral. En este sentido, el modelo implica que pequeños incrementos en el ancho total de la escalera incrementan el flujo en una relación lineal con el ancho efectivo. Este mismo principio es actualmente aplicado como parte de los fundamentos de los cálculos hidráulicos para evacuación en ingeniaría desarrollado por Nelson y Mowrer para el SFPE *Handbook of Fire Protection Engineering*. Consecuentemente, una parte fundamental de este modelo hidráulico es el uso del concepto de ancho efectivo para cada elemento de la ruta de evacuación que es analizada. Por ende, el SFPE *Handbook of Fire Protection Engineering* sugiere valores para el especio de margen o separación para los diferentes elementos que se encuentran en las rutas de evacuación.

Sin embargo, en el caso de aberturas, como puertas y arcos, hay pocos estudios empíricos en el ancho efectivo que permitan justificar los valores del espacio de margen sugerido por el SFPE handbook. Es de esta forma que este proyecto usa el Kinect v2 como una novedosa forma de tecnología para el seguimiento peatonal, empleándolo como una herramienta técnica que permite medir las dimensiones del espacio de margen en tres escenarios distintos, considerando exclusivamente flujos de baja densidad.

Los resultados obtenidos a través de este proyecto muestran como los valores sugeridos por la Society of Fire Protection Engineers (SFPE) están muy cercanos a los obtenidos de forma experimental para los escenarios considerados de baja densidad entre 0.38 a 0.56 ocupantes por metro cuadrado. Sin embargo, estos valores no son completamente conservativos en el caso de flujos de baja densidad ya que no consideran el posible impacto de las puertas en la abertura. Adicionalmente, este estudio experimental permitió observar como las dimensiones del espacio de margen, considerando flujos de baja densidad, no son estáticas. Los hallazgos indican que el espacio de margen cambia sus dimensiones dependiendo del ancho total de la abertura, consecuentemente se encuentra una clara dependencia con el número máximo de carriles que se pueden observar para aberturas de diferentes dimensiones.

Acknowledgements

This project was the final step to finish the International Master of Science in Fire Safety Engineering programme. I started this international adventure with the aim to learn about fire safety and the fire problem from several perspectives. However, little did I know that this master degree programme would not only become an academic adventure but also allow me to grow so much as a person. This section of the thesis is dedicated to all who were a special part of this extraordinary experience.

To my family in Colombia, who provided me with unconditional support through the whole duration of this programme. My father, mother and sisters especially, who always believed in me even when I did not.

To Enrico Ronchi, who was an outstanding supervisor. I would not have been able to complete this project without your guidance, advice, and support. Your continuous supervision and open doors helped me overcome every obstacle along the way.

To the management board of IMFSE, for creating and managing this internationally recognized programme. I thank you for giving me the opportunity of joining this wonderful programme and community.

Finally, I want to acknowledge all the incredible persons I have met throughout the past two years. I am proud to say I have incredible friends from all around the globe. Without your support and friendship, I would not have been able to complete this extraordinary adventure.

Table of Contents

List of Figures

List of Tables

List of equations

1. Introduction and objectives

Pedestrian tracking has proved to be a valuable tool to collect empirical data on pedestrian dynamics. Data obtained by empirical studies of pedestrian dynamics can be used to calibrate computational and mathematical models that are used by fire engineers to estimate evacuation times. One of the most commonly used calculations is the estimation of flow through doorways and openings using the hydraulic method suggested in the SFPE Handbook of Fire Protection Engineering (Gwynne and Rosenbaum, 2016), this method uses the effective width as one of the variables to calculate the flow through an opening. However, there is limited experimental research conducted on the effective width and the boundary layers in openings, therefore the value suggested by the SFPE Handbook needs more experimental support from empirical data.

The recent introduction of affordable 3D sensors has opened new options on how fire engineers can collect data in a more accurate and efficient way. The Kinect v2 device, introduced to the market in 2014, is one of such devices that can be used for pedestrian tracking (Brščić et al., 2013; Capecci et al., 2016; Corbetta et al., 2014; Seer et al., 2014). This study uses the Microsoft Kinect v2 as a tool to, through simple experiments, assess the capability of the sensor to accurately track the relevant body joints (e.g. right and left arm) in a 3-dimensional coordinate system to assess the dimension of the boundary layer and hence the effective width at openings.

1.1. Objectives

The objective of this project is to review the suitability of Microsoft Kinect v2 for pedestrian tracking aimed at observing the effective width in doorways and openings. Considering effective width, it is of interest for design optimization to assess the capability of Kinect v2 to perform such measurements. Therefore, this project aims to utilise this as a tool to (1) determine if by using this technology it is possible to analyse effective widths in openings through experimental data, generating a better understanding of the boundary layers, and (2) if it is possible to assess the results from the measurements to validate the suggested input data values for the boundary layer provided by the SFPE Handbook of Fire Protection Engineering and other similar evacuation calculation methodologies.

1.2. Literature review

This section includes a comprehensive review of relevant literature. This is intended to provide an insight on the importance of pedestrian tracking and techniques used as a tool for experimental data collection regarding pedestrian dynamics. Additionally, this section

emphasises the most commonly used models in engineering to calculate flows through openings using the concept of effective width. Finally, this section attempts to illustrate how the Microsoft Kinect has been previously used as a valuable tool for pedestrian tracking, and as such illustrate the capabilities of the device as a valuable tool in the field of pedestrian dynamics.

1.2.1. Pedestrian tracking

Pedestrian tracking is the process of investigating people trajectories. The focus of this thesis is pedestrian tracking when approaching an opening. Data acquired from simple experimental setups such as the ones performed at Lund University in 2006 (Frantzich et al., 2007) can provide valuable data, which can be used to calibrate computational models that can estimate evacuation times and flows through openings (Ronchi and Nilsson, 2012). Techniques used for pedestrian tracking are usually focussed on collection and sharing of empirical data on pedestrian dynamics. The purpose of this type of research is to generate and share techniques for capturing data of interest about individuals and groups; this can be done using novel approaches such as automated image processing and machine learning (Greenwood et al., 2014) in contrast with less effective manual counting and non-automated video analysis.

Different techniques and devices are used for pedestrian tracking with varying types of data that can be collected from each one of them. The most common method is using video cameras to generate recordings from which the data is extracted after the events occur. A good example of this type of procedure is the study on pedestrian flow through bottlenecks by Liao, in which Bumblebee XB3 cameras were used on an overhead setting and trajectories were automatically extracted from the video recordings using software *PeTrack* (Liao et al., 2014). Pedestrian recognition can also be performed in laboratory settings using specific colour recognition (Jo et al., 2014) as well as binary code to allow semi-automatic software to perform identification and follow with a manual comparison of records (Bukáček et al., 2014).

In more recent years, 3D range sensors have become available on the market, these come in three representative types: structured light cameras, time-of-flight cameras, and multi-layer laser scanners. Structured light cameras measure range based on a camera view of a projected light pattern, these sensors have a short range and the maximum range for correct measurements is around 5 meters; Microsoft Kinect v1 is an example of such type of sensors (Brščić et al., 2013). A different approach is the time-of-flight (ToF) cameras that work measuring the time a projected light needs to travel to an object in order to determine distance and have a similar range to the structured light camera sensors (Corti et al., 2016), Microsoft Kinect v2 works in such a way. The final type of common 3D sensors are the multi-layer laser scanners which use multiple laser scanning units rotating together that obtain 3D

measurements (Brščić et al., 2014; Fridholm and Rasmusson, 2017), these sensors have a longer range than the previous two and have very little influence from external light.

3D sensors have been used for several pedestrian flow and tracking studies for large data collection; Brščić, Zanlungo and Kanda performed yearlong pedestrian tracking measurements using the three different kind of sensors in the Asia and Pacific Trade Center in Osaka (Brščić et al., 2014). Moreover, Fridholm and Rasmusson used the laser scanner RPLIDAR from RoboPeak to measure personal flow through door openings in the fire laboratory at the Faculty of Engineering in Lund University (Fridholm and Rasmusson, 2017) showing how this technology has potential of measuring flow through door openings in simple scenarios. Studies using time-of-flight cameras have also been performed by Corbetta, who used the Microsoft Kinect v2 to perform large scale trajectory tracking and data collection at Eindhoven University of Technology (Corbetta, 2016). The use of these sensors allows to perform pedestrian tracking measurements in real time while providing accurate data.

The flexibility and precision of the 3D sensor devices makes it particularly interesting to perform automated tracking in both natural and laboratory setups. The result of such studies can therefore generate a better understanding of "walking behaviour" whilst offering the possibility to collect reliable data that can be used for modelling in both normal and emergency contexts (Haghani and Sarvi, 2018).

1.2.2. Flow through openings and the effective-width model

Pedestrian dynamics are a fundamental part of the egress calculations often performed by fire engineers around the globe. As such, the assessment of the expected performance of an egress configuration has traditionally required the use of empirically derived equations to predict flows and evacuation times (Gwynne et al., 2009). This results in the use of some numerical data that sometimes has no sufficient experimental background to support it. Therefore, it becomes of importance to provide a detailed description of the assumptions adopted in order to generate transparency in code numbers, this would enhance users' understanding of the codes leading to an improved application and increased safety in building design (Gissi et al., 2017).

Flow calculations associated with openings assume that when individuals move through an evacuation route of a building, a boundary layer of clearance is maintained between themselves and walls or other stationary objects (Hurley et al., 2016), this is derived from the "Effective-Width Model" conceived by Pauls and originally intended for stairwells (Pauls, 1982), in which the effective width of stairs is considered smaller than the absolute clear width for evacuation calculations.

The effective width model accounts for the edge effect as well as lateral body sway. When conceived, the model related stair width, population capacity, and flow time. The model is based on empirical findings from studies in high rise buildings (Pauls, 1982) in which the mean flow, plotted against stair width, is a linear function and thus small increments in the stair width add to crowd flow capacity (Pauls, 1984), therefore the model assumed a linear function between effective width and flow in which the effective width, W_e, is the absolute/code credited width, W, minus the boundary layers of clearance B_L.

$$W_e = W - 2 \cdot B_L$$

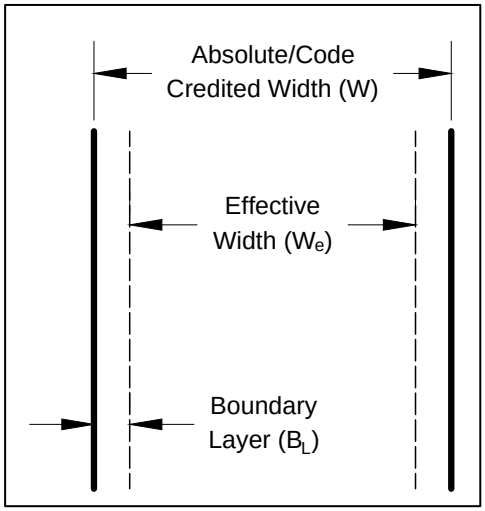

Figure 1: Principles of the effective width model. Adapted from (Pauls, 1984).

Similar research has been conducted in corridors for pedestrian flows adjacent to walls by Habicht and Braaksma. In this case, video recordings were taken and analysed by estimating the locations of pedestrians as they passed a specific cross section of tunnel at Carleton University, they derived a formula to calculate effective width in corridors and obtained a value ranging from 15.3 to 20.1 cm of effective width reduction due to walls (Habicht and Braaksma, 1984). Nevertheless, the proposed formulas are only intended for corridors and cannot be used for openings.

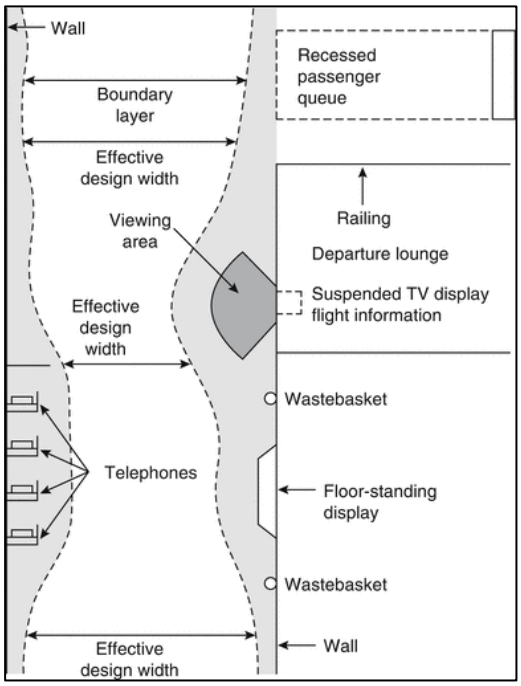

Figure 2: Public corridor effective width. Graphical representation of the boundary layer in corridors (Gwynne and Rosenbaum, 2016).

Consequently, further studies are required to assess effective width measurements using modern technological advances (Pauls et al., 2007), this is especially relevant for doors and archways since, to the authors' knowledge, no data has been collected whilst the effective width of doorways is still used for flow calculations. A good example of this is the engineering approach presented in the Society of Fire Protection Engineers (SFPE) Handbook (Gwynne and Rosenbaum, 2016), in which a reduction of 15 cm (6 in.) is considered from each edge of the opening. This value, however, corresponds to the one obtained by Pauls from his experimental studies for stairwells (Pauls, 1987, 1984, 1982).

The methodology presented in the SFPE handbook was developed by Nelson and Mowrer and is presented in the 2016 edition of the SFPE handbook by Gwynne and Rosenbaum (Gwynne and Rosenbaum, 2016). The work developed in this chapter of the SFPE handbook by Nelson and Mowrer is based on the work of Fruin (Fruin and Strakosch, 1987), Predtechenskii and Milinskii (Predtechenskiĭ and Milinskii, 1978), and Pauls (Pauls, 1982). This hydraulic method assumes that the population evacuates simultaneously, providing a reservoir of people to ensure assumed flow rates; occupant decision-making does not interrupt the flow produced; and the flow is not influenced by the presence of the movement impaired, thus population speeds are considered uniform (Gwynne et al., 2009).

The proposed engineering approach depends on population density, D, (occupants/m^2 or occupants/ft^2); velocity, S, (m/s or ft/min); effective doorway width, W_e, (m or ft); and specific flow rate, F_s, of the opening (occupants/m/s or occupants/ft/min). Occupant density, D, can

vary between 0.54 and 3.8 occupants/m^2 (0.05 and 0.35 occupants/ft^2) and the movement speed, *S*, depends linearly on the density by the following relationship:

Equation 1: Walking speed formula as stated in the SFPE handbook

$$S = k - akD$$

where *a* and *k* are constants whose values vary according to the component and the units used. Thus, the method specifies that for a doorway $k = 1.4$ and $a = 0.266$ for the speed in m/s and $k = 275$ and $a = 2.86$ for the speed in ft/min, thus the linear relation between speed and density becomes:

Equation 2: Walking speed formula for doorways in m/s or ft/min

$$\text{(m/s)}\ S = 1.4 - 0.37D$$
$$\text{(ft/min)}\ S = 275 - 786.5D$$

Once speed is calculated, it is possible to determine the specific flow of the opening, F_s, using the following expression:

Equation 3: Specific flow for corridors, aisles, ramps and doorways as stated in the SFPE handbook considering SI units

$$F_s = SD = kD - akD^2 = k(D - aD^2)$$
$$F_s = 1.4D - 0.37D^2$$

This expression leads to a maximum specific flow for corridors, aisles, ramps and doorways of 1.3 Occupants/s/m of effective width (24 Occupants/min/ft of effective width). Therefore, the calculated flow, F_c, in occupants/s depends directly on the effective width, W_e, of the element being considered ($F_c = F_s W_e$). Thus, the calculated flow for the egress element linearly depends on the effective width and hence it becomes of interest to assess the validity of the suggested value for doorways since it merely corresponds to the value obtained for stairs from research done in the 1980s by Pauls (Pauls, 1987, 1984, 1982).

The abovementioned method recommended in the SFPE handbook indicates that the flow increases in a continuous, in contrast to a stepwise, function as the width of the opening increases. This has been corroborated by Seyfried and Schadschneider when performing experiments in 2006 in the wardroom of the “Bergische Kaserne Düsseldorf” with a test group comprised of soldiers (Seyfried and Schadschneider, 2010). In these experiments, the pedestrian dynamics at bottlenecks were studied in laboratory conditions using an experimental setup that allowed to review the influence of the bottleneck width and length on the flow.

Moreover, research on the impact of several variables including width of a doorway or opening has been performed in the Netherlands (Daamen and Hoogendoorn, 2010). This experimental research, performed at Delft University of Technology, shows how the capacity of evacuation doors is affected by the evacuation door width, population composition, the presence of an open door, and stress induced to simulate evacuation conditions. Findings from this study provide insight on how flows can vary due to the change in door width amongst the other variables. Nevertheless, this study only considered the total width of the opening without considering the impact of effective width of the archway which could, to some extent, provide some explanation on why the capacity per meter of opening did not always increase when the opening size was increased.

1.2.3. Microsoft Kinect as a tool for pedestrian tracking

Pedestrian dynamics pose a challenge for fire engineers as individual trajectories are presented as stochastic variables that cannot be fully predicted by deterministic models. Corbetta proposes that, although singular routes might appear to be random, the analysis of large quantities of data can provide insights into a preferred behaviour from which all other trajectories are mere deviations (Corbetta, 2016). Considering this, 24/7 measurements of pedestrian trajectories were performed at Eindhoven University of Technology using an overhead Microsoft Kinect to prove pedestrians have preferred paths and observe pedestrian behaviour (Corbetta et al., 2014). This study provided evidence of the potential benefits of the Kinect in relation to pedestrian dynamics and experimental data collection.

Similar research has been performed by Seer, Brändle, and Ratti (Seer et al., 2014) in which walking experiments under real world conditions in the Massachusetts Institute of Technology (MIT) Infinite Corridor were performed. This work attested how the Kinect allows the automated capture of human motion trajectories with high accuracy without privacy issues. Additionally, this study provided insight on how the Kinect has a Multiple Object Tracking Precision (MOTP) of relatively small values of around 4 cm with a pedestrian detection rate ranging from 94 to 96% (Seer et al., 2014). Therefore, the adoption of the Kinect can be useful for the development and calibration of pedestrian models as well as a useful tool to understand human crowd behaviour providing new input data that can be used for existing and new models.

Moreover, studies on how the Kinect v2 functions, in order to determine the location of pedestrians in buildings, have also been performed in Lund University, considering both normal conditions and smoke-filled environments (Pettersson and Lundh, 2017). The results of these tests have shown how the device performs well in normal conditions having the potential to analyse body movements and behaviour patterns, hence demonstrating how the

device has potential to be used as a low-cost tool for pedestrian tracking used as a lateral or frontal device and not only as an overhead camera sensor.

1.3. Limitations

Research performed on effective width has, to the author's knowledge, not been specifically focused on openings such as doorways and archways, therefore there is no experimental data or research available to compare and validate the results of the tests performed during this study. Furthermore, it is of foremost importance to acknowledge that the automated pedestrian tracking was performed under laboratory conditions, and although it is an attempt to resemble real-life conditions, the results inherently carry a bias since measurements were not taken from real-life evacuation drills nor of unaware pedestrians.

Additionally, the sample size and type constitutes a limitation for this research project, ideally the samples for group experiments should have comprised small to large groups with a varying population, this would have allowed to assess the relationship between effective width and varying densities in the flow. However, this was not possible due to time constraints and the chosen recruitment method. Thus, the focus of this study was narrowed to the effect of the opening size on the dimensions of the boundary layer. Therefore, occupant density was not the object of the study and was not measured but calculated using empirical formulas as illustrated in section 2.6, nonetheless it is relevant to highlight that the considered occupant densities ranged between 0.38 to 0.56 occupants per square meter. Moreover, it is essential to clarify that the flow through the openings was not measured directly by the Kinect v2 sensor but was obtained from video recordings and is intended to provide context regarding the type of flow being studied (e.g. low or high density) rather than an actual result from the collected experimental data.

The obtained flows were calculated using video recordings which in which the time from the first to last pedestrian of the group experiments to walk through the opening was measured, as opposed to pre-determined time steps used to measure the flow directly when counting the number of pedestrians. Flows were therefore calculated using the time until the whole group walked through the opening, subsequently the total number of occupants was divided by this measured time value obtained. This intrinsically means that the uncertainty was in the determination on when the time measurement started and finished with an accuracy of 1 second.

The number of scenarios also constitute a major constraint on the outputs of this study. In this case, only three scenarios were chosen based on table 4 from the Approved Document B, which is the prescriptive code that applies for the United Kingdom (Great Britain and Office of the Deputy Prime Minister, 2013). However, the hybrid standard for the United Kingdom

BS9999(British Standards Institution, 2008), the NFPA 101 Life Safety Code (National Fire Protection Association, 2017), International Building Code (Thornburg and Henry, 2009), and Swedish Boverket's Building Regulations (Swedish National Board of Housing, Building and Planning (Boverket), 2016) were also reviewed in order to assess if the chosen values were indeed similar to those provided in these codes, this is described in section 2.3.

Likewise, the Microsoft Kinect v2 has both software and hardware limitations that have an impact on how the measurements of the different body joints were taken as well as the accuracy of such measurements, hence the average error due to the way the sensor collects data was considered based on previous studies on the accuracy of the device (Capecci et al., 2016; Seer et al., 2014; Wang et al., 2015; Yang et al., 2015). The Kinect sensor uses the time-of-flight approach for depth sensing, generating a 3-dimensional coordinate system for the skeletal joints tracked by the device using the body index map and skeleton data sources, included as a part of the framework of the Kinect for Windows Software Developer Kit (SDK) v2. The point where the skeletal joint is in the coordinate system is the perceived centre of the joint by the device, hence, the orientation of the different parts of the body when performing measurements influences how the body joint can be perceived either towards the "outside" or "inside" of the body, producing a slight lateral displacement of the joint in the coordinate system.

Furthermore, the line-of-sight nature of the Kinect sensor is an additional constraint when studying groups instead of individuals with an individual Kinect sensor since, occasionally, when walking through an opening the pedestrian were obstructed by the individual walking in front of them throughout the time in which the measurements were of interest, consequently, when such event occurred data of relevance to this study could not be collected. Hence, as shown in section 3.2, for the group experiments the amount of data collected is below 100%.

2. Methodology

This section will discuss and portray the methodology followed to perform this experimental study on effective width in openings. This section illustrates the experimental methodology that was followed, as well as provide insight on how data was collected and analysed. Moreover, this section provides insight on the considered scenarios, including an overview on the participants and the technical characteristics of the Kinect v2 device that were considered as relevant for this study. Furthermore, the methodology section illustrates how data was treated to obtain the results that are portrayed in section 3, including the usage of the equations for hydraulic flow calculations that are commonly used.

2.1. Participants and recruitment

Participants were recruited from the student population at Lund University. The only requirement to participate in the experiment was not having any injury or physical/mental disability that may affect walking normally; an informed consent was signed by all the participants prior conducting the experiments. Participants also filled in a background questionnaire (see Table 1). Individual tests were performed with 5 different participants, this was done in order to broadly investigate the accuracy of the Kinect, as well as providing insight on how effective width can be measured and its implications. Therefore, individual experiments were aimed to be used for calibration purposes before the group experiments. Group experiments, on the other hand, were performed in groups of 10 and 14 participants at the same time. The group experiments were aimed to provide valuable data to analyse the width of the boundary layer in openings when considering more realistic scenarios. In total 15 students participated in this experimental analysis.

Table 1: Demographics of the participants in the experiments according to the data provided by them in the background questionnaire

Participant Characteristics	
Female	40.00%
Male	60.00%
Left Handed	13.33%
Right Handed	86.67%
Age Range	21-29 years
Number of Countries	13
Height Range	156-190 cm
Weight Range	55-99 kg
Percentage of participants from countries that drive on the right	60%
Percentage of participants from countries that drive on the left	40%

Table 1 shows the demographics of the participants. It is particularly relevant to remark that the group was very diverse, comprising 13 different nationalities. Table 2, on the other hand, shows the different countries from which the participants came from, including information regarding which side of the road they drive in each one of the countries. The information displayed on these tables, thus, not only displays the demographics of the participants but also attempts to provide data that can explain some of the behaviours observed, including a tendency to naturally walk towards the right or left hand side in relation with the country of origin of each one of the individuals.

Table 2: Countries to which the participants came from including the side of the road that is used for driving in each country information obtained from (World Standards, 2018).

List of Countries	
Country	**Driving side of the road**
Bangladesh	Left
Belarus	Right
Colombia	Right
El Salvador	Right
Greece	Right
India	Left
Italy	Right
Kazakhstan	Right
New Zealand	Left
Philippines	Right
Serbia	Right
Singapore	Left
Turkey	Right

2.2. Experimental setup and equipment

This section describes the experimental setup as well as the Microsoft Kinect v2 technical characteristics. These include constraints and an assessment on the device accuracy. Moreover, the chosen setup is further discussed in order to account for the chosen scenarios as well as the positioning of the device and use of video camera.

2.2.1. Setup

The experimental phase of this study took place in the basement of the V-building at LTH in Lund University. To generate an artificial corridor, wardrobes were used as illustrated in Figure 4; the dimensions of the corridor and the different opening sizes are explained in depth in section 2.3. Additionally, the setup included the Kinect v2 sensor, which was located 1.95 m away from the opening and shifted towards the right side of the artificial doorway when looking from behind the device. It is of importance to remark that the distance of 1.95 m was chosen since it is within the ideal range for the Kinect v2 sensor in which the device is the most accurate for 3-Dimensional space measurements, this is further discussed in section 2.2.2. However, preliminary tests were performed while the device was being programmed, these tests showed that the distances in which the best results were obtained ranged between 1 and 2.5 meters, hence a distance of 1.95 meters was used as it was deemed as accurate. Nonetheless, for further tests other distances can be used with the same level of accuracy by defining the distance on the programmed code.

The sensor was placed at a height of 0.67 m measured from the centre of the depth sensor and the lateral shift to the right side was of 0.64 m from the centre of the corridor, bearing in mind that the depth sensor is a reference point since it is the element that generates the 3-D coordinate system, this positioning of the sensor can be clearly seen in Figure 3. It is important to remark that the device's displacement to the right side was done with the intention of pedestrians not modifying their trajectory, avoiding in this way interactions between the sensor and normal movement of people.

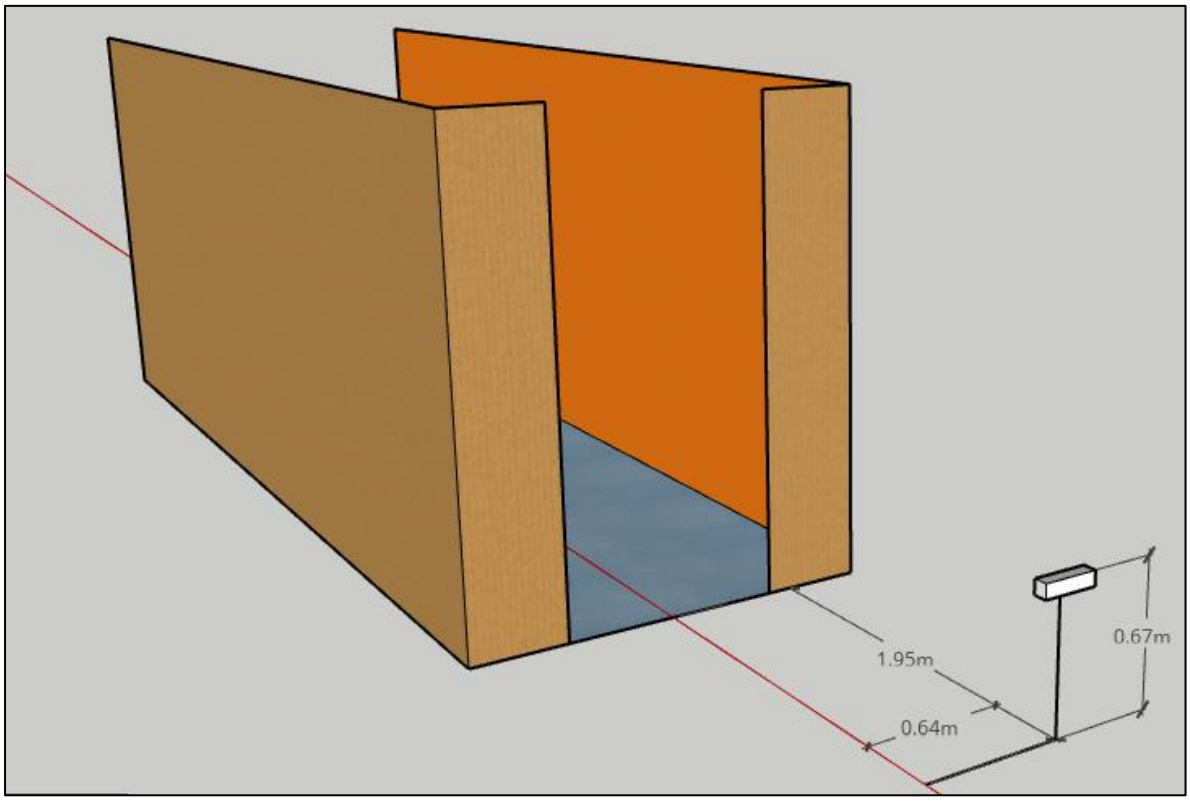

Figure 3: Positioning of the Kinect v2 sensor.

Supplementary to the artificial corridor setup and the Kinect v2 device it was necessary to generate video recordings from each one of the experiments using a GoPro HERO4 camera on a tripod behind the Kinect sensor. This camera has a continuous shooting speed of 10 frames per second and a video resolution of 3840 x 2160 (CNET, 2018). The video recording was done to identify the pedestrians using numbers attached to the front of their clothes, it also permitted to measure the time it took for the entire group of pedestrians to walk through the opening. This allowed to assess if the individual's background such as the country of origin, considering if they usually drive on the right or left side of the road, had any effect on individual behaviour. Moreover, the video recording allowed to determine when two lanes were created, thus allowing to identify towards which side of the opening each pedestrian was leaning to when multiple lanes were present. Finally, it is of interest to remark that flows were estimated based on the video feed as is explained in section 2.6.

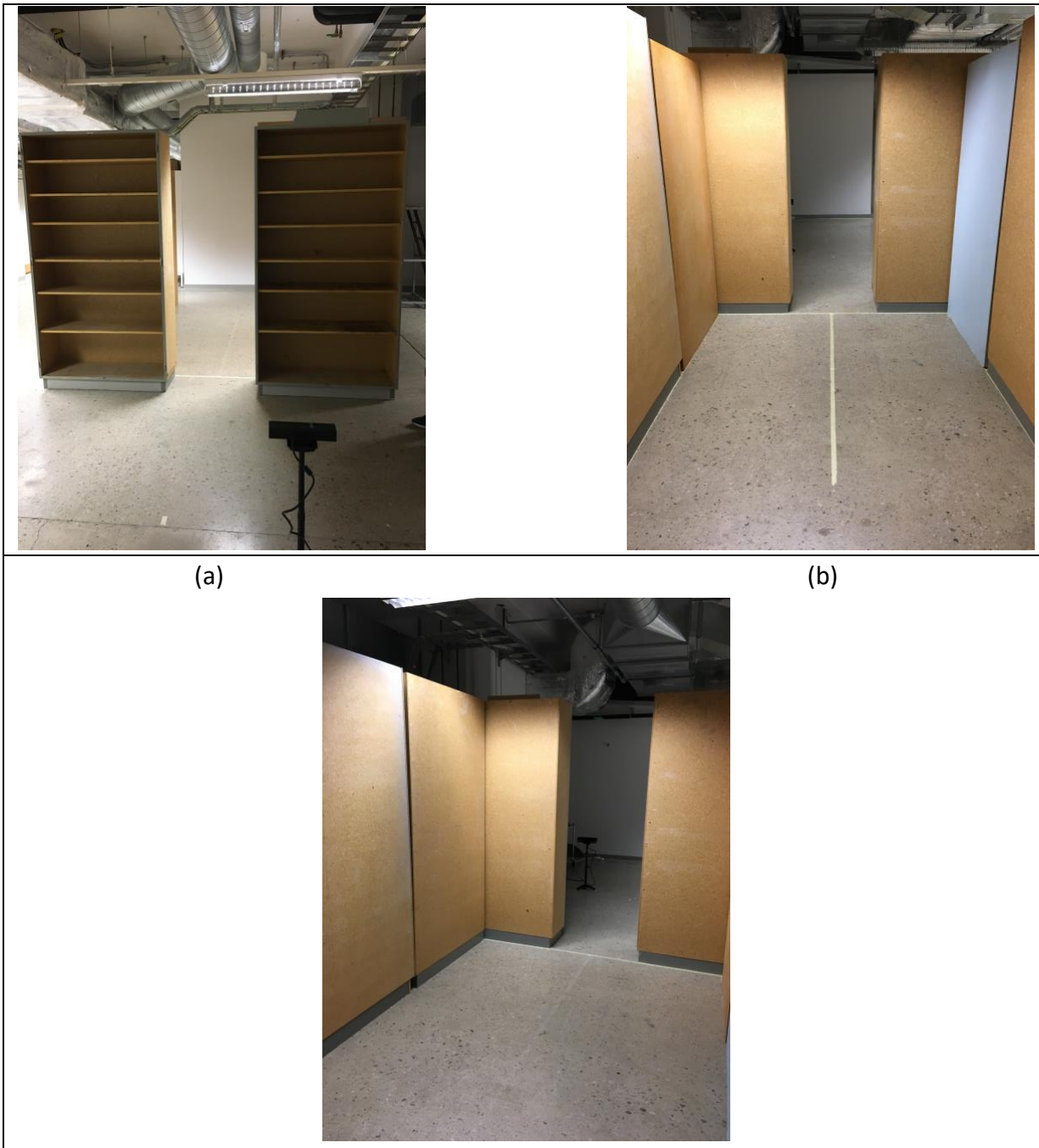

Figure 4: (a) Frontal view of the setup. (b) View from the corridor toward the opening. (c) Diagonal view of the corridor setup

2.2.2. Microsoft Kinect v2 technical characteristics

The Microsoft Kinect v2 is a camera-like sensor composed by infrared (IR) emitters/lasers, depth sensor, RGB camera, and a 4-element microphone array. This device is an accessory of the Xbox One, that reconstructs a scene and identifies the player's body position for

interaction with virtual reality (Corti et al., 2016). Kinect v2 uses Time-of-Flight (ToF) method for depth sensing and measurement. This method uses the active sensors to measure the distance of a surface by calculating the round-trip time of a pulse of light (Yang et al., 2015). This device is one of the most efficient low-cost ToF cameras available in the market.

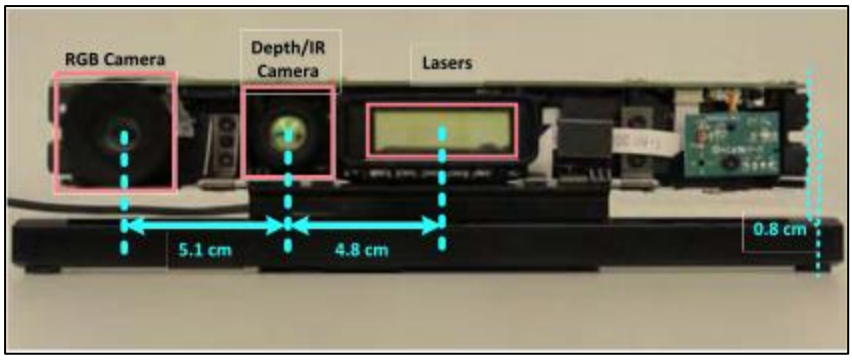

Figure 5: Microsoft Kinect v2 sensor components (Yang et al., 2015)

Figure 6: Coordinate mapping for the Kinect v2 (Microsoft Developer Network (MSDN), 2018a)

The depth sensor of the device provides the coordinate mapping using the location of the sensor as the reference point, as illustrated in Figure 6. This coordinate system generates 3-dimensional coordinates for the skeletal joints tracked by the Kinect using the body index map and skeleton data sources included as a part of the framework of the Kinect for Windows Software Developer Kit (SDK) v2. Additionally, the sensor can track up to 25 body joints for a total of six people simultaneously (Microsoft Developer Network (MSDN), 2018b).

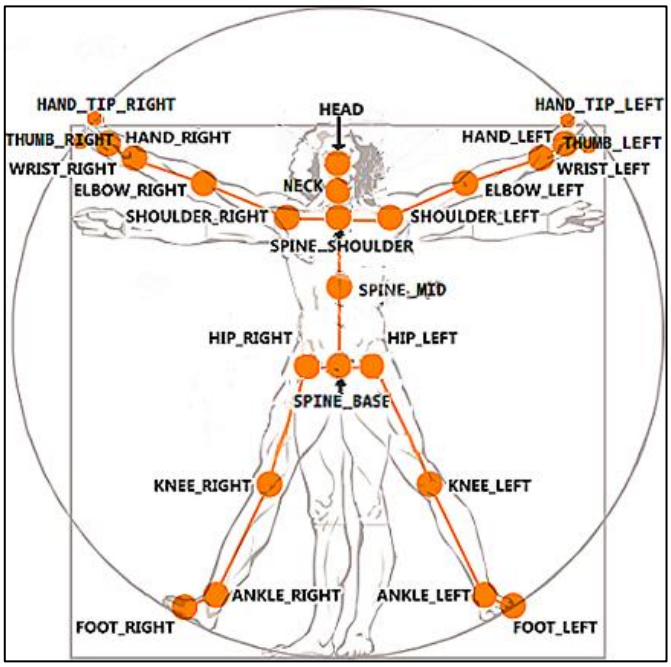

Figure 7: Joint type enumeration for the Microsoft Kinect sensor v2(Microsoft Developer Network (MSDN), 2018c)

Since its release in 2014, the Kinect v2 has been deemed as an improved version of the Kinect v1, having a better quality in the depth images than its predecessor (Microsoft Developer Network (MSDN), 2014). However, it is of interest to mention that the Kinect v1 has proved to have an ideal range between 1 to 3 meters in which the relative 3-D coordinates can be captured with minor errors (<1cm), and as such the Kinect v2 has proven to be equally good in this range, with errors below 4 mm for depth sensing applications (Yang et al., 2015). However, previous studies have shown that the Kinect can produce errors up to 10cm for ranges longer than 3 meters. Moreover, the tracking algorithm can frequently fail due to occlusions, non-distinguishing depth (limbs very close to the body) or clutter (Jungong Han et al., 2013). Nevertheless, for this study the considered error will be of $\pm$4 cm considering the results from Seer, Brändle and Ratti for Multiple Object Tracking Precision (MOTP) using Kinect v2 with pedestrian detection rate ranging from 94 to 96% (Seer et al., 2014), this is consistent with Capecci's findings in which the maximum error for the distance between elbows for lateral tilt of the trunk, as part of a research on the accuracy of Kinect v2 during dynamic movements for rehabilitation scenarios, was of 8.3 cm (Capecci et al., 2016), therefore an error 4 cm per joint can be considered as consistent.

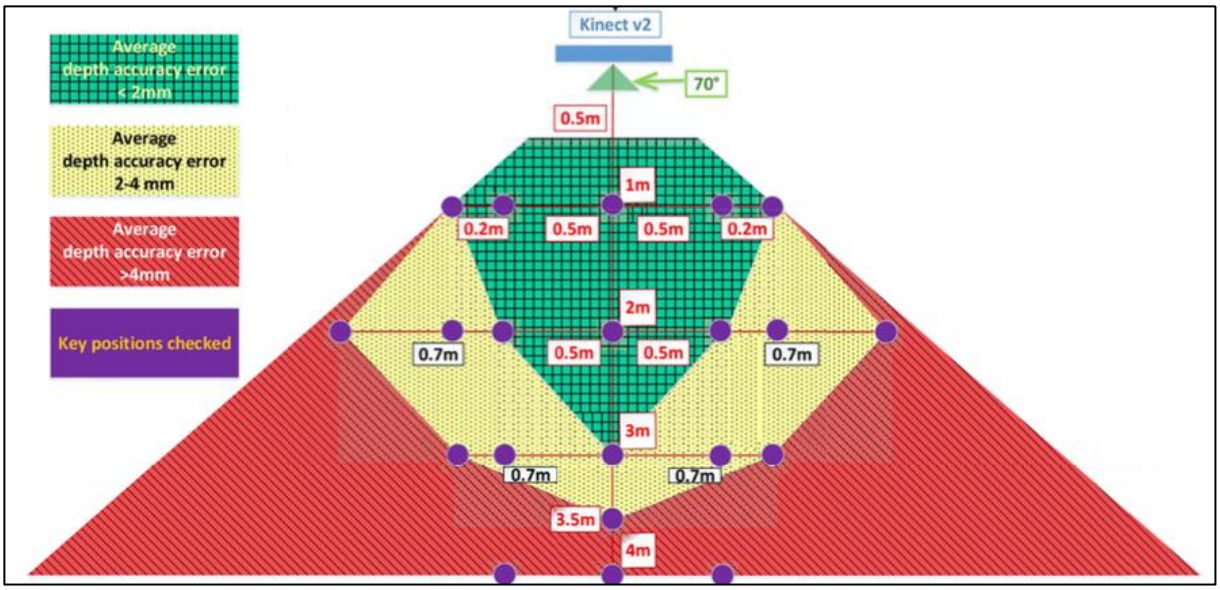

Figure 8: Accuracy error distribution of Kinect for Windows v2 for depth sensing applications on the horizontal plane(Yang et al., 2015)

2.3. Scenarios

Three different opening configurations were considered for the experiments. The configurations were chosen based on table 4 from the Approved Document B, which is the prescriptive code that applies for the United Kingdom (Great Britain and Office of the Deputy Prime Minister, 2013). Therefore, the configurations consisted of a corridor of 6 meters of length and 2 meters of width. British Standard 9999 requires a minimum corridor width of 1.2 meters, thus a 2 meters wide corridor complied with the standard that is being considered (British Standards Institution, 2008). The opening varied from 0.75, 0.85, and 1.05 meters of width as shown in Figure 9. These values are similar to the required values by the NFPA 101 life safety code of minimum 32 inches (0.81 meters) and the Swedish Boverket's Building Regulations minimum width of 0.8 meters (National Fire Protection Association, 2017; Swedish National Board of Housing, Building and Planning (Boverket), 2016), the International Building Code requires an egress width of 0.2 inches per occupant and thus was not considered in this analysis (Thornburg and Henry, 2009).

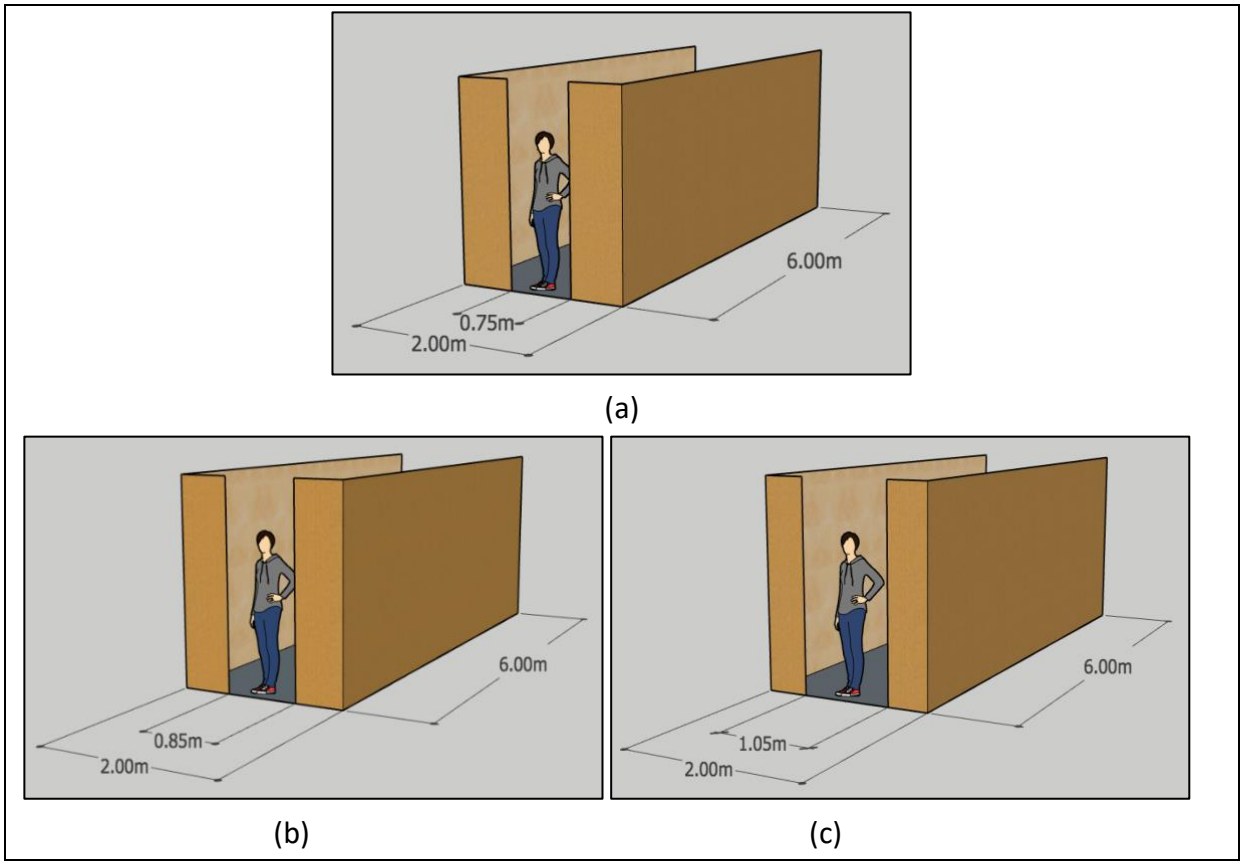

Figure 9: Layout of the three different configurations. (a) Opening of 0.75 m (b) Opening of 0.85 m (c) Opening of 1.05 m

2.4. Procedure

The aim of the experimental procedure was to generate movement through openings as natural as possible considering that the measurements were done on an artificial setup. One of the constraints was the line-of-sight nature of the detector, thus generating as many measurements as possible allowed the collection of sufficient data, especially when considering the group experiments in which an individual might obstruct partially the line-of-sight for the next pedestrian's relevant body joints.

A GoPro Hero 4 camera was used to record the pedestrians and identify in which order the opening was crossed, therefore allowing to analyse data points that compose rare events (e.g. a very tall individual or an overweight person). To do this in the group experiments, a number was assigned to each person, this number was physically placed in the front of the pedestrian as a number in a piece of paper attached to their clothes. This was also documented in the questionnaire, allowing to identify age, height, gender, weight and any medical conditions each individual might have, this were used as explanatory variables for the movement behaviour in case any abnormal measurements were reported.

2.4.1. Single pedestrian experiments

A single individual was asked to walk at their regular pace through the corridor, once the pedestrian crossed the opening he/she went towards a pre-defined point behind the sensor, this was done repeatedly until the experiment was performed 5 times. The instructions were delivered orally. Once this was done, the configuration was changed and the procedure was repeated until completing all three configurations. This was done while recording the data and video feed using the Kinect v2 sensor and a GoPro Hero 4 camera. The sensor, as mentioned previously in section 2.2.1, was located 1.95 meters away from the opening, the location of the sensor determined the axis for the X-coordinate in the system, the sensor was displaced from the centre of the opening 0.64 meters as shown in Figure 3, avoiding in this way any interaction between the apparatus and the normal flow of pedestrians. These experiments were executed with 5 individuals separately with the objective to perform a data analysis and calibration of the sensor.

2.4.2. Group experiments

A group of pedestrians was asked to walk at their regular pace through the corridor, once each individual crossed the opening he/she went towards a pre-defined point behind the sensor, this was done repeatedly until the experiment had been performed 5 times. The instructions were, once again, delivered orally. Additionally, in these set of experiments each person was assigned a number that was attached to their clothes, allowing the a-posteriori analysis of the video footage in order to relate each pedestrian to the information collected in the questionnaire. Once this was done, the configuration was changed and the procedure was repeated until completing all three configurations. This was done while recording the data and video feed using the Kinect v2 sensor and a GoPro Hero 4 camera. The sensor was, as previously mentioned, located 1.95 meters away from the opening and the horizontal displacement of the sensor determined the axis for the X-coordinate in the system as shown in Figure 3, avoiding in this way any interaction between the apparatus and the normal flow of pedestrians. These experiments were done with two groups of 10 and 14 individuals each, with the objective to perform a data analysis of effective widths on a more realistic scenario.

2.5. Data Collection

Considering that the objective of the experiments was to measure the effective width through openings 10 relevant body joints were selected:

1. Head
2. Spine Shoulder
3. Spine Mid

4. Spine Base/Core
5. Right Shoulder
6. Right Elbow
7. Right Wrist
8. Left Shoulder
9. Left Elbow
10. Left Wrist

These joints were chosen to provide a reasonable amount of data, which in turn would allow the creation of a heat map of space usage as well as an insight on the dimensions of the boundary layer. Joints 1, 2, and 3 were meant to provide a visual reference of the body, joint 4 was considered the core and centre of gravity of the individual being tracked, thus it could be used as a complement to the video feed in order to determine towards which side each pedestrian was leaning to. The remaining joints are the ones that provide information on which part of the body is located closer to the edge of the opening, allowing to measure the dimensions of the boundary layer and therefore producing a better understanding of the effective width through openings. Figure 10 illustrates how the selected body joints were displayed by the IR video feed while Figure 11 shows the data provided by the depth sensor using the body index map and skeleton data sources.

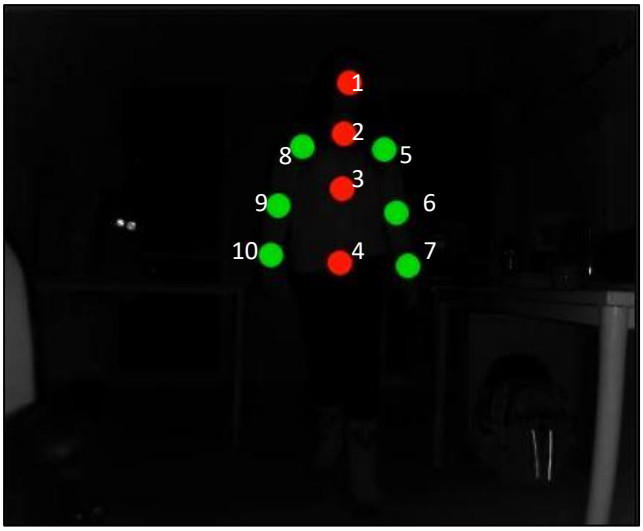

Figure 10: IR feed of the 10 selected body joints

Figure 11: Coordinates in meters of each of the 10 selected body joints using the reference coordinate system.

2.6. Data Analysis

This section illustrates how the collected data was analysed throughout this experimental study. This includes the equations used to calculate flows and densities that are included to provide context.

2.6.1. Individual Experiments

For the individual experiments, the data analysis was focused exclusively in the tracking of the relevant body joints, particularly the joints that represent each arm. In this way for each time the pedestrians crossed the opening all ten relevant joints were tracked. Following this procedure, the data from the two arms was transformed from the relative coordinate system obtained from the Kinect v2 sensor into a system with the origin located at the centre of the opening at a height of 0 m. Thus, generating a X-Y coordinate system that allowed to plot the data for each one of the relevant joints. This information was gathered for each one of the three scenarios and an aggregate result was generated in the form of a heat map. Additionally, the mean, maximum, and minimum distances to the closest edge for each of the joints were calculated based on the dimensions of the opening, thus allowing to see how single individuals moved in each one of the three proposed scenarios. The standard deviation for the distance of each one of the body joints was also calculated.

2.6.2. Group Experiments

For the group experiments, the data analysis included the tracking of the relevant body joints, and the measurement of flows. Thus, for each time a pedestrian crossed the opening all ten relevant joints were tracked, while flow was estimated using the video feed. In this case, the flow considered the whole group as the number of occupants, while the time it took the

whole group to cross the opening was calculated from the moment the first pedestrian crossed the opening until the last person of the group crossed that same point, hence using a "first-in last-out" approach. Since this was performed 5 times per scenario an average flow was calculated.

Equation 4: Calculated or measured flow

$$F_c = \frac{Number\ of\ persons\ in\ the\ group}{\Delta t}$$

Once the flow was estimated it was possible to normalize the value by dividing by the effective width of the corridor, thus obtaining the specific flow for the corridor. Once the specific flow was obtained the density was calculated based on the formulas used in the hydraulic method proposed by the SFPE handbook (Gwynne and Rosenbaum, 2016):

Equation 5: Specific flow formula parting from the definition of calculated flow in the SFPE handbook

$$F_{s_{corridor}}\left(\frac{occupants}{m/second}\right) = \frac{F_c}{W_{e_{corridor}}}$$

Additionally, the reference density had to be calculated for the corridor since the doorway itself has no density as it is a threshold and not an area. Density can be calculated in several manners. One way is to use the concept of momentary density, in which the immediate number of persons at a given time is counted for a reference area section, and thus the density at a specific time can be calculated; Seyfried, Steffen, Klingsch and Boltes (Seyfried et al., 2005), however, found this method problematic when a small number of pedestrians is involved. Hence in their experiments, performed in the auditorium Rotunde at the Central Institute for Applied Mathematics (ZAM) of the Research Centre Jülich, they calculated the density in 1-dimension and then transform this line-density into area-density considering the average width of a person (α=0.46 m) and the increased width due to velocity of movement considering body sway (β between 0.05s and 0.3s). Therefore, in their research the area-density is calculated as $\rho_{1D} \rightarrow \rho_{2D} = \frac{\rho_{1D}}{\alpha + \beta\, v}$ where v is the velocity in m/s.

Nonetheless, in this research density was not calculated in such ways since the relevant variables were not measured directly. Thus, in this case the density was calculated using the formula for the specific flow that is suggested for the hydraulic calculations in the SFPE handbook in which density depends on the effective width of the corridor:

Equation 6: Density formula for corridors, aisles, ramps and doorways derived from the specific flow formula form the SFPE handbook

$$D\left(\frac{occupants}{m^2}\right) = \frac{-1.4 \pm \sqrt{1.4^2 - 4\left(-F_{s_{corridor}}\right)(-0.37)}}{2(-0.37)}$$

$$Fs: \begin{cases} F_{s_{corridor}} \leq 1.3, & F_{s_{corridor}} = F_{s_{corridor}} \\ F_{s_{corridor}} > 1.3, & F_{s_{corridor}} = 1.3 \end{cases}$$

Performing these calculations made possible to assess the type of density range that the flow reflected for each one of the scenarios according to the hydraulic model under scrutiny. The results of this procedure are shown in section 3. However, it is of outmost importance to acknowledge that this was only done to provide context.

Most importantly, the data from the two arms that was recorded by the Kinect v2 sensor was transformed from the relative coordinate system obtained from the Kinect v2 sensor into a system with the origin located at the centre of the opening at a height of 0 m. Thus, generating a X-Y coordinate system that allowed to plot the data for each one of the relevant joints. This information was gathered for each one of the three scenarios and an aggregate result was generated in the form of a heat map. Additionally, the mean, maximum, and minimum distances to the closest edge for each of the joints was calculated based on the dimensions of the opening, thus allowing to see how single individuals moved in each one of the three proposed scenarios. The standard deviation for the distance of each one of the body joints was also calculated.

3. Results

Results from the experimental study on effective width in openings using the Kinect v2 sensor are presented in this section. Heat maps are used to illustrate the areas in the Cartesian coordinate plane in which data was seen repetitively for the tracked joints. In this sense, a red colour in the heat map illustrates that joints within that region were repetitive whilst blue indicates spaces where no joints were tracked. Additionally, the mean values for the relevant joints are plotted, this is fundamental since the average value shows an indication on how pedestrians, for this limited number of tests, use the space more commonly and therefore this generates a better understanding of the boundary layer. Additionally, tables present the boundary layer dimensions, highlighting the mean value of the joint that was on average closer to each respective edge.

Additionally, as it was previously mentioned, measurements performed by the Kinect v2 sensor although very accurate intrinsically will have a random error of 4 cm. The treatment of this error in the global results will be addressed in the discussion section of this thesis, nonetheless it is of interest to keep it in mind when reviewing these results. Nevertheless, the standard error of the mean was calculated in order to provide some insight as to how much the mean varies within different experiments.

3.1. Individual Experiments

The results obtained from individual experiments are presented in this section. Individual experiments were carried out separately for each pedestrian, however the values obtained were aggregated later to illustrate how single pedestrians tend to behave when unimpeded. Moreover, in the case of individual tests the results and measurements were not affected by obstruction, thus for these scenarios the data collected was 100%.

Experimental data from the individual experiments for the different scenarios, as previously mentioned, was used to generate mean values as well as the heat map that would, in turn, generate a more visual understanding on the capability of the Kinect v2 device to measure the position of the relevant joints and thus become a useful tool to generate a better understanding of boundary layers for openings.

3.1.1. Opening of 0.75 m

Table 3 shows the most relevant values for the distances between joints and their respective edge for an opening of 0.75 m obtained from the individual experimental phase. The mean values displayed on Table 3 are the same as those in Figure 12, this was done to provide a visual representation for which is the width being considered. Additionally, the standard deviation illustrates how, overall amongst five different individuals, the variation of the distances to the edges for individual experiments through this opening scenario oscillates from the mean value selected as the dimension of the boundary layer; this was done for all individual experiments. In this particular scenario, the values that constitute the boundary layer for individuals are of 14 cm on the right edge and 13 cm on the left, thus leading to an effective width of 47 cm.

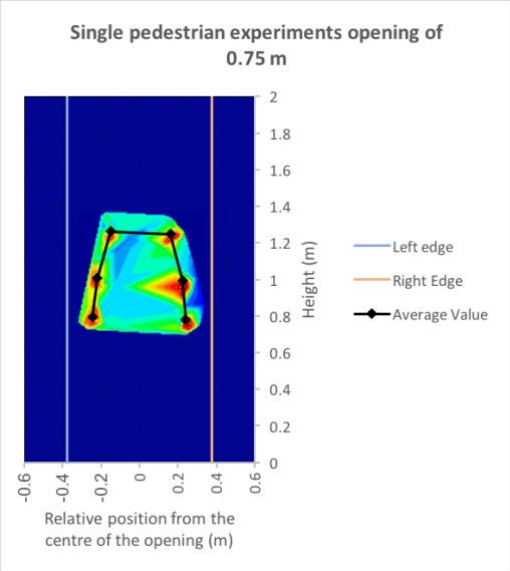

Figure 12: Heat map of aggregate results from individual experiments for an opening of 0.75 m

Table 3: Results for the dimensions of the boundary layer obtained from individual experiments for an opening of 0.75 m. The text in red is the minimum distance to the edge found on average for the scenario and thus the dimensions of the boundary layers.

Single pedestrian experiments aggregate results for opening of 0.75 m					
Joint	**Mean distance to edge(m)**	**Max distance to edge (m)**	**Min distance to edge (m)**	**Standard Deviation**	**Standard Error of the mean**
Right Wrist	**0.14**	0.22	0.04	0.04	0.009
Right Elbow	0.15	0.20	0.08	0.03	0.007
Right Shoulder	0.21	0.27	0.15	0.03	0.007
Left Wrist	**0.13**	0.21	0.06	0.04	0.009
Left Elbow	0.16	0.25	0.11	0.04	0.009
Left Shoulder	0.23	0.33	0.18	0.04	0.009

3.1.2. Opening of 0.85 m

Table 4 shows the most relevant values for the distances between joints and their respective edge for an opening of 0.85 m obtained from the individual experimental phase. The mean values displayed on Table 4 are the same as those in Figure 13 for the mean values. In this scenario, the values that constitute the boundary layer for individuals are of 21 cm on the right edge and 15 cm on the left. This shows an increment of boundary layer in contrast to the opening of 0.75 m of width, nevertheless the effective width of the opening of 49 cm which is still above the one for an opening of 0.75 m.

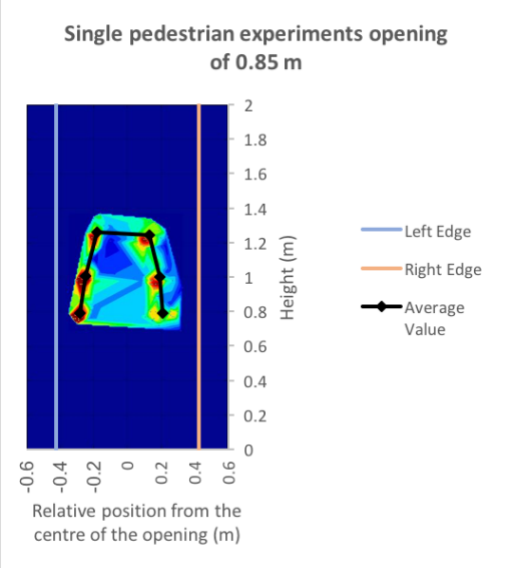

Figure 13: Heat map of aggregate results from individual experiments for an opening of 0.85 m

Table 4: Results for the dimensions of the boundary layer obtained from individual experiments for an opening of 0.85 m. The text in red is the minimum distance to the edge found on average for the scenario and thus the dimensions of the boundary layers.

Single pedestrian experiments aggregate results for opening of 0.85 m					
Joint	**Mean distance to edge(m)**	**Max distance to edge (m)**	**Min distance to edge (m)**	**Standard Deviation**	**Standard Error of the mean**
Right Wrist	**0.21**	0.32	0.11	0.06	0.013
Right Elbow	0.23	0.34	0.10	0.06	0.013
Right Shoulder	0.29	0.39	0.20	0.06	0.013
Left Wrist	**0.15**	0.23	0.08	0.04	0.009
Left Elbow	0.18	0.27	0.12	0.04	0.009
Left Shoulder	0.25	0.33	0.18	0.04	0.009

3.1.3. Opening of 1.05 m

Table 5 shows the most relevant values for the distances between joints and their respective edge for an opening of 1.05 m obtained from the individual experimental phase. The mean values displayed on Table 5 are the same as those in Figure 14 for the mean values. In this scenario, the values that constitute the boundary layer for individuals are of 28 cm on the right edge and 26 cm on the left. This shows an increment of boundary layer in contrast to the openings of 0.75 m and 0.85 m of width, nevertheless the effective width of the opening of 51 cm which is still above the one for an opening of 0.75 m and 0.85 m.

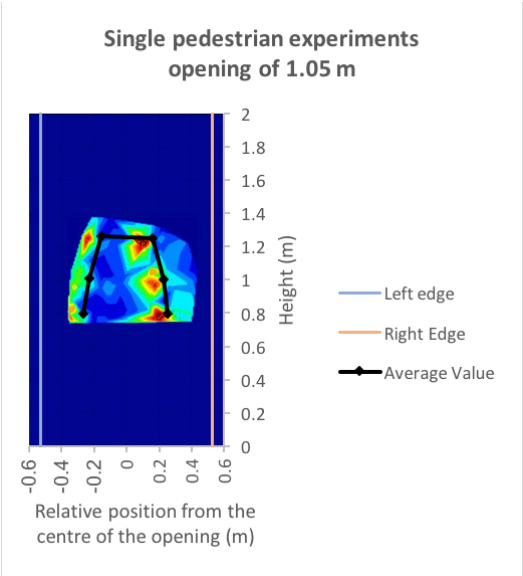

Figure 14: Heat map of aggregate results from individual experiments for an opening of 1.05 m

Table 5: Results for the dimensions of the boundary layer obtained from individual experiments for an opening of 1.05 m. The text in red is the minimum distance to the edge found on average for the scenario and thus the dimensions of the boundary layers.

Single pedestrian experiments aggregate results for opening of 1.05 m					
Joint	**Mean distance to edge(m)**	**Max distance to edge (m)**	**Min distance to edge (m)**	**Standard Deviation**	**Standard Error of the mean**
Right Wrist	**0.28**	0.40	0.12	0.09	0.020
Right Elbow	0.30	0.40	0.09	0.09	0.020
Right Shoulder	0.37	0.46	0.15	0.09	0.020
Left Wrist	**0.26**	0.49	0.17	0.09	0.020
Left Elbow	0.30	0.52	0.19	0.10	0.022
Left Shoulder	0.37	0.60	0.26	0.10	0.022

3.2. Group Experiments

The results obtained from group experiments are presented in this section. Additionally, it is important to observe that for openings of 0.75 and 0.85 m only one lane was formed as seen in figures 15 and 16. However, for the opening of 1.05 m two lanes were formed when pedestrians crossed through the opening as seen in figure 17. Moreover, tables 6-8 show the average, minimum, and maximum distances from each joint to the corresponding edge as well as the standard deviation that resulted from the experimental data. Furthermore, in the tables is highlighted the value that is considered to represent the dimension of the boundary layer. In this case, the boundary layer dimension was measured as the mean value of the joint closest to the edge. Finally, each section will comment on how some data was lost due to the line-of-sight nature of the device.

3.2.1. Opening of 0.75 m

Experimental data from the group experiments for an opening of 0.75 m in displayed in this section. For the case of the 10 pedestrians crossing the opening 100% of the data was collected satisfactorily, whilst for the group of 14 pedestrians 71.43% of the data was collected. This is due to obstructions of the line-of-sight for some pedestrians in the opening by a person walking in front of them. This will be discussed with further detail in section 4. Additionally, from the obtained results it can be observed from tables 6 and 7 that the dimension of the boundary layer was, on average, of 15 cm for both edges thus leading to an effective width of 45 cm.

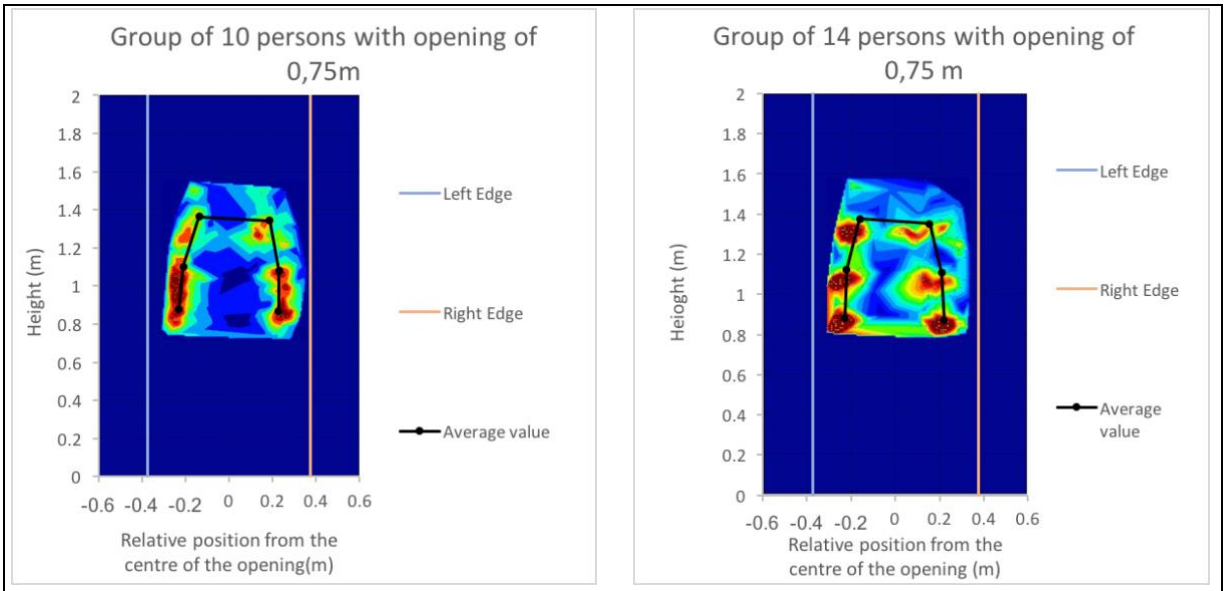

(a)100% of the total data collected (b)71.43% of the total data collected

Figure 15: Heat map of results for group experiments with an opening of 0.75 m: (a) Experiments with 10 pedestrians. (b)Experiments with 14 pedestrians

Table 6 Results for group experiments with an opening of 0.75 m with 10 pedestrians. The text in red is the minimum distance to the edge found on average for the scenario and thus the dimensions of the boundary layers.

Group of 10 persons with opening of 0.75 m						
	Right Wrist	**Right Elbow**	**Right Shoulder**	**Left Wrist**	**Left Elbow**	**Left Shoulder**
Average Distance to Edge	**0.15**	0.15	0.19	**0.15**	0.16	0.24
Minimum Distance to Edge	0.05	0.02	0.06	0.07	0.10	0.13
Maximum Distance to Edge	0.50	0.30	0.31	0.31	0.33	0.42
Standard deviation	0.09	0.06	0.06	0.05	0.05	0.06
Standard error of the mean	0.013	0.008	0.008	0.007	0.007	0.008

Table 7: Results for group experiments with an opening of 0.75 m with 14 pedestrians. The text in red is the minimum distance to the edge found on average for the scenario and thus the dimensions of the boundary layers.

Group of 14 persons with opening of 0.75 m						
	Right Wrist	**Right Elbow**	**Right Shoulder**	**Left Wrist**	**Left Elbow**	**Left Shoulder**
Average Distance to Edge	**0.15**	0.16	0.22	**0.15**	0.16	0.22
Minimum Distance to Edge	0.04	0.03	0.06	0.06	0.06	0.10
Maximum Distance to Edge	0.26	0.26	0.36	0.32	0.34	0.42
Standard deviation	0.06	0.07	0.08	0.06	0.06	0.07
Standard error of the mean	0.008	0.010	0.011	0.008	0.008	0.010

3.2.2. Opening of 0.85 m

Experimental data from the group experiments for an opening of 0.85 m is displayed in this section. For the case of the 10 pedestrians crossing the opening 87.14% of the data was collected satisfactorily, whilst for the group of 14 pedestrians 72.86% of the data was collected. This is due to obstructions of the line-of-sight for some pedestrians in the opening by a person walking in front of them. This will be discussed with further detail in section 4. Additionally, from the obtained results it can be observed from tables 8 and 9 that the dimension of the boundary layer was, on average, of 19 to 22 cm for both edges. Therefore, considering that the value closest to the edge represents the best use of the opening, this results on an effective width of 47 cm on average, thus even though the boundary layer increased significantly there is still an increased effective width and, according to theory explained in the literature review in which flow depends linearly on effective width, the flow through this opening still increased when only a small modification of the total width was considered.

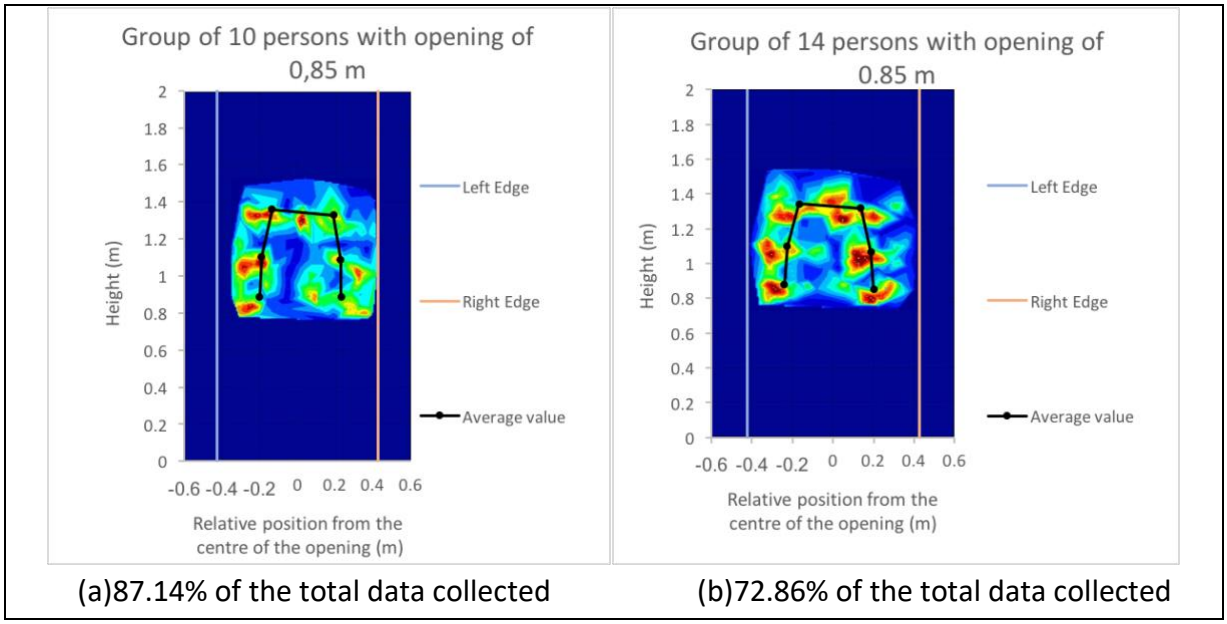

(a)87.14% of the total data collected (b)72.86% of the total data collected

Figure 16: Heat map of results for group experiments with an opening of 0.85 m: (a) Experiments with 10 pedestrians. (b)Experiments with 14 pedestrians

Table 8: Results for group experiments with an opening of 0.85 m with 10 pedestrians. The text in red is the minimum distance to the edge found on average for the scenario and thus the dimensions of the boundary layers.

Group of 10 persons with opening of 0.85 m						
	Right Wrist	**Right Elbow**	**Right Shoulder**	**Left Wrist**	**Left Elbow**	**Left Shoulder**
Average Distance to Edge	**0.19**	0.20	0.24	0.22	0.23	0.29
Minimum Distance to Edge	0.00	0.00	0.02	0.08	0.08	0.12
Maximum Distance to Edge	0.42	0.42	0.44	0.54	0.57	0.60
Standard deviation	0.12	0.12	0.13	0.11	0.13	0.13
Standard error of the mean	0.018	0.018	0.020	0.017	0.020	0.020

Table 9: Results for group experiments with an opening of 0.85 m with 14 pedestrians. The text in red is the minimum distance to the edge found on average for the scenario and thus the dimensions of the boundary layers.

Group of 14 persons with opening of 0.85 m						
	Right Wrist	**Right Elbow**	**Right Shoulder**	**Left Wrist**	**Left Elbow**	**Left Shoulder**
Average Distance to Edge	0.22	0.24	0.29	**0.19**	0.20	0.26
Minimum Distance to Edge	0.02	0.00	0.06	0.04	0.02	0.10
Maximum Distance to Edge	0.54	0.50	0.46	0.48	0.50	0.54
Standard deviation	0.11	0.11	0.11	0.10	0.11	0.11
Standard error of the mean	0.015	0.015	0.015	0.014	0.015	0.015

3.2.3. Opening of 1.05

Experimental data from the group experiments for an opening of 1.05 m is displayed in this section, these experiments showed the formation of two lanes when pedestrians walked through the opening. For the case of the 10 pedestrians crossing the opening 94.29% of the data was collected satisfactorily, whilst for the group of 14 pedestrians 95.71% of the data was collected. This is due to obstructions of the line-of-sight for some pedestrians in the opening by a person walking in front of them. This will be discussed with further detail in section 4. These scenarios are far more complex than the previous analysed since lanes and a small sense of crowd behaviour can be seen due to large opening that allows the formation of two lanes. Results from these tests show a boundary layer of 9 to 13 cm on average. This, considering the result closest to the opening to be the effective width leads to a width reduction of 18 cm thus leading to an effective width of 87 cm.

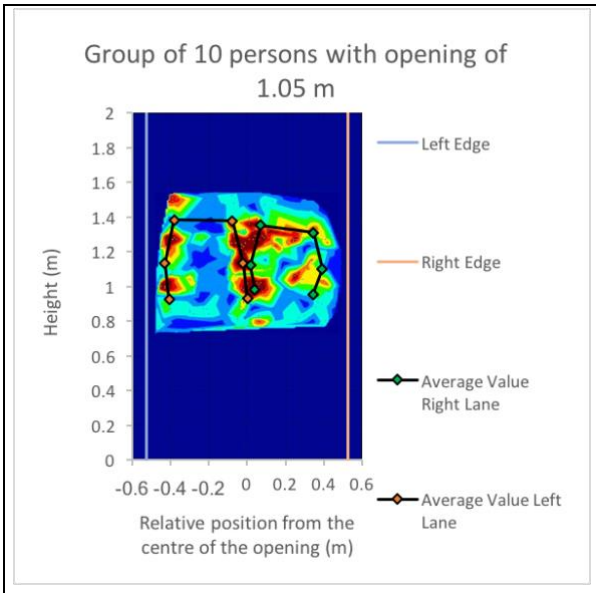

(a)94.29% of the total data collected

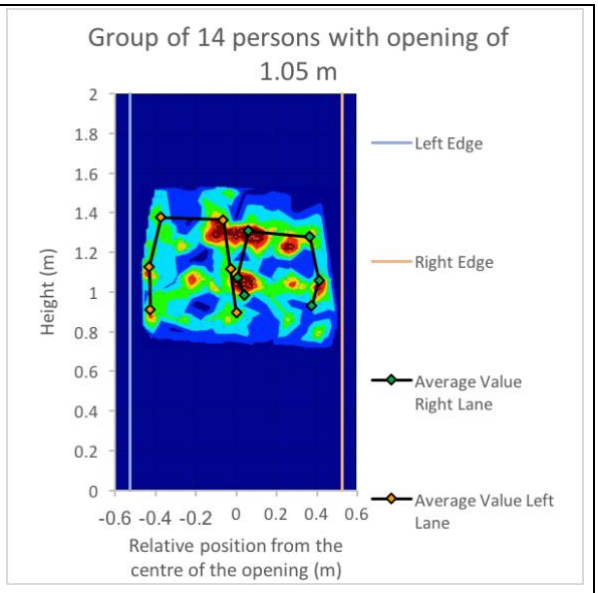

(b)95.71% of the total data collected

Figure 17: Heat map of results for group experiments with an opening of 1.05 m: (a) Experiments with 10 pedestrians. (b)Experiments with 14 pedestrians

Table 10: Results for group experiments with an opening of 1.05 m with 10 pedestrians. The text in red is the minimum distance to the edge found on average for the scenario and thus the dimensions of the boundary layers.

Group of 10 persons with opening of 1.05 m					
Right arm values for pedestrians in right lane					
	Average distance to edge (m)	Minimum distance to edge (m)	Maximum distance to edge (m)	Standard Deviation	Standard error of the mean
Right Shoulder	0.18	0.09	0.28	0.06	0.009
Right Elbow	**0.13**	0.04	0.27	0.06	0.009
Right Wrist	0.18	0.04	0.39	0.10	0.015
Left arm values for pedestrians in left lane					
	Average distance to edge (m)	Minimum distance to edge (m)	Maximum distance to edge (m)	Standard Deviation	Standard error of the mean
Left Shoulder	0.14	0.12	0.19	0.02	0.003
Left Elbow	**0.09**	0.07	0.13	0.02	0.003
Left Wrist	0.12	0.05	0.26	0.06	0.009

Table 11: Results for group experiments with an opening of 1.05 m with 14 pedestrians. The text in red is the minimum distance to the edge found on average for the scenario and thus the dimensions of the boundary layers.

Group of 14 persons with opening of 1.05 m					
Right arm values for pedestrians in right lane					
	Average distance to edge (m)	Minimum distance to edge (m)	Maximum distance to edge (m)	Standard Deviation	Standard error of the mean
Right Shoulder	0.16	0.10	0.27	0.06	0.007
Right Elbow	**0.12**	0.04	0.19	0.04	0.005
Right Wrist	0.15	0.02	0.33	0.09	0.011
Left arm values for pedestrians in left lane					
	Average distance to edge (m)	Minimum distance to edge (m)	Maximum distance to edge (m)	Standard Deviation	Standard error of the mean
Left Shoulder	0.15	0.10	0.23	0.04	0.002
Left Elbow	**0.09**	0.07	0.14	0.02	0.001
Left Wrist	0.10	0.06	0.17	0.03	0.004

3.2.4. Aggregate results for group experiments regarding flows and densities

As mentioned in section 2.4.2, densities and flows were calculated using the video recordings for each one of the group experiment scenarios. Flows were estimated using the measured time it took from first-in to last-out of the pedestrians through the opening using Equation 4. The reference density, however, corresponds to the area-density calculated using Equation 6. This density corresponds to the corridor; therefore, the normalized or specific flow of the corridor is required. This, consequently, was calculated using an effective width of the corridor of 1.6 meters for Equation 5. This effective width is used since the corridor is 2 meters wide and the SFPE uses a boundary layer reduction of 0.2 meters for corridors, this value is derived from the findings of Habitch and Braaksma (Gwynne and Rosenbaum, 2016; Habicht and Braaksma, 1984).

The specific flow through the opening was calculated by dividing the measured flow by the effective width obtained from the results previously displayed. The result of this calculation shows that the density of the scenarios was, in general, low and thus the flow corresponds to a nearly unimpeded speed scenario for all cases. These results are displayed in tables 12 and 13.

Table 12: Flow and density calculations for scenarios with 10 pedestrians

Scenario	Measured flow (Occ/s)	Normalized flow for corridor (Occ/s/m)	Density (Occ/m2)
10 pedestrians opening of 0,75m	0.76	0.48	0.38
10 pedestrians opening of 0,85m	0.80	0.50	0.40
10 pedestrians opening of 1,05m	0.88	0.55	0.44

Table 13: Flow and density calculations for scenarios with 14 pedestrians

Scenario	Measured flow (Occ/s)	Normalized flow for corridor (Occ/s/m)	Density (Occ/m2)
14 pedestrians opening of 0,75m	0.91	0.57	0.46
14 pedestrians opening of 0,85m	0.99	0.62	0.51
14 pedestrians opening of 1,05m	1.06	0.66	0.56

In this case, the specific flow through openings would be very large ranging from 1.01 to 2.1 occupants/s/m of effective width. These results are explained by the large value obtained for the dimensions of the boundary layer which in turn results in a reduced effective width. This is mentioned to provide context; however these values should be treated with caution as they do not represent the actual flow through the opening and therefore are only mentioned in this section but will not be displayed explicitly.

4. Discussion

This section includes the critical analysis of the interpretation of the data obtained during the experimental phase of this thesis. Analysis on the implications of the findings and their limitations is included. Moreover, a comprehensive analysis of the Kinect v2 capability to measure the position of joints in 3-dimensional space and hence measure boundary layer dimensions is included. The findings of the experimental data for both individual and group experiments are compared and an evaluation of the effects this has on the way effective width is analysed. This, in turn, allows to discuss about how further experimental tests are required to generate a better understanding on the boundary layer dimensions in openings.

Additionally, this section will examine how the retrieved data shows discrepancies with the linear relationship model between effective width and flow through openings in case of almost unimpeded movement (e.g. low densities), as the total width determines if one or several pedestrians can cross the opening simultaneously (i.e. if there are one or more lanes at the same time) and therefore this will influence the maximum flow that can be achieved. Consequently, this section incorporates a further analysis on the relationship between the maximum number of lanes that can be observed for the width of an opening in case of almost unimpeded movement and the dimensions of the boundary layers that can be observed.

4.1. Kinect v2 capability to measure effective width

One of the main objectives of this project was to determine if Kinect v2 can be used to analyse effective widths in openings through experimental data collection, generating a better understanding of the boundary layers. Therefore, the device was programmed to measure the desired joints at a specific distance of 1.95 m from the device and generate an output of the positioning of such joints in a two dimensional X-Y coordinate system. This allowed to obtain the desired data from the experimental tests and provide some insight on how boundary layer in openings can be measured.

4.1.1. Accuracy and error treatment

As mentioned in the methodology section, multiple researchers (Capecci et al., 2016; Jungong Han et al., 2013; Seer et al., 2014; Yang et al., 2015) have investigated the accuracy of the Kinect v2 device for depth sensing measurements. It has been observed that the sensor can provide an accurate position of body joints and objects for several ranges, however the ideal range has proven to be between 1 and 3 meters of distance between the sensor and the person whose joints are being tracked. Within this range, the static 3-dimensional coordinates can be captured with minor errors below 4mm, however for longer ranges it has been observed that the errors can go up to 10cm (Yang et al., 2015).

Nonetheless, this study focuses on pedestrians walking and therefore the measurements were not performed under static scenarios but dynamic ones. Therefore, the accuracy is reduced due to the movement of the tracked joints, the changing position of the limbs and additional cluttering which introduce a new source of random error.

Studies on the accuracy of the Kinect v2 for dynamic scenarios have also been performed in the past (Capecci et al., 2016; Seer et al., 2014). Considering the maximum error that has been observed in these studies, it has been determined that a maximum random error of 4 cm for dynamic tracking can be observed for the Kinect v2 device. This error is random in nature and as such it is intrinsically reduced by performing multiple measurements, this is proven by the standard error of the mean which shows the reduction of the random error when multiple measurements are performed.

This, in turn, means than an analysis of the trend of convergence allows to obtain useful information of the data under consideration. Hence, it is possible to assess behavioural uncertainty and therefore estimate the impact of the use of stochastic variables in models (Ronchi et al., 2014). This same principle can be applied to experimental setups in which the number of performed tests is determined by the convergence of the values obtained, hence reducing the random error to acceptable values.

Additionally, the standard deviation of the results was presented for each set of data collected. This fundamentally assumes that the data collected has a normal distribution. Since several individuals were used for both individual and group experiments multiple measurements were performed and as such it could be observed that the standard error of the mean was very low for all cases, therefore the mean values could be deemed as sufficiently accurate for this study as the standard error of the mean presented small variations and was within a range below 2 cm for all joints considered as relevant to provide the dimension of the boundary layer. Thus, it can be also confirmed that there is, intrinsically, a pattern of behaviour from which all other observations are deviations as was proposed by Corbetta (Corbetta, 2016).

4.1.2. Advantages and limitations

The Kinect v2 is a device that uses the depth sensor to track positions within a coordinate system with origin at the location of the sensor using a Time-of-Flight method. Using this, or any other methodology, for depth sensing requires a direct line of sight between the device and the individuals being tracked. Consequently, when a pedestrian was obstructed by a person in front of them it was not possible to track the desired joints and data was not collected. Moreover, the algorithm used by this device returns as an output for the joint

location the relative centre of the joint, hence orientation of the limbs, clothing, fat and skin constitute an extra layer that is not accounted for, nevertheless this limitation is included as part of the random error of 4 cm, although it was not possible to accurately measure how much impact it has on the output.

Nevertheless, the Kinect v2 sensor has proven to be useful and has overall taken most of the data from the experiments, proving to dynamically track multiple pedestrians at the same time as well as rapidly recognizing the next pedestrian once the line of sight is unobstructed, while protecting individual privacy as the face is not recognizable from the video feed. However, this was done in low density flows as indicated in section 3.2.4, higher density flow might, on the other hand, result in more occlusion and limbs closer to the body, generating a lower data collection since the tracking might be impaired. Nonetheless, this device proved to be accurate and low cost providing valuable results for simple scenarios.

Increasing accuracy of the Kinect device as a tool for pedestrian tracking, regarding for effective width applications, could be done by the use of multiple devices. Using both overhead and frontal tracking at the same time to, in turn, increase the precision as triangulation on the 3-dimensional space would be possible. Moreover, the use of multiple devices could also reduce the effect of clutter and obstruction of the line-of-sight, as if one of the devices is obstructed it is still possible for the others to still have a direct line-of-sight and hence track the desired joints accurately. Multiple overhead devices have been used simultaneously in the past for trajectory tracking experiments performed by Corbetta (Corbetta, 2016).

4.2. Individual experiments

Single pedestrian experiments were performed for calibration of the device as well as to retrieve data on how the boundary layer works when a completely unimpeded walking pace was present. Additional to this, individual experiments shed some light on individual walking behaviour in openings.

The individual results for the three different configurations, show how individuals tend to walk in the centre of the opening. However, when individual results are analysed separately, it becomes evident that pedestrians with different countries of origin had small deviations from this behaviour. Thus, it was observed that individuals coming from countries in which the norm is to drive in the right side of the road naturally tended to be inclined to walk slightly to the right side whilst pedestrians coming from countries in which the norm is to drive on the left side of the road tended to walk closer to the left side of the opening. This supports previous findings such the ones presented by Corbetta in yearlong measurements for pedestrian tracking (Corbetta, 2016) in which a tendency for individuals to walk in the relative

right was observed in the Netherlands, where the norm is to drive on the right side of the road.

Regarding effective width, individual experiments allowed to measure the dimensions of the boundary layer for a simple scenario with unimpeded walking speed. This, additionally allowed to ascertain that the Kinect v2 device can perform such measurements in a simple dynamic scenario, and therefore allowed to prepare a more complex experiment in which group behaviour could be assessed. Moreover, individual experiments due to their simplicity allowed to corroborate the benefits of using the infrared sensor for depth sensing as variation of light had no significant impact on the measured outputs.

4.3. Group experiments

Group experiments were performed in order to reproduce a more realistic scenario of a low-density flow through the three different opening sizes. Nonetheless, since the device had never been used for boundary layer measurements, considering flow through openings, in a frontal position the densities had to be low to ensure that sufficient data was collected, therefore small groups were used. This pilot experimental study did, however, shed some light on how the boundary layer is influenced in low density conditions by the width of the opening as well as by the number of individuals that can cross through the opening simultaneously, therefore the effect of one or multiple lanes was seen. Nevertheless, the effect of higher density flows was not assessed due to the nature of the experimental setup and consequently the effect of density is not accounted for through this analysis.

4.3.1. Relationship between dimensions of boundary layer and total width of openings in low density flows

The results from the group experiments, although considering exclusively low density flows, showed that even a small increase of 10 cm in the opening size resulted in an increase of the flow, this is similar to the findings by Pauls in the 1980s (Pauls, 1987) and thus is not new to the field since the methodology presented by the SFPE handbook is based on this assumption. However, the dimension of the effective width has been considered to increase equally as the increase of the total width of the opening. Nevertheless, the results obtained in this experimental study at low density conditions showed that the formation of lanes has a significant effect on the dimensions of the boundary layer. Thus, it has come to attention that the dimensions of the boundary layer might not be static for the case of openings but dynamic dependent on the total width of the opening and possibly being affected by local densities.

The relationship between the dimension of the boundary layer and the total width of the opening was not evident until group experiments were performed. For the low-density flows

that were considered in this study, it became clear that the width of the opening determines the number of lanes that can be formed to cross through the opening simultaneously. However, for the 0.85 and 0.75 m wide openings it was noted an increased flow even if the change of total width was small; nonetheless in both cases only one lane was observed but the effective width for these openings also increased as the opening dimensions augmented. Yet, this increment on the effective width was not the same as the increment in the total opening size and thus the boundary layer dimensions changed and were not static as is assumed currently for engineering calculations. Furthermore, when the opening was increased to 1.05 m the formation of two lanes was observed and with it the dimensions of the boundary layer dropped significantly.

This observation on the varying dimensions of the boundary layer could be explained by the merging process. As even if the same number of lanes is formed, the merging process might be improved due to the additional width in the opening. The reason for the effective width to be augmented, in these low-density flow scenarios, would be the merging process occurring before the opening and thus, although the effective width increases as the opening becomes larger, the limitation on the number of lanes only allows one pedestrian to cross through the doorway at a time and hence the amount of space used becomes significantly less than the total width of the opening. This, in turn, means that the dimensions of the boundary layer augmented with the increased width of the opening. However, when the size of the opening is increased enough for a second lane to be formed the observed results showed that the dimensions of the boundary layer dropped significantly as now most of the space was used since it was just enough to fit the two lanes. Hence, if the trend observed for the increase from one to two lanes applies for multiple lanes, then the same behaviour for the boundary layer would be expected if the opening size is further increased until there is enough space to have a third lane of pedestrians walking through the archway, point in which the dimensions of the boundary layer would reduce again.

These results, therefore, seem to indicate that there is a minimum and maximum value for the boundary layer. Nonetheless, further studies are needed to assess the point at which the opening becomes sufficiently large to have two lanes are of interest in order to determine the minimum and maximum dimensions of the boundary layer that can be observed and the impact that varying densities may have on lane formation. This is only considered for multiple lanes as openings with dimensions that are only capable of generating a single lane should not go below the minimum requirements and, in any case, not below 0.75 m which was the lowest value allowed by the reviewed codes.

In this experimental study, the formation of lanes proved to be very relevant when considering the flow through the opening in low-density situations. Intuitively, in the case of lane formation, a step-wise increase of capacity with the width appears to be natural (Schadschneider and Seyfried, 2009). This has been corroborated previously in studies

performed by Hoogendoorn and Daamen (Hoogendoorn and Daamen, 2005) in which the capacity of a bottleneck increases in a step-wise fashion. This is based on the observation that inside the bottleneck the formation of lanes occurs, and hence the "zipper" effect is detected as the merging behaviour produced when pedestrians enter the bottleneck. Nevertheless the study by Seyfried, Passon, Steffen, Boltes, Rupprecht and Klingsch (Seyfried et al., 2009) suggests that the lane distance in bottlenecks increases continuously, in contrast to a step-wise approach. Therefore, the impact of lane formation should be further studied to assess the dimensions of the boundary layers.

However, this experimental study focussed exclusively in low-density flows. And hence it is possible that for larger densities the pedestrian dynamics change. It has been observed in the past that the cross section of a person, as seen from above, is of an oval and as such individuals can shrink their projected body width against the opening by twisting their shoulders (Imanishi et al., 2015). Hence, for higher densities this behaviour should be considered as it implies that in such cases more persons would be able to fit in the opening and therefore the results from this study would reflect the most conservative approach, as the boundary layers would, therefore, be reduced when a higher density occurs.

Additionally, as mentioned in the literature review, research on the impact of several variables including width of a doorway or opening has been performed in the Netherlands (Daamen and Hoogendoorn, 2010). Findings from this study provide insight on how flows can vary due to the change in door width amongst the other variables. Nevertheless, this study only considered the total width of the opening without considering the impact of effective width of the archway which could, to some extent, provide some explanation on why the capacity per meter of opening did not always increase when the opening size was increased. This was especially true for doors were the opening of 270 cm was used in which the capacity, in Persons/m/s, was lower than for the opening of 220 cm. However, it is possible that for the opening of 270 cm the dimensions of the boundary layers were considerably larger (i.e. perhaps no extra lane was formed) and hence the effective width might be nearly the same for both openings, which in turn would mean that the capacity per meter of effective width of both openings is much more similar than what is portrayed in the results when the possible fluctuation of the boundary layer due to the formation of lanes is not considered.

4.3.2. Experimental boundary layer findings and the SFPE handbook

In relation to the dimensions for the boundary layer suggested in the SFPE handbook, the results from the experiments show much variation and thus further experiments should be performed. Nevertheless, values obtained ranged between 9 to 19 cm for the width of the boundary layer. Therefore, the 15 cm (6 in) value suggested in the SFPE handbook is reasonably in line with the obtained results. It is important to point out that the contemplated scenarios only considered low-density conditions, which is possibly the most conservative

case since, as previously mentioned, for higher densities it is possible for people to rotate their shoulders or torso reducing their projected width, (Imanishi et al., 2015) consequently allowing more pedestrians to walk through the opening at the same time when density increases. However, this value is not conservative in itself and should be revised as the present case does not consider the possible further reduction in width due to the presence of a door (Gwynne et al., 2009).

These set of experiments, however, only considered low density flows and therefore it is out of the scope of this thesis to ascertain whether the dimensions of the boundary layer used in the SFPE handbook of fire safety engineering are sufficient without further experimental tests. Therefore, additional experimental studies are of interest to investigate the dimensions of the boundary layer when considering higher density flows and scenarios that show the relationship lane formations (Hoogendoorn and Daamen, 2005; Schadschneider and Seyfried, 2009; Seyfried et al., 2009), shoulder rotation at openings (Imanishi et al., 2015) and flows. Thus, it is possible that higher densities will yield a reduction on the dimensions of the boundary layer (i.e. increased effective width) and perhaps in higher density flows the boundary layer can become less variable in relation to the width of the opening and, possibly, become nearly fixed due to high densities.

4.4. Group vs individual experiments

As previously mentioned, both individual and group experiments allowed to observe several specific behaviours regarding flow through openings with unimpeded or nearly unimpeded walking speed. However, comparing the results from individual and group experiments is fundamental as it also sheds some additional light on the differences and similarities between individual and group pedestrian dynamics regarding openings.

4.4.1. Effect of single vs multiple pedestrians

When analysing the results and comparing the dimensions of the boundary layer for single vs group experiments, it became evident that the opening of 1.05 m is the one that has the largest difference. This is due to the fact that, in individual experiments, only one person walked through the opening and, as mentioned previously, this led to the individuals on aggregate to tend to walk through the centre of the opening and therefore having the largest boundary layer for individual experiments. However, group experiments for the opening of 1.05 m showed the appearance of two lanes instead of a single lane, thus substantially reducing the size of the boundary layer in comparison to single pedestrian experiments. Hence, it is possible to ascertain that for the same opening the boundary layer was directly influenced by the group behaviour in which a creation of a second lane occurred.

Nevertheless, when considering the results from the openings of 0.75 and 0.85 m of width it becomes apparent that there are some similitudes and some differences regarding the openings when group and individual experiments were carried out and only a single lane was observed. As a starting point, it was relatively clear that the dimensions of the boundary layer for the opening of 0.75 m were very similar in both cases converging towards the value of 0.15 m which is the same value obtained suggested by the SFPE handbook. The opening of 0.85 m, on the other hand, showed a more evident variation between individual and group experimental results, having boundary layers that oscillated far more, this is due to the additional space and therefore it is observed that a tendency to have an increment on the boundary layer is observed in both individual and group experiments for this opening. Considering that the densities for the group experiments were very low, it is possible that the results of these experiments illustrate in a very clear way the change on the boundary layer dimensions when unimpeded speed is present when the opening restricts the flow to a single lane. This is evident as, even if there is some variation from individual to group experiment results, the average values for the dimensions of the boundary layer when only one lane was present were very close for both individual and group trials.

5. Conclusions

This experimental study of effective width through opening using the Kinect v2 allowed to demonstrate that the device can be used with sufficient accuracy for frontal pedestrian tracking, considering the dynamic characteristic of the measurements. This was demonstrated by a low standard error of the mean value. Additionally, since the major source of error is random in nature, when more measurements are taken a smaller error will be expected as a pattern or tendency will develop and all other measurements outside the observed average behaviour become mere deviations from the observed tendency.

The single use of Kinect v2, proved to have some limitations for this type of study. As a line-of-sight device, it becomes necessary to avoid occlusion of joints of the pedestrians that are tracked. Nevertheless, per the nature of the study the device had to be placed on frontal position and thus some occlusion was bound to occur. Therefore, after performing the tests it became evident that for high density flows the use of only one device might not be sufficient to collect all the desired data. Hence, for further studies it would be ideal to use several devices, preferably one leaning towards each side of the opening and a third one overhead, thus allowing to triangulate the position of each individual. This would not only allow to collect more data but also increase the reliability and accuracy of the obtained results.

The results obtained from the experimental trials, regarding the individual tests, also allowed to corroborate the natural tendency individuals to lean towards one side when walking completely unimpeded. Hence, from a qualitative perspective, it was observed that individuals that came from countries in which the norm is to drive in the right side of the road naturally tended to lean towards the right, whilst individuals that came from countries in which the norm is to drive on the left side of the road naturally leaned to the left side.

Moreover, the results from the group tests showed an insight on the effective width on openings, especially regarding the dimensions of the boundary layer. In this case, the influence of the maximum number of lanes observed to flow on the opening became evident. Therefore, the results from this study suggest that there is a “lane effect” which directly affects the dimensions of the boundary layer in case of low density conditions. This, in turn, indicates that there are maximum and minimum values of boundary layer dimensions that would be observed when slowly increasing the opening size until the limit in which an additional lane can be observed. Hence, these observations indicate that the boundary layer is nor static for low-density flows and consequently, for openings, it should be treated dynamically. However, the effect of density was not studied in this research and its influence, especially considering higher density flows, has not been properly assessed. Therefore, further studies on the effective width and the possible effects of the observed maximum number of lanes on a specific opening size and at different density conditions and population

types (i.e not exclusively healthy young students) must be performed. This would allow to assess the true nature of the boundary layer through openings considering additional relevant variables that, due to time and experimental setup constraints, could not be considered in this study.

Finally, this study attempted to assess the results from the measurements to validate the suggested input data values for the boundary layer provided by the SFPE Handbook of Fire Protection Engineering. In this case, the obtained values from the experimental study were very close to the values presented by the SFPE handbook. However, the results from these low-density flow experiments show that the value of 15 cm used in the SFPE handbook would not be conservative especially when considering the results from the opening of 0.85 m in which the dimensions of the boundary layer increased to a minimum of 19 cm; this results in a reduction of an additional 8 cm on the effective width in comparison to the SFPE handbook. Nevertheless the values suggested by the SFPE are in line with the experimental findings for openings in low-density flow conditions, however, this does not account for the presence of doors.

Nonetheless, further studies on effective width through openings, considering the impact of doors, lanes and higher densities should be considered before ascertaining that the values suggested by the hydraulic method in the SFPE handbook are appropriate for all scenarios.

6. References

British Standards Institution (Ed.), 2008. Code of practice for fire safety in the design, management and use of buildings BS9999, British standards publication. BSI, London.

Brščić, D., Kanda, T., Ikeda, T., Miyashita, T., 2013. Person Tracking in Large Public Spaces Using 3-D Range Sensors. IEEE Trans. Hum.-Mach. Syst. 43, 522–534. https://doi.org/10.1109/THMS.2013.2283945

Brščić, D., Zanlungo, F., Kanda, T., 2014. Density and Velocity Patterns during One Year of Pedestrian Tracking. Transp. Res. Procedia 2, 77–86. https://doi.org/10.1016/j.trpro.2014.09.011

Bukáček, M., Hrabák, P., Krbálek, M., 2014. Experimental Study of Phase Transition in Pedestrian Flow. Transp. Res. Procedia 2, 105–113. https://doi.org/10.1016/j.trpro.2014.09.014

Capecci, M., Ceravolo, M.G., Ferracuti, F., Iarlori, S., Longhi, S., Romeo, L., Russi, S.N., Verdini, F., 2016. Accuracy evaluation of the Kinect v2 sensor during dynamic movements in a rehabilitation scenario. IEEE, pp. 5409–5412. https://doi.org/10.1109/EMBC.2016.7591950

CNET, 2018. GoPro Hero4 Black Specs [WWW Document]. CNET. URL https://www.cnet.com/products/gopro-hero4-black/specs/ (accessed 4.26.18).

Corbetta, A., 2016. Multiscale crowd dynamics: physical analysis, modelling and applications. Technische Universiteit Eindhoven, Eindhoven.

Corbetta, A., Bruno, L., Muntean, A., Toschi, F., 2014. High Statistics Measurements of Pedestrian Dynamics. Transp. Res. Procedia 2, 96–104. https://doi.org/10.1016/j.trpro.2014.09.013

Corti, A., Giancola, S., Mainetti, G., Sala, R., 2016. A metrological characterization of the Kinect V2 time-of-flight camera. Robot. Auton. Syst. 75, 584–594. https://doi.org/10.1016/j.robot.2015.09.024

Daamen, W., Hoogendoorn, S., 2010. Capacity of doors during evacuation conditions. Procedia Eng. 3, 53–66. https://doi.org/10.1016/j.proeng.2010.07.007

Frantzich, H., Nilsson, D., Eriksson, O., 2007. Utvärdering och validering av utrymningsprogram [Evaluation and validation of evacuation programs] (No. 3143). Lund: Brandteknik och rikshantering, LTH, Lund.

Fridholm, V., Rasmusson, K., 2017. Test av ny mätmetod för att mäta personflöde genom öppningar [Test of new method to measure personal flow through door openings]. Division of Fire Safety Engineering Lund University, Lund.

Fruin, J.J., Strakosch, G.R., 1987. Pedestrian Planning and Design. Elevator World.

Gissi, E., Ronchi, E., Purser, D.A., 2017. Transparency vs magic numbers: The development of stair design requirements in the Italian Fire Safety Code. Fire Saf. J. 91, 882–891.

Great Britain, Office of the Deputy Prime Minister, 2013. The Building Regulations 2010: fire safety : approved document B. Vol. 2, Vol. 2,. NBS (RIBA Enterprises), London.

Greenwood, D., Sharma, S., Johansson, A., 2014. Gap Analysis of Current Industrial Challenges and the State-of-the-Art in Pedestrian Modelling. Transp. Res. Procedia 2, 219–227. https://doi.org/10.1016/j.trpro.2014.09.040

Gwynne, S.M.V., Kuligowski, E.D., Kratchman, J., Milke, J.A., 2009. Questioning the linear relationship between doorway width and achievable flow rate. Fire Saf. J. 44, 80–87. https://doi.org/10.1016/j.firesaf.2008.03.010

Gwynne, S.M.V., Rosenbaum, E.R., 2016. Employing the Hydraulic Model in Assessing Emergency Movement, in: Hurley, M.J., Gottuk, D., Hall, J.R., Harada, K., Kuligowski, E., Puchovsky, M., Torero, J., Watts, J.M., Wieczorek, C. (Eds.), SFPE Handbook of Fire Protection Engineering. Springer New York, New York, NY, pp. 2115–2151. https://doi.org/10.1007/978-1-4939-2565-0_59

Habicht, A.T., Braaksma, J.P., 1984. Effective Width of Pedestrian Corridors. J. Transp. Eng. 110, 80–93. https://doi.org/10.1061/(ASCE)0733-947X(1984)110:1(80)

Haghani, M., Sarvi, M., 2018. Crowd behaviour and motion: Empirical methods. Transp. Res. Part B Methodol. 107, 253–294. https://doi.org/10.1016/j.trb.2017.06.017

Hoogendoorn, S.P., Daamen, W., 2005. Pedestrian Behavior at Bottlenecks. Transp. Sci. 39, 147–159. https://doi.org/10.1287/trsc.1040.0102

Hurley, M.J., Gottuk, D., Hall, J.R., Harada, K., Kuligowski, E., Puchovsky, M., Torero, J., Watts, J.M., Wieczorek, C. (Eds.), 2016. SFPE Handbook of Fire Protection Engineering. Springer New York, New York, NY. https://doi.org/10.1007/978-1-4939-2565-0

Imanishi, M., Sano, T., Hagiwara, I., Nunota, K., 2015. EFFECTS OF HUMAN BODY ON PEDESTRIAN FLOW CHARACTERISTICS AT OPENINGS. J. Archit. Plan. Trans. AIJ 80, 1799–1806. https://doi.org/10.3130/aija.80.1799

Jo, A., Sano, T., Ikehata, Y., Ohmiya, Y., 2014. Analysis of Crowd Flow Capacity through a Door Connected to a Crowded Corridor. Transp. Res. Procedia 2, 10–18. https://doi.org/10.1016/j.trpro.2014.09.003

Jungong Han, Ling Shao, Dong Xu, Shotton, J., 2013. Enhanced Computer Vision With Microsoft Kinect Sensor: A Review. IEEE Trans. Cybern. 43, 1318–1334. https://doi.org/10.1109/TCYB.2013.2265378

Liao, W., Seyfried, A., Zhang, J., Boltes, M., Zheng, X., Zhao, Y., 2014. Experimental Study on Pedestrian Flow through Wide Bottleneck. Transp. Res. Procedia 2, 26–33. https://doi.org/10.1016/j.trpro.2014.09.005

Microsoft Developer Network (MSDN), 2018a. Coordinate mapping [WWW Document]. Microsoft Dev. Netw. MSDN. URL https://msdn.microsoft.com/en-us/library/dn785530.aspx# (accessed 3.5.18).

Microsoft Developer Network (MSDN), 2018b. Features [WWW Document]. Microsoft Dev. Netw. MSDN. URL https://msdn.microsoft.com/en-us/library/dn782025.aspx (accessed 3.5.18).

Microsoft Developer Network (MSDN), 2018c. JointType Enumeration [WWW Document]. Microsoft Dev. Netw. MSDN. URL https://msdn.microsoft.com/en-us/library/microsoft.kinect.jointtype.aspx (accessed 2.23.18).

Microsoft Developer Network (MSDN), 2014. The Kinect for Windows v2 sensor and free SDK 2.0 public preview are here – Kinect for Windows Product Blog [WWW Document]. Kinect Window Prod. Blog. URL https://blogs.msdn.microsoft.com/kinectforwindows/2014/07/15/the-kinect-for-windows-v2-sensor-and-free-sdk-2-0-public-preview-are-here/ (accessed 4.26.18).

National Fire Protection Association, 2017. NFPA 101: life safety code 2017. NATL FIRE PROTECTION ASSO, S.l.

Pauls, J.L., 1987. Calculating evacuation times for tall buildings. Fire Saf. J. 12, 213–236. https://doi.org/10.1016/0379-7112(87)90007-5

Pauls, J.L., 1984. The movement of people in buildings and design solutions for means of egress. Fire Technol. 20, 27–47. https://doi.org/10.1007/BF02390046

Pauls, J.L., 1982. Effective-Width Model for Crowd Evacuation Flow on Stairs, in: Proceedings of Sixth International Fire Protection Seminar. Presented at the Sixth International Fire Protection Seminar, Karlsruche, Germany, pp. 295–306.

Pauls, J.L., Fruin, J.J., Zupan, J.M., 2007. Minimum Stair Width for Evacuation, Overtaking Movement and Counterflow — Technical Bases and Suggestions for the Past, Present and Future, in: Waldau, N., Gattermann, P., Knoflacher, H., Schreckenberg, M. (Eds.), Pedestrian and Evacuation Dynamics 2005. Springer Berlin Heidelberg, Berlin, Heidelberg, pp. 57–69. https://doi.org/10.1007/978-3-540-47064-9_5

Pettersson, F., Lundh, K., 2017. Microsoft Kinect för utrymning i smarta byggnader. Division of Fire Safety Engineering Lund University, Lund.

Predtechenskiĭ, V.M., Milinskii, A.I., 1978. Planning for foot traffic flow in buildings. Amerind, New Delhi.

Ronchi, E., Nilsson, D., 2012. Evaluation of an Evacuation and Fire Model (No. 7037). Department of Fire Safety Engineering and Systems Safety Lund University, Lund.

Ronchi, E., Reneke, P.A., Peacock, R.D., 2014. A Method for the Analysis of Behavioural Uncertainty in Evacuation Modelling. Fire Technol. 50, 1545–1571. https://doi.org/10.1007/s10694-013-0352-7

Schadschneider, A., Seyfried, A., 2009. Empirical Results for Pedestrian Dynamics and their Implications for Cellular Automata Models, in: Pedestrian Behavior. pp. 27–43. https://doi.org/10.1108/9781848557512-002

Seer, S., Brändle, N., Ratti, C., 2014. Kinects and human kinetics: A new approach for studying pedestrian behavior. Transp. Res. Part C Emerg. Technol. 48, 212–228. https://doi.org/10.1016/j.trc.2014.08.012

Seyfried, A., Passon, O., Steffen, B., Boltes, M., Rupprecht, T., Klingsch, W., 2009. New Insights into Pedestrian Flow Through Bottlenecks. Transp. Sci. 43, 395–406. https://doi.org/10.1287/trsc.1090.0263

Seyfried, A., Schadschneider, A., 2010. Empirical Results for Pedestrian Dynamics at Bottlenecks, in: Wyrzykowski, R., Dongarra, J., Karczewski, K., Wasniewski, J. (Eds.), Parallel Processing and Applied Mathematics. Springer Berlin Heidelberg, Berlin, Heidelberg, pp. 575–584. https://doi.org/10.1007/978-3-642-14403-5_62

Seyfried, A., Steffen, B., Klingsch, W., Boltes, M., 2005. The fundamental diagram of pedestrian movement revisited. J. Stat. Mech. Theory Exp. 2005, P10002–P10002. https://doi.org/10.1088/1742-5468/2005/10/P10002

Swedish National Board of Housing, Building and Planning (Boverket), 2016. Boverket's building regulations – mandatory provisions and general recommendations, BBR. BFS 2011:6 with amendments up to BFS 2016:6.

Thornburg, D.W., Henry, J.R., 2009. Significant changes to the international building code, 2009 ed. ed. Delmar Cengage Learning, Australia ; United States.

Wang, Q., Kurillo, G., Ofli, F., Bajcsy, R., 2015. Evaluation of Pose Tracking Accuracy in the First and Second Generations of Microsoft Kinect. IEEE, pp. 380–389. https://doi.org/10.1109/ICHI.2015.54

World Standards, 2018. List of left- & right-driving countries [WWW Document]. World Stand. URL https://www.worldstandards.eu/cars/list-of-left-driving-countries/ (accessed 4.13.18).

Yang, L., Zhang, L., Dong, H., Alelaiwi, A., Saddik, A.E., 2015. Evaluating and Improving the Depth Accuracy of Kinect for Windows v2. IEEE Sens. J. 15, 4275–4285. https://doi.org/10.1109/JSEN.2015.2416651

7. Appendices

Appendix 1: Individual Experiments: Opening of 0.75 m

Pedestrian 1

Pedestrian 1 position and distance to edge of body joints for left and right arm relative to the centre of the opening (0.75m)

Relative position with centre of opening: Left Shoulder (m)

X	Y	Distance to Edge
-0.13	1.21	0.245
-0.14	1.2	0.235
-0.16	1.2	0.215
-0.16	1.21	0.215
-0.12	1.17	0.255

Relative position with centre of opening: Right Shoulder (m)

X	Y	Distance to Edge
0.14	1.2	0.235
0.16	1.23	0.215
0.12	1.19	0.255
0.11	1.21	0.265
0.13	1.17	0.245

Relative position with centre of opening: Left Elbow (m)

X	Y	Distance to Edge
-0.2	0.96	0.175
-0.23	1	0.145
-0.23	0.96	0.145
-0.25	0.98	0.125
-0.22	0.95	0.155

Relative position with centre of opening: Right Elbow (m)

X	Y	Distance to Edge
0.22	0.93	0.155
0.22	0.96	0.155
0.21	0.94	0.165
0.2	0.93	0.175
0.19	0.96	0.185

Relative position with centre of opening: Left Wrist (m)

X	Y	Distance to Edge
-0.24	0.76	0.135
-0.28	0.77	0.095
-0.29	0.76	0.085
-0.3	0.77	0.075
-0.29	0.75	0.085

Relative position with centre of opening: Right Wrist (m)

X	Y	Distance to Edge
0.22	0.74	0.155
0.22	0.7	0.155
0.21	0.75	0.165
0.21	0.73	0.165
0.24	0.7	0.135

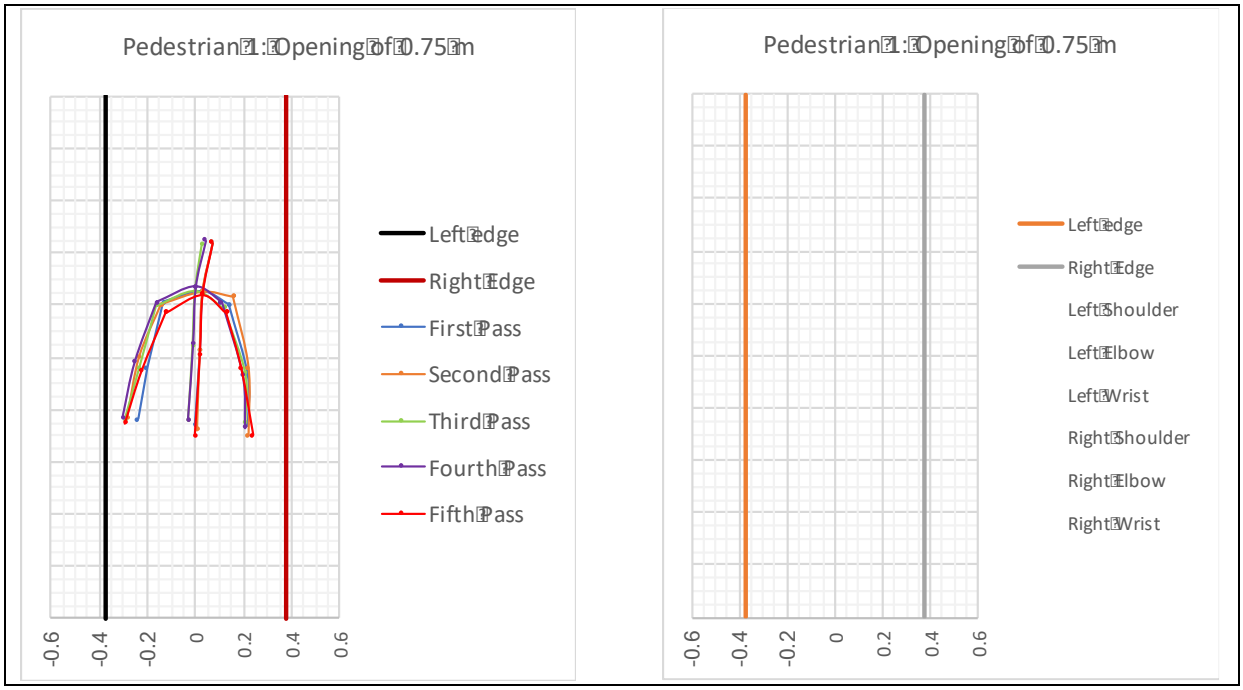

Pedestrian 2

Pedestrian 2 position and distance to edge of body joints for left and right arm relative to the centre of the opening (0.75m)

Relative position with centre of opening: Left Shoulder (m)

X	Y	Distance to Edge
-0.2	1.35	0.175
-0.19	1.35	0.185
-0.2	1.35	0.175
-0.17	1.37	0.205
-0.17	1.34	0.205

Relative position with centre of opening: Right Shoulder (m)

X	Y	Distance to Edge
0.14	1.32	0.235
0.13	1.35	0.245
0.14	1.33	0.235
0.16	1.34	0.215
0.16	1.32	0.215

Relative position with centre of opening: Left Elbow (m)

X	Y	Distance to Edge
-0.25	1.07	0.125
-0.23	1.11	0.145
-0.23	1.08	0.145
-0.24	1.09	0.135
-0.23	1.07	0.145

Relative position with centre of opening: Right Elbow (m)

X	Y	Distance to Edge
0.18	1.09	0.195
0.18	1.09	0.195
0.18	1.08	0.195
0.18	1.08	0.195
0.2	1.06	0.175

Relative position with centre of opening: Left Wrist (m)

X	Y	Distance to Edge
-0.27	0.85	0.105
-0.24	0.86	0.135
-0.25	0.83	0.125
-0.25	0.86	0.125
-0.25	0.83	0.125

Relative position with centre of opening: Right Wrist (m)

X	Y	Distance to Edge
0.18	0.84	0.195
0.18	0.85	0.195
0.19	0.85	0.185
0.16	0.85	0.215
0.22	0.85	0.155

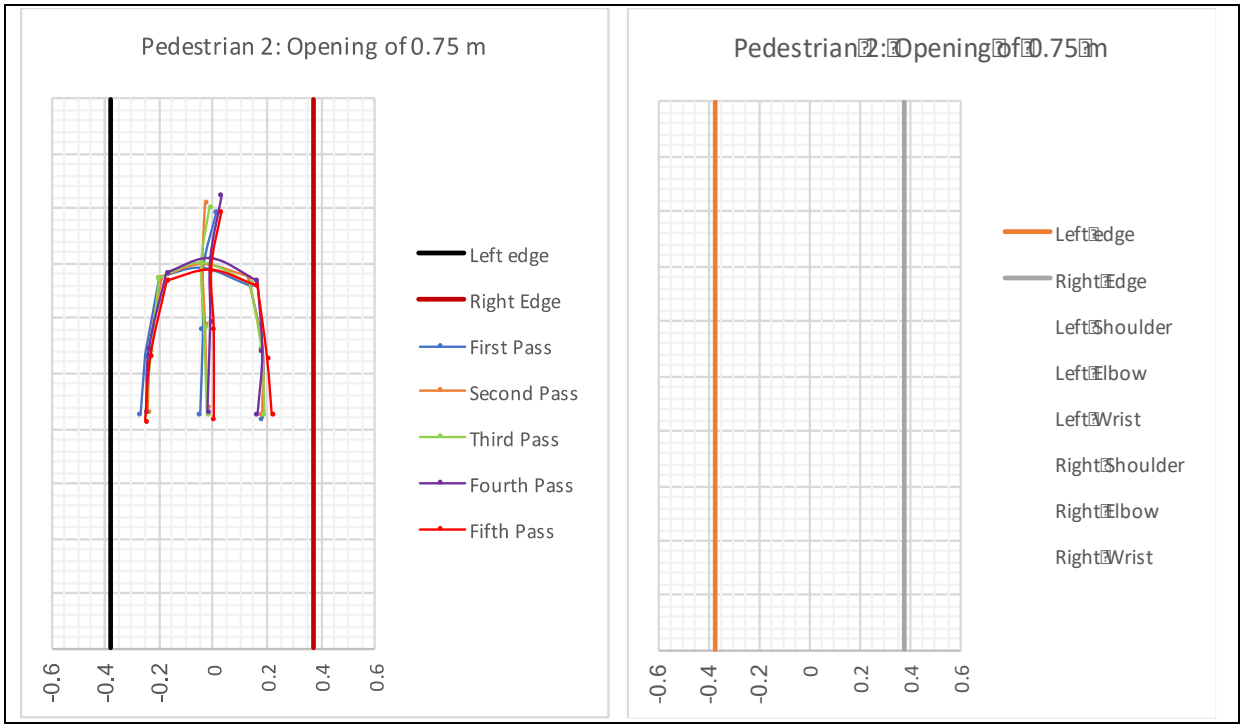

Pedestrian 3

Pedestrian 3 position and distance to edge of body joints for left and right arm relative to the centre of the opening (0.75m)

Relative position with centre of opening: Left Shoulder (m)

X	Y	Distance to Edge
-0.17	1.24	0.205
-0.15	1.23	0.225
-0.18	1.24	0.195
-0.18	1.24	0.195
-0.2	1.21	0.175

Relative position with centre of opening: Right Shoulder (m)

X	Y	Distance to Edge
0.15	1.22	0.225
0.17	1.21	0.205
0.15	1.22	0.225
0.14	1.21	0.235
0.12	1.18	0.255

Relative position with centre of opening: Left Elbow (m)

X	Y	Distance to Edge
-0.24	0.98	0.135
-0.24	0.97	0.135
-0.25	0.98	0.125
-0.25	0.97	0.125
-0.27	0.95	0.105

Relative position with centre of opening: Right Elbow (m)

X	Y	Distance to Edge
0.23	0.96	0.145
0.23	0.97	0.145
0.23	0.96	0.145
0.21	0.96	0.165
0.2	0.93	0.175

Relative position with centre of opening: Left Wrist (m)

X	Y	Distance to Edge
-0.24	0.78	0.135
-0.32	0.77	0.055
-0.27	0.76	0.105
-0.27	0.77	0.105
-0.27	0.73	0.105

Relative position with centre of opening: Right Wrist (m)

X	Y	Distance to Edge
0.26	0.74	0.115
0.27	0.75	0.105
0.28	0.76	0.095
0.26	0.76	0.115
0.24	0.71	0.135

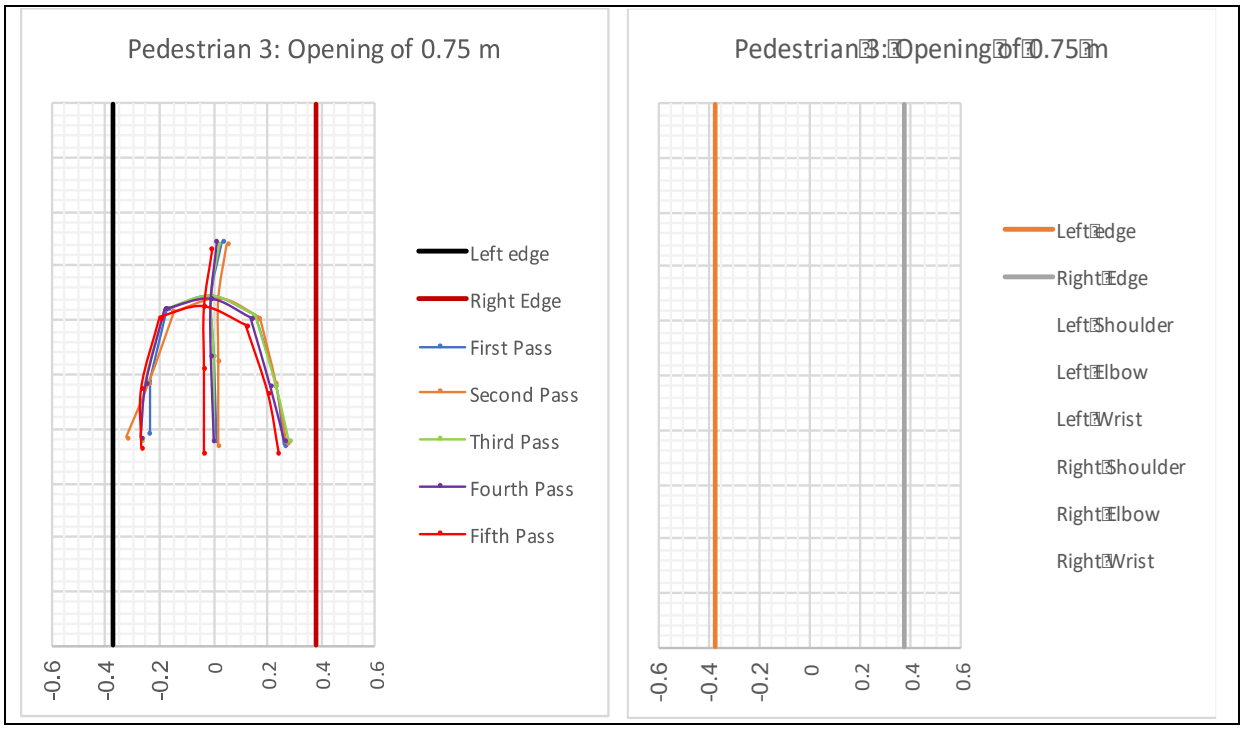

Pedestrian 4

Pedestrian 4 position and distance to edge of body joints for left and right arm relative to the centre of the opening (0.75m)

Relative position with centre of opening: Left Shoulder (m)		
X	Y	Distance to Edge
-0.15	1.31	0.225
-0.19	1.29	0.185
-0.16	1.25	0.215
-0.16	1.3	0.215
-0.14	1.26	0.235

Relative position with centre of opening: Right Shoulder (m)		
X	Y	Distance to Edge
0.19	1.28	0.185
0.15	1.27	0.225
0.17	1.24	0.205
0.18	1.29	0.195
0.19	1.26	0.185

Relative position with centre of opening: Left Elbow (m)		
X	Y	Distance to Edge
-0.22	1.04	0.155
-0.25	1.04	0.125
-0.24	1.03	0.135
-0.22	1.02	0.155
-0.22	1.01	0.155

Relative position with centre of opening: Right Elbow (m)		
X	Y	Distance to Edge
0.25	1.05	0.125
0.24	1.02	0.135
0.24	1.02	0.135
0.25	1.02	0.125
0.27	1	0.105

Relative position with centre of opening: Left Wrist (m)		
X	Y	Distance to Edge
-0.25	0.83	0.125
-0.24	0.84	0.135
-0.22	0.85	0.155
-0.22	0.8	0.155
-0.2	0.85	0.175

Relative position with centre of opening: Right Wrist (m)		
X	Y	Distance to Edge
0.24	0.81	0.135
0.34	0.87	0.035
0.24	0.86	0.135
0.26	0.8	0.115
0.26	0.78	0.115

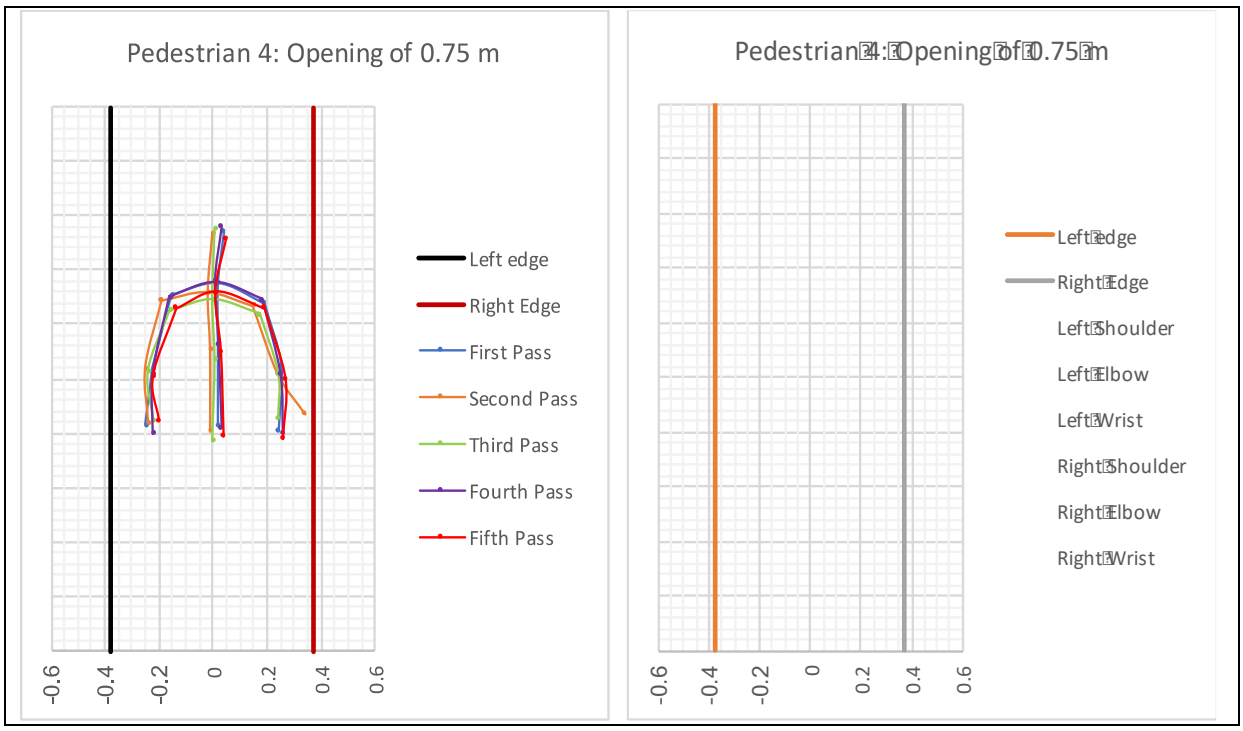

Pedestrian 5

Pedestrian 5 position and distance to edge of body joints for left and right arm relative to the centre of the opening (0.75m)

Relative position with centre of opening: Left Shoulder (m)		
X	Y	Distance to Edge
-0.12	1.26	0.255
-0.07	1.23	0.305
-0.05	1.23	0.325
-0.1	1.24	0.275
-0.08	1.26	0.295

Relative position with centre of opening: Right Shoulder (m)		
X	Y	Distance to Edge
0.18	1.24	0.195
0.22	1.22	0.155
0.22	1.22	0.155
0.19	1.24	0.185
0.23	1.26	0.145

Relative position with centre of opening: Left Elbow (m)		
X	Y	Distance to Edge
-0.17	0.99	0.205
-0.17	0.98	0.205
-0.13	0.96	0.245
-0.16	0.97	0.215
-0.15	0.99	0.225

Relative position with centre of opening: Right Elbow (m)		
X	Y	Distance to Edge
0.21	0.99	0.165
0.26	0.95	0.115
0.28	0.94	0.095
0.3	1.01	0.075
0.25	0.97	0.125

Relative position with centre of opening: Left Wrist (m)		
X	Y	Distance to Edge
-0.19	0.76	0.185
-0.2	0.77	0.175
-0.17	0.75	0.205
-0.21	0.77	0.165
-0.18	0.76	0.195

Relative position with centre of opening: Right Wrist (m)		
X	Y	Distance to Edge
0.23	0.76	0.145
0.27	0.77	0.105
0.31	0.75	0.065
0.27	0.76	0.105
0.24	0.77	0.135

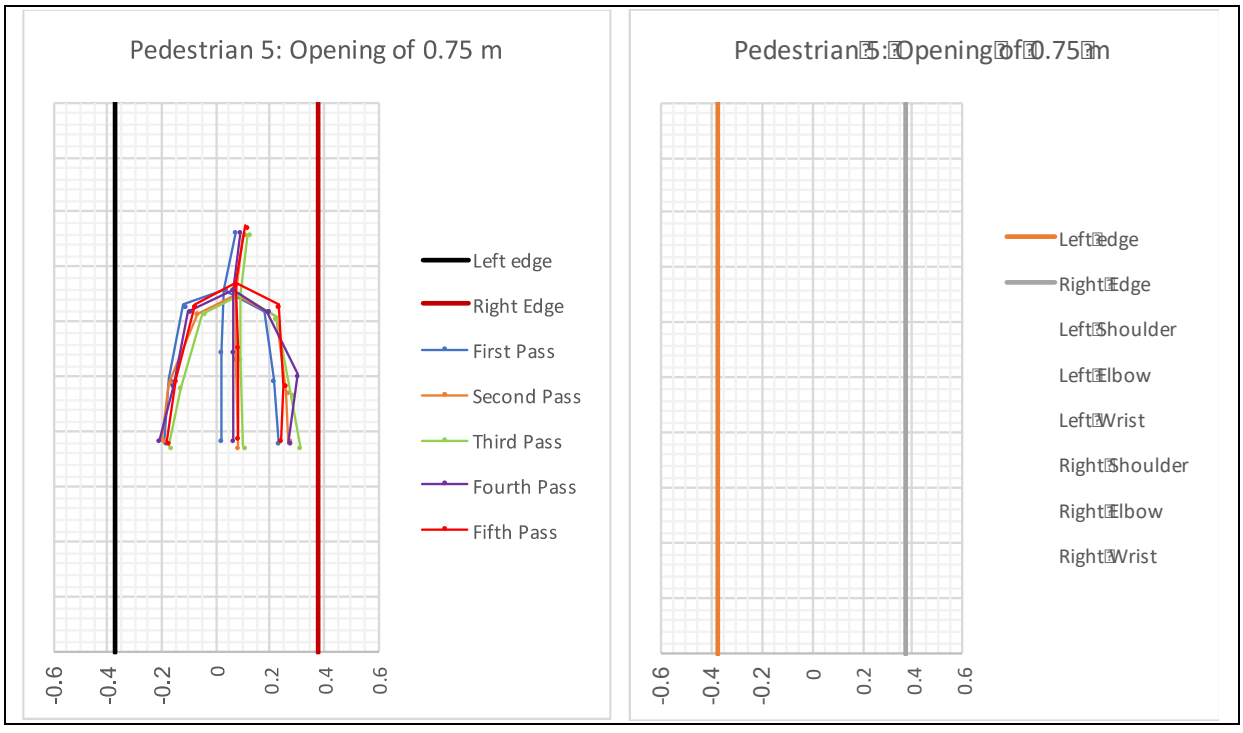

Appendix 2: Individual Experiments: Opening of 0.85 m

Pedestrian 1

Pedestrian 1 position and distance to edge of body joints for left and right arm relative to the centre of the opening (0.85m)

Relative position with centre of opening: Left Shoulder (m)

X	Y	Distance to Edge
-0.18	1.18	0.245
-0.15	1.17	0.275
-0.2	1.19	0.225
-0.19	1.21	0.235
-0.21	1.21	0.215

Relative position with centre of opening: Right Shoulder (m)

X	Y	Distance to Edge
0.1	1.18	0.325
0.12	1.17	0.305
0.08	1.19	0.345
0.1	1.22	0.325
0.06	1.21	0.365

Relative position with centre of opening: Left Elbow (m)

X	Y	Distance to Edge
-0.25	0.94	0.175
-0.24	1	0.185
-0.27	0.96	0.155
-0.25	0.97	0.175
-0.27	0.96	0.155

Relative position with centre of opening: Right Elbow (m)

X	Y	Distance to Edge
0.17	0.94	0.255
0.14	0.96	0.285
0.16	0.93	0.265
0.17	0.96	0.255
0.15	0.96	0.275

Relative position with centre of opening: Left Wrist (m)

X	Y	Distance to Edge
-0.3	0.73	0.125
-0.29	0.78	0.135
-0.33	0.77	0.095
-0.29	0.75	0.135
-0.32	0.76	0.105

Relative position with centre of opening: Right Wrist (m)

X	Y	Distance to Edge
0.2	0.77	0.225
0.15	0.75	0.275
0.19	0.72	0.235
0.2	0.75	0.225
0.2	0.76	0.225

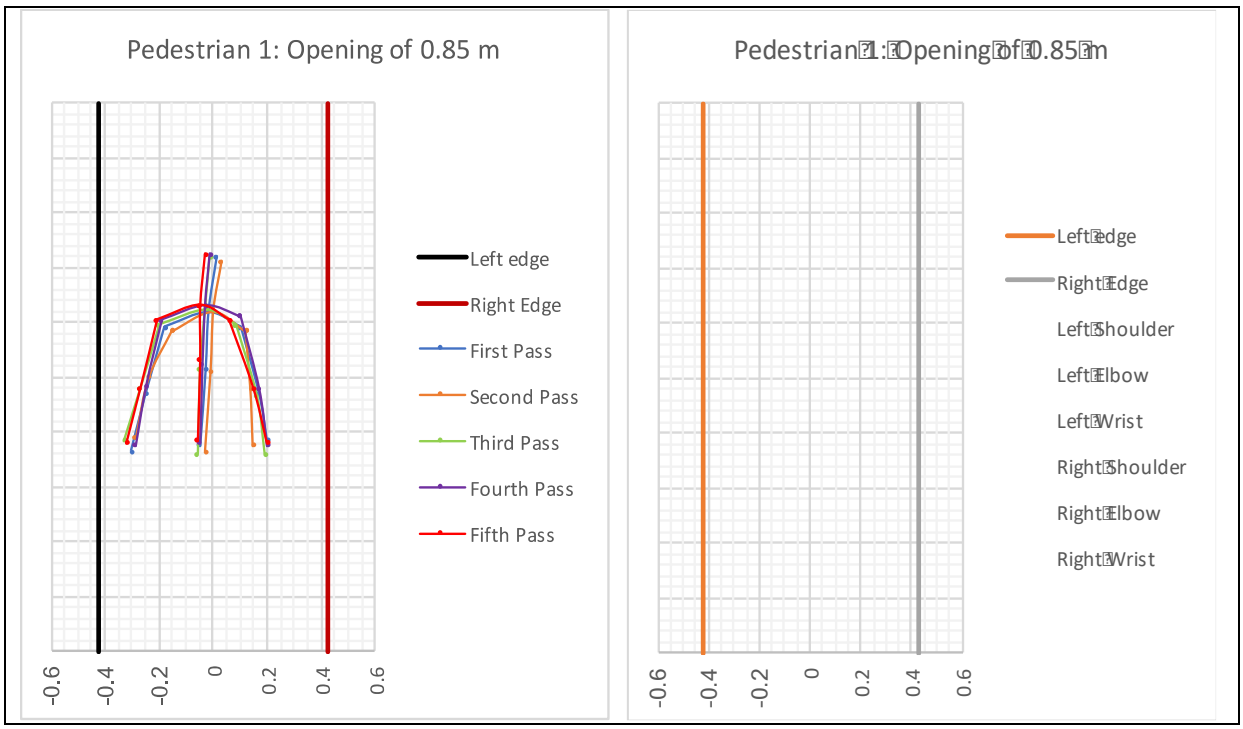

Pedestrian 2

Pedestrian 2 position and distance to edge of body joints for left and right arm relative to the centre of the opening (0.85m)

Relative position with centre of opening: Left Shoulder (m)

X	Y	Distance to Edge
-0.18	1.35	0.245
-0.2	1.35	0.225
-0.16	1.36	0.265
-0.16	1.37	0.265
-0.2	1.34	0.225

Relative position with centre of opening: Right Shoulder (m)

X	Y	Distance to Edge
0.15	1.32	0.275
0.14	1.34	0.285
0.17	1.31	0.255
0.17	1.32	0.255
0.13	1.32	0.295

Relative position with centre of opening: Left Elbow (m)

X	Y	Distance to Edge
-0.24	1.08	0.185
-0.25	1.08	0.175
-0.25	1.1	0.175
-0.2	1.11	0.225
-0.24	1.07	0.185

Relative position with centre of opening: Right Elbow (m)

X	Y	Distance to Edge
0.19	1.08	0.235
0.18	1.06	0.245
0.18	1.06	0.245
0.19	1.07	0.235
0.18	1.06	0.245

Relative position with centre of opening: Left Wrist (m)

X	Y	Distance to Edge
-0.28	0.86	0.145
-0.26	0.85	0.165
-0.26	0.87	0.165
-0.27	0.87	0.155
-0.26	0.83	0.165

Relative position with centre of opening: Right Wrist (m)

X	Y	Distance to Edge
0.18	0.89	0.245
0.18	0.85	0.245
0.18	0.83	0.245
0.17	0.84	0.255
0.19	0.89	0.235

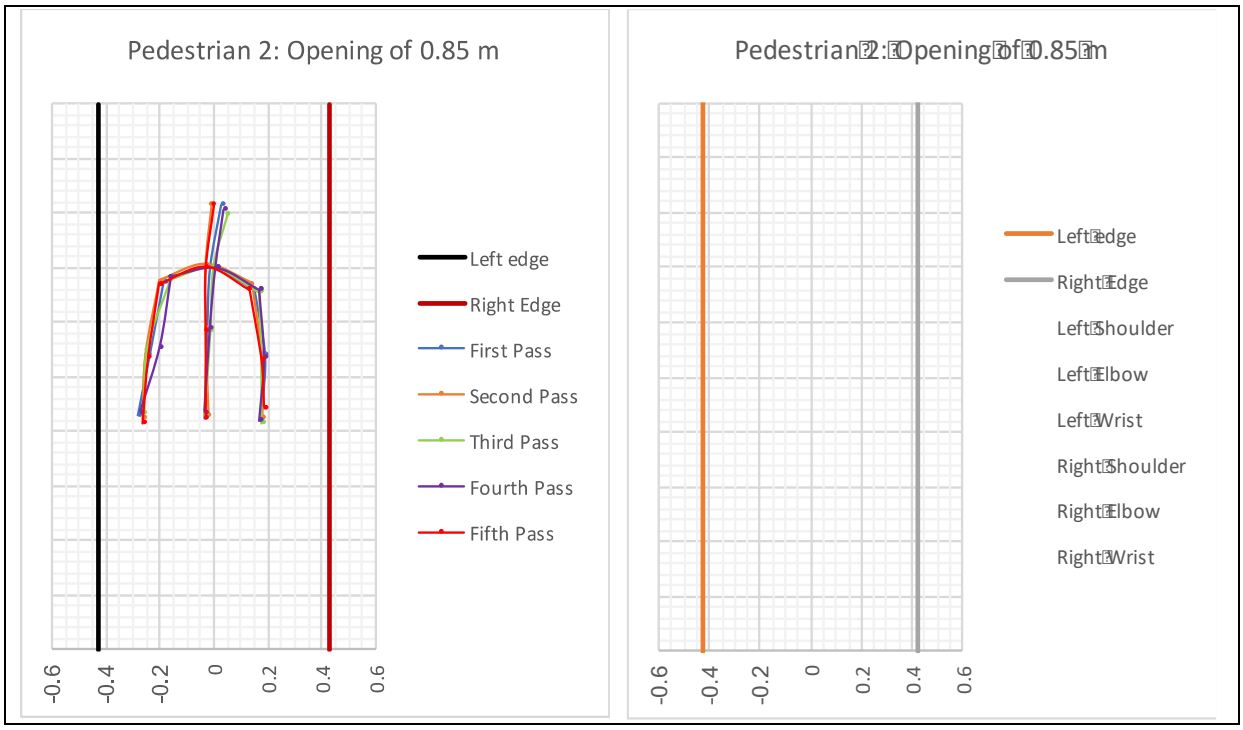

Pedestrian 3

Pedestrian 3 position and distance to edge of body joints for left and right arm relative to the centre of the opening (0.85m)

Relative position with centre of opening: Left Shoulder (m)

X	Y	Distance to Edge
-0.1	1.21	0.325
-0.17	1.24	0.255
-0.21	1.23	0.215
-0.2	1.2	0.225
-0.2	1.22	0.225

Relative position with centre of opening: Right Shoulder (m)

X	Y	Distance to Edge
0.23	1.19	0.195
0.15	1.22	0.275
0.11	1.22	0.315
0.13	1.19	0.295
0.12	1.21	0.305

Relative position with centre of opening: Left Elbow (m)

X	Y	Distance to Edge
-0.2	0.98	0.225
-0.26	0.97	0.165
-0.27	0.99	0.155
-0.26	0.94	0.165
-0.28	0.96	0.145

Relative position with centre of opening: Right Elbow (m)

X	Y	Distance to Edge
0.33	0.94	0.095
0.23	0.98	0.195
0.19	0.96	0.235
0.2	0.99	0.225
0.19	0.98	0.235

Relative position with centre of opening: Left Wrist (m)

X	Y	Distance to Edge
-0.23	0.76	0.195
-0.29	0.76	0.135
-0.29	0.79	0.135
-0.3	0.74	0.125
-0.33	0.77	0.095

Relative position with centre of opening: Right Wrist (m)

X	Y	Distance to Edge
0.32	0.69	0.105
0.28	0.77	0.145
0.22	0.75	0.205
0.26	0.8	0.165
0.25	0.79	0.175

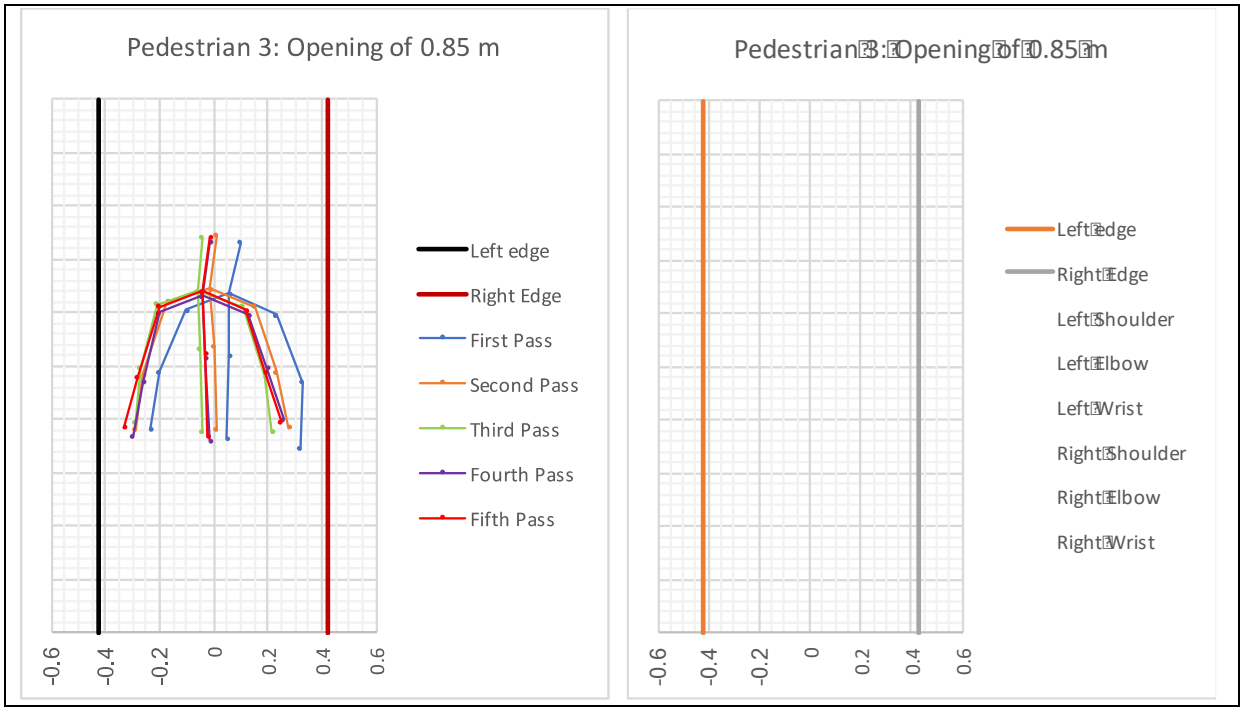

Pedestrian 4

Pedestrian 4 position and distance to edge of body joints for left and right arm relative to the centre of the opening (0.85m)					
Relative position with centre of opening: Left Shoulder (m)			Relative position with centre of opening: Right Shoulder (m)		
X	Y	Distance to Edge	X	Y	Distance to Edge
-0.14	1.3	0.285	0.19	1.27	0.235
-0.14	1.25	0.285	0.2	1.23	0.225
-0.1	1.29	0.325	0.23	1.28	0.195
-0.16	1.26	0.265	0.18	1.24	0.245
-0.11	1.3	0.315	0.22	1.26	0.205
Relative position with centre of opening: Left Elbow (m)			Relative position with centre of opening: Right Elbow (m)		
X	Y	Distance to Edge	X	Y	Distance to Edge
-0.22	1.03	0.205	0.25	1.05	0.175
-0.22	1.02	0.205	0.27	0.98	0.155
-0.16	1.03	0.265	0.29	1.02	0.135
-0.22	0.99	0.205	0.23	1.03	0.195
-0.18	1.04	0.245	0.29	1.01	0.135
Relative position with centre of opening: Left Wrist (m)			Relative position with centre of opening: Right Wrist (m)		
X	Y	Distance to Edge	X	Y	Distance to Edge
-0.26	0.82	0.165	0.26	0.84	0.165
-0.22	0.81	0.205	0.29	0.76	0.135
-0.2	0.83	0.225	0.3	0.8	0.125
-0.27	0.78	0.155	0.26	0.78	0.165
-0.21	0.81	0.215	0.27	0.77	0.155

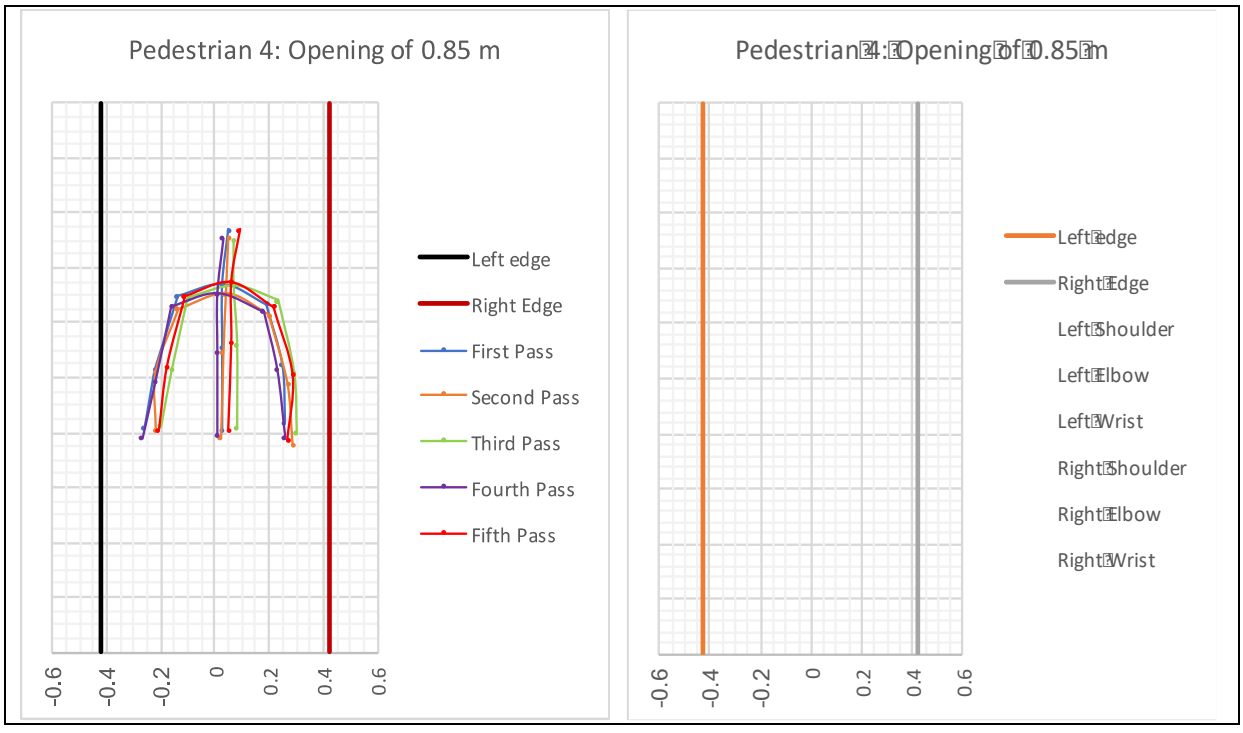

Pedestrian 5

Pedestrian 5 position and distance to edge of body joints for left and right arm relative to the centre of the opening (0.85m)

Relative position with centre of opening: Left Shoulder (m)

X	Y	Distance to Edge
-0.23	1.25	0.195
-0.19	1.26	0.235
-0.25	1.26	0.175
-0.25	1.24	0.175
-0.19	1.24	0.235

Relative position with centre of opening: Right Shoulder (m)

X	Y	Distance to Edge
0.06	1.24	0.365
0.1	1.25	0.325
0.04	1.25	0.385
0.04	1.22	0.385
0.11	1.23	0.315

Relative position with centre of opening: Left Elbow (m)

X	Y	Distance to Edge
-0.29	1	0.135
-0.25	1	0.175
-0.3	0.98	0.125
-0.31	0.98	0.115
-0.25	0.98	0.175

Relative position with centre of opening: Right Elbow (m)

X	Y	Distance to Edge
0.11	1	0.315
0.14	0.98	0.285
0.1	1.01	0.325
0.09	0.98	0.335
0.15	0.98	0.275

Relative position with centre of opening: Left Wrist (m)

X	Y	Distance to Edge
-0.31	0.78	0.115
-0.27	0.77	0.155
-0.31	0.76	0.115
-0.35	0.79	0.075
-0.28	0.77	0.145

Relative position with centre of opening: Right Wrist (m)

X	Y	Distance to Edge
0.14	0.8	0.285
0.16	0.76	0.265
0.11	0.77	0.315
0.13	0.81	0.295
0.17	0.8	0.255

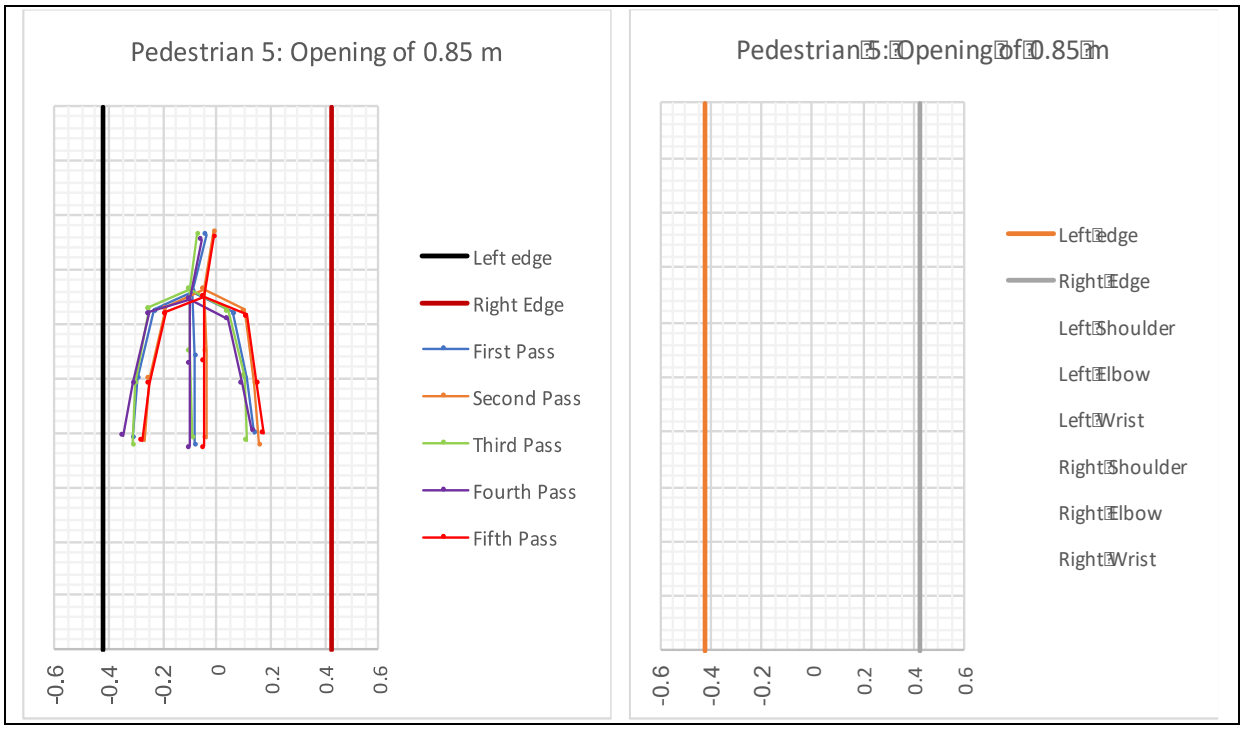

Appendix 3: Individual Experiments: Opening of 1.05 m

Pedestrian 1

Pedestrian 1 position and distance to edge of body joints for left and right arm relative to the centre of the opening (1.05 m)

Relative position with centre of opening: Left Shoulder (m)

X	Y	Distance to Edge
-0.16	1.2	0.365
-0.1	1.19	0.425
-0.15	1.21	0.375
-0.17	1.21	0.355
-0.06	1.21	0.465

Relative position with centre of opening: Right Shoulder (m)

X	Y	Distance to Edge
0.11	1.19	0.415
0.17	1.19	0.355
0.11	1.2	0.415
0.1	1.22	0.425
0.21	1.2	0.315

Relative position with centre of opening: Left Elbow (m)

X	Y	Distance to Edge
-0.23	0.96	0.295
-0.16	0.95	0.365
-0.23	0.97	0.295
-0.22	0.98	0.305
-0.12	0.95	0.405

Relative position with centre of opening: Right Elbow (m)

X	Y	Distance to Edge
0.18	0.95	0.345
0.26	0.96	0.265
0.19	0.94	0.335
0.19	0.97	0.335
0.3	0.96	0.225

Relative position with centre of opening: Left Wrist (m)

X	Y	Distance to Edge
-0.27	0.74	0.255
-0.21	0.74	0.315
-0.28	0.76	0.245
-0.25	0.77	0.275
-0.16	0.75	0.365

Relative position with centre of opening: Right Wrist (m)

X	Y	Distance to Edge
0.21	0.78	0.315
0.3	0.78	0.225
0.22	0.75	0.305
0.23	0.76	0.295
0.33	0.77	0.195

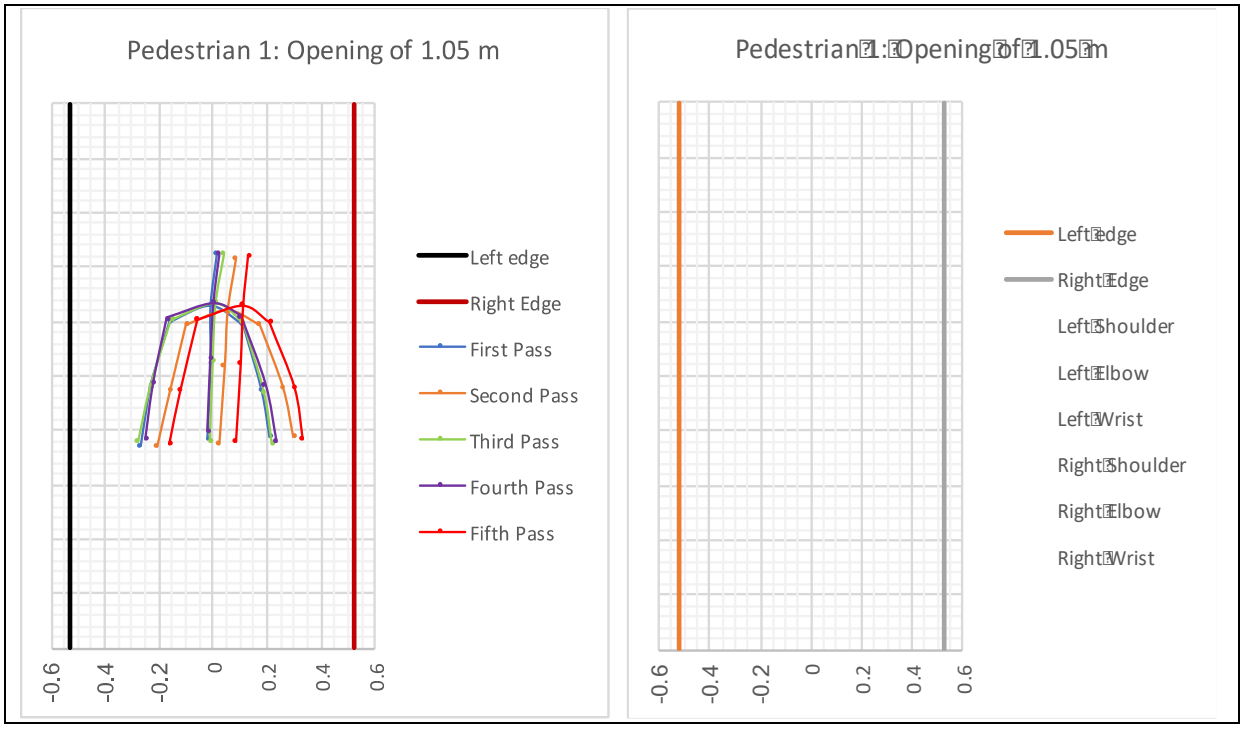

Pedestrian 2

Pedestrian 2 position and distance to edge of body joints for left and right arm relative to the centre of the opening (1.05 m)

Relative position with centre of opening: Left Shoulder (m)		
X	Y	Distance to Edge
-0.17	1.36	0.355
-0.21	1.38	0.315
-0.09	1.37	0.435
-0.19	1.34	0.335
-0.22	1.34	0.305

Relative position with centre of opening: Right Shoulder (m)		
X	Y	Distance to Edge
0.16	1.33	0.365
0.12	1.33	0.405
0.23	1.31	0.295
0.14	1.31	0.385
0.11	1.31	0.415

Relative position with centre of opening: Left Elbow (m)		
X	Y	Distance to Edge
-0.26	1.12	0.265
-0.29	1.11	0.235
-0.18	1.11	0.345
-0.26	1.08	0.265
-0.28	1.07	0.245

Relative position with centre of opening: Right Elbow (m)		
X	Y	Distance to Edge
0.22	1.06	0.305
0.15	1.09	0.375
0.25	1.07	0.275
0.17	1.06	0.355
0.15	1.06	0.375

Relative position with centre of opening: Left Wrist (m)		
X	Y	Distance to Edge
-0.33	0.92	0.195
-0.34	0.88	0.185
-0.22	0.88	0.305
-0.3	0.85	0.225
-0.32	0.84	0.205

Relative position with centre of opening: Right Wrist (m)		
X	Y	Distance to Edge
0.29	0.81	0.235
0.15	0.85	0.375
0.23	0.82	0.295
0.18	0.87	0.345
0.16	0.86	0.365

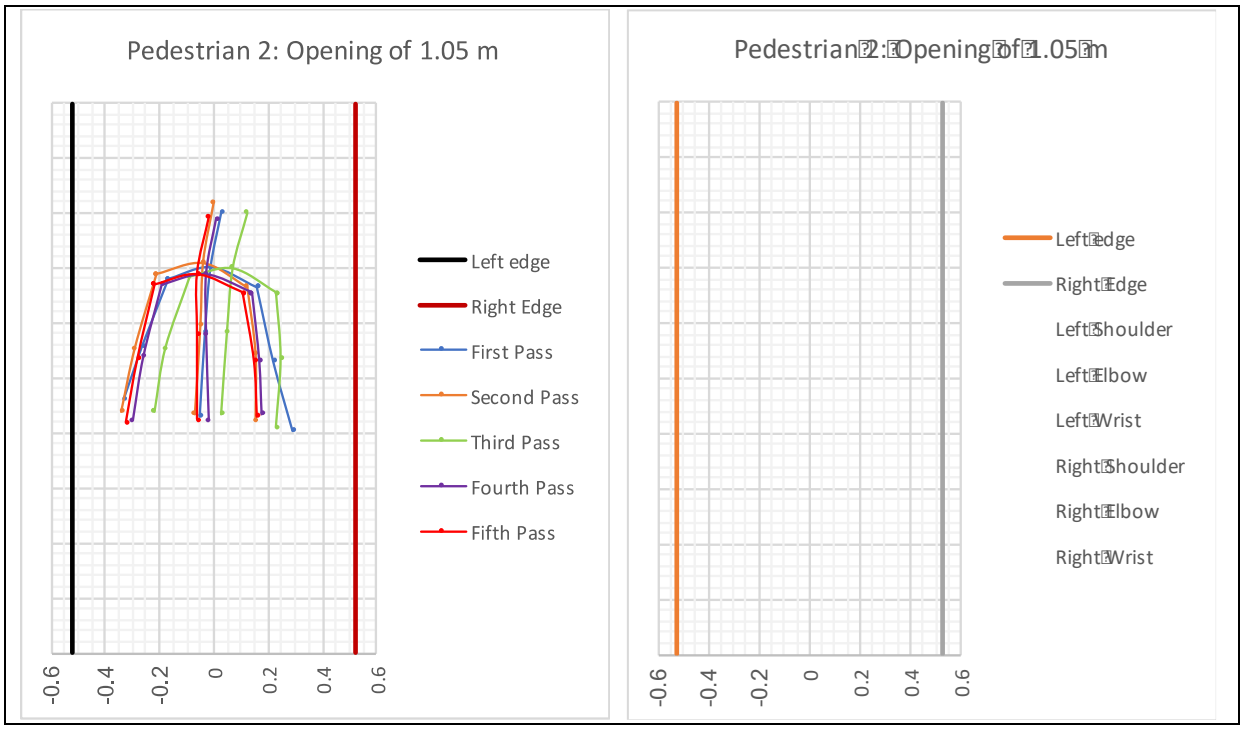

Pedestrian 3

Pedestrian 3 position and distance to edge of body joints for left and right arm relative to the centre of the opening (1.05 m)

Relative position with centre of opening: Left Shoulder (m)

X	Y	Distance to Edge
-0.22	1.24	0.305
-0.24	1.24	0.285
-0.22	1.23	0.305
-0.24	1.24	0.285
-0.23	1.23	0.295

Relative position with centre of opening: Right Shoulder (m)

X	Y	Distance to Edge
0.11	1.22	0.415
0.08	1.23	0.445
0.1	1.21	0.425
0.08	1.23	0.445
0.1	1.2	0.425

Relative position with centre of opening: Left Elbow (m)

X	Y	Distance to Edge
-0.3	0.96	0.225
-0.32	0.96	0.205
-0.3	0.97	0.225
-0.34	0.95	0.185
-0.29	0.96	0.235

Relative position with centre of opening: Right Elbow (m)

X	Y	Distance to Edge
0.17	0.98	0.355
0.15	0.97	0.375
0.15	0.98	0.375
0.17	0.98	0.355
0.17	0.98	0.355

Relative position with centre of opening: Left Wrist (m)

X	Y	Distance to Edge
-0.31	0.75	0.215
-0.34	0.74	0.185
-0.34	0.79	0.185
-0.35	0.74	0.175
-0.34	0.77	0.185

Relative position with centre of opening: Right Wrist (m)

X	Y	Distance to Edge
0.22	0.79	0.305
0.2	0.77	0.325
0.2	0.77	0.325
0.18	0.77	0.345
0.22	0.79	0.305

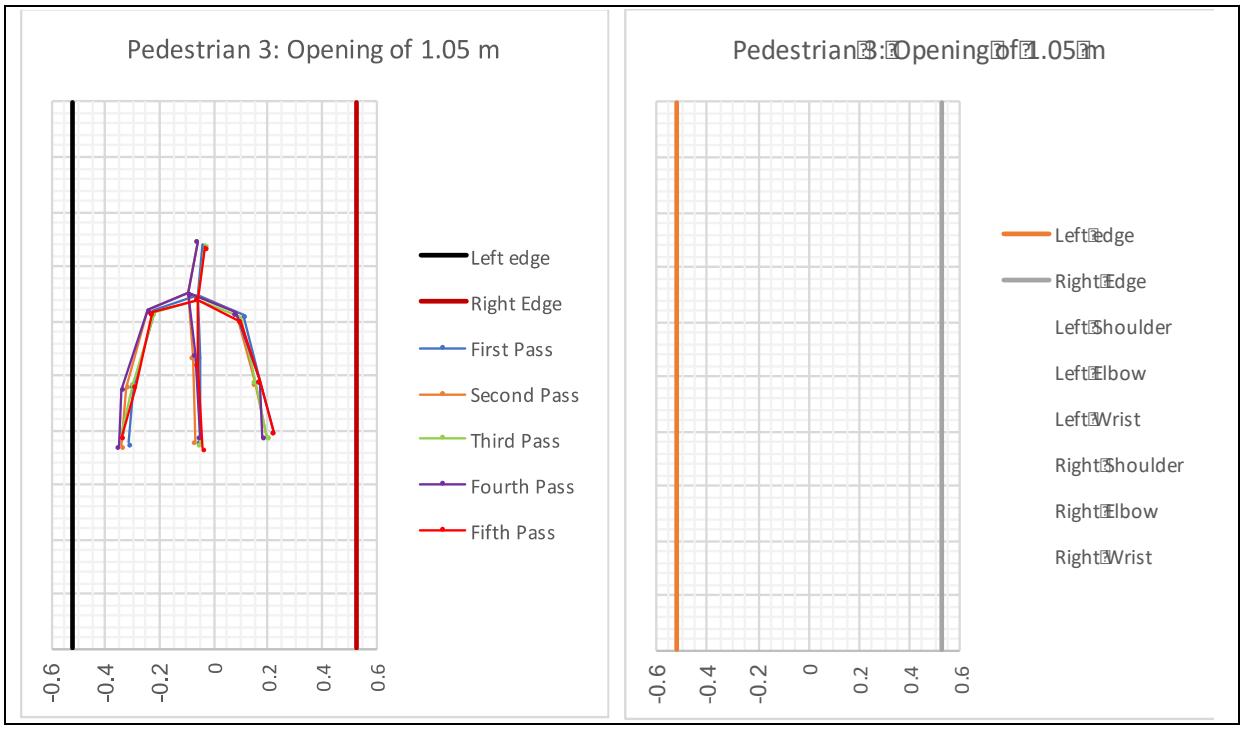

Pedestrian 4

Pedestrian 4 position and distance to edge of body joints for left and right arm relative to the centre of the opening (1.05 m)					
Relative position with centre of opening: Left Shoulder (m)			Relative position with centre of opening: Right Shoulder (m)		
X	Y	Distance to Edge	X	Y	Distance to Edge
-0.23	1.28	0.295	0.11	1.27	0.415
-0.22	1.25	0.305	0.12	1.24	0.405
-0.16	1.26	0.365	0.17	1.25	0.355
-0.27	1.27	0.255	0.07	1.27	0.455
-0.26	1.27	0.265	0.08	1.26	0.445
Relative position with centre of opening: Left Elbow (m)			Relative position with centre of opening: Right Elbow (m)		
X	Y	Distance to Edge	X	Y	Distance to Edge
-0.3	1.03	0.225	0.18	1.03	0.345
-0.3	1.05	0.225	0.18	1.04	0.345
-0.23	1	0.295	0.25	1.03	0.275
-0.34	1.03	0.185	0.13	1.04	0.395
-0.34	1.05	0.185	0.14	1.02	0.385
Relative position with centre of opening: Left Wrist (m)			Relative position with centre of opening: Right Wrist (m)		
X	Y	Distance to Edge	X	Y	Distance to Edge
-0.36	0.81	0.165	0.23	0.87	0.295
-0.35	0.8	0.175	0.19	0.81	0.335
-0.28	0.79	0.245	0.29	0.79	0.235
-0.34	0.81	0.185	0.16	0.79	0.365
-0.35	0.84	0.175	0.13	0.82	0.395

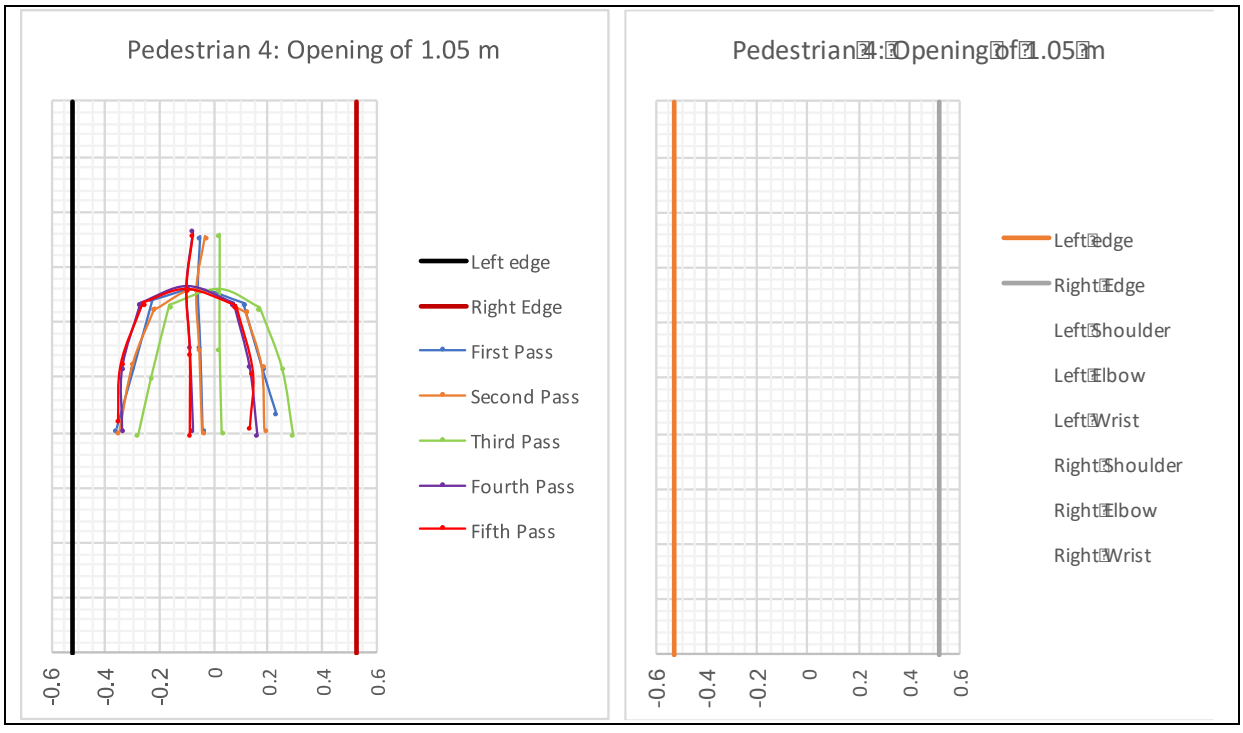

Pedestrian 5

Pedestrian 5 position and distance to edge of body joints for left and right arm relative to the centre of the opening (1.05 m)

Relative position with centre of opening: Left Shoulder (m)

X	Y	Distance to Edge
0.04	1.25	0.565
-0.07	1.26	0.455
0.01	1.25	0.535
-0.04	1.26	0.485
0.07	1.24	0.595

Relative position with centre of opening: Right Shoulder (m)

X	Y	Distance to Edge
0.35	1.23	0.175
0.22	1.25	0.305
0.31	1.25	0.215
0.25	1.26	0.275
0.38	1.22	0.145

Relative position with centre of opening: Left Elbow (m)

X	Y	Distance to Edge
-0.03	0.98	0.495
-0.15	1.03	0.375
-0.08	0.99	0.445
-0.11	0.98	0.415
-0.01	1.02	0.515

Relative position with centre of opening: Right Elbow (m)

X	Y	Distance to Edge
0.4	0.97	0.125
0.28	1	0.245
0.44	1.05	0.085
0.4	0.97	0.125
0.4	0.94	0.125

Relative position with centre of opening: Left Wrist (m)

X	Y	Distance to Edge
-0.07	0.77	0.455
-0.2	0.82	0.325
-0.12	0.82	0.405
-0.14	0.75	0.385
-0.04	0.82	0.485

Relative position with centre of opening: Right Wrist (m)

X	Y	Distance to Edge
0.41	0.79	0.115
0.29	0.82	0.235
0.4	0.77	0.125
0.41	0.79	0.115
0.4	0.75	0.125

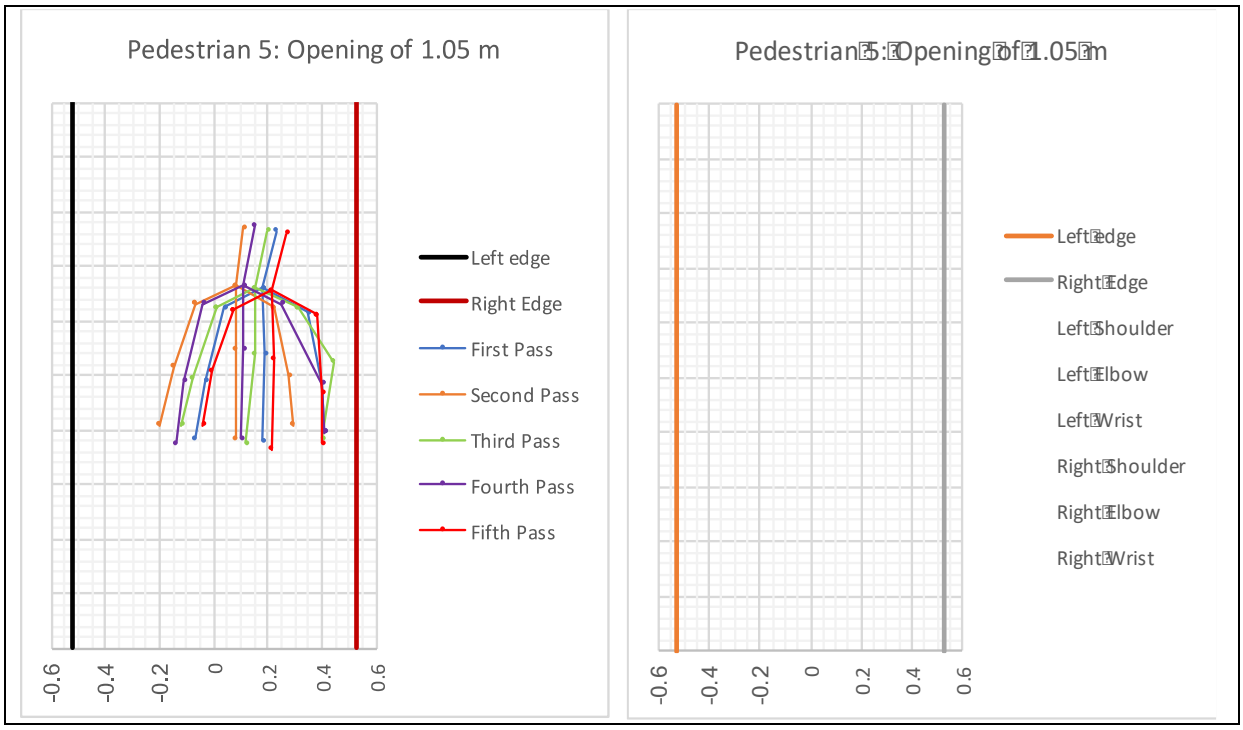

Appendix 4: Group Experiments with 10 pedestrians: Opening of 0.75 m

Right Arm

Position and distance to edge of body joints for right arm relative to the centre of the opening (0.75 m)												
Right Wrist				Right Elbow				Right Shoulder			
ID[1]	X	Y	Distance(m)	ID[1]	X	Y	Distance(m)	ID[1]	X	Y	Distance(m)
2	0.28	0.88	0.10	2	0.14	1.23	0.24	2	0.24	1.51	0.14
	0.28	0.91	0.10		0.25	1.18	0.13		0.15	1.49	0.23
	0.22	0.97	0.16		0.22	1.19	0.16		0.15	1.48	0.23
	0.25	0.95	0.13		0.22	1.19	0.16		0.16	1.49	0.22
	0.32	0.95	0.06		0.31	1.2	0.07		0.26	1.47	0.12
3	0.2	0.72	0.18	3	0.2	0.95	0.18	3	0.14	1.24	0.24
	0.24	0.8	0.14		0.24	0.99	0.14		0.19	1.24	0.19
	0.2	0.73	0.18		0.18	0.96	0.20		0.14	1.23	0.24
	0.24	0.73	0.14		0.18	0.97	0.20		0.13	1.29	0.25
	0.29	0.73	0.09		0.28	0.95	0.10		0.28	1.25	0.10
4	0.25	0.98	0.13	4	0.26	1.21	0.12	4	0.2	1.47	0.18
	0.3	0.97	0.08		0.31	1.21	0.07		0.26	1.49	0.12
	0.26	1.02	0.12		0.27	1.25	0.11		0.17	1.51	0.21
	0.26	0.99	0.12		0.26	1.23	0.12		0.16	1.49	0.22
	0.25	1.04	0.13		0.25	1.25	0.13		0.17	1.52	0.21
7	0.28	0.97	0.10	7	0.28	1.12	0.10	7	0.22	1.4	0.16
	0.24	0.87	0.14		0.24	1.1	0.14		0.2	1.38	0.18
	0.31	0.87	0.07		0.32	1.12	0.06		0.27	1.38	0.11
	0.33	0.89	0.05		0.32	1.13	0.06		0.27	1.38	0.11
	0.29	0.87	0.09		0.3	1.13	0.08		0.25	1.4	0.13
10	0.33	0.85	0.05	10	0.36	1.06	0.02	10	0.32	1.31	0.06
	0.24	0.85	0.14		0.24	1.08	0.14		0.2	1.34	0.18
	0.26	0.88	0.12		0.19	1.07	0.19		0.14	1.31	0.24
	0.32	0.81	0.06		0.32	1.04	0.06		0.29	1.34	0.09
	0.24	0.85	0.14		0.24	1.07	0.14		0.21	1.34	0.17
11	0.22	0.87	0.16	11	0.18	1.07	0.20	11	0.16	1.32	0.22
	0.28	0.83	0.10		0.27	1.08	0.11		0.27	1.33	0.11
	0.22	0.83	0.16		0.19	1.05	0.19		0.13	1.33	0.25
	0.25	0.83	0.13		0.25	1.06	0.13		0.2	1.32	0.18
	0.15	0.82	0.23		0.14	1.05	0.24		0.12	1.3	0.26
12	0.31	0.79	0.07	12	0.31	0.99	0.07	12	0.27	1.23	0.11
	0.25	0.79	0.13		0.23	0.99	0.15		0.16	1.25	0.22
	0.28	0.72	0.10		0.28	0.97	0.10		0.22	1.24	0.16
	0.17	0.75	0.21		0.23	1	0.15		0.16	1.24	0.22
	-0.01	1.04	0.39		0.19	1.05	0.19		0.11	1.25	0.27
16	0.19	0.9	0.19	16	0.22	1.12	0.16	16	0.17	1.37	0.21
	0.15	0.85	0.23		0.18	1.12	0.20		0.16	1.36	0.22
	0.2	0.85	0.18		0.21	1.07	0.17		0.19	1.33	0.19
	0.13	0.89	0.25		0.13	1.11	0.25		0.08	1.37	0.30
	0.15	0.84	0.23		0.19	1.09	0.19		0.14	1.34	0.24
17	0.28	0.88	0.10	17	0.28	1.07	0.10	17	0.22	1.32	0.16
	0.23	0.84	0.15		0.18	1.04	0.20		0.1	1.28	0.28
	0.25	0.84	0.13		0.18	1.01	0.20		0.1	1.26	0.28
	-0.12	1.03	0.50		0.08	1.07	0.30		0.15	1.31	0.23
	0.16	0.83	0.22		0.14	1.06	0.24		0.07	1.33	0.31
20	0.08	0.81	0.30	20	0.15	0.97	0.23	20	0.21	1.21	0.17
	0.24	0.86	0.14		0.26	1.03	0.12		0.18	1.26	0.20
	0.02	0.79	0.36		0.12	0.99	0.26		0.13	1.27	0.25
	0.27	0.84	0.11		0.27	1.05	0.11		0.19	1.26	0.19
	0.33	0.89	0.05		0.24	1.07	0.14		0.26	1.31	0.12

[1] ID refers to the pedestrian number that was assigned to the participants during the experiments.

Left Arm

Position and distance to edge of body joints for left arm relative to the centre of the opening (0.75 m)											
Left Wrist				**Left Elbow**				**Left Shoulder**			
ID[2]	X	Y	Distance to edge (m)	ID[2]	X	Y	Distance to edge (m)	ID[2]	X	Y	Distance to edge (m)
2	-0.11	1.51	0.27	2	-0.17	1.21	0.21	2	-0.18	0.96	0.20
	-0.16	1.49	0.22		-0.23	1.17	0.15		-0.25	0.89	0.13
	-0.18	1.51	0.20		-0.25	1.22	0.13		-0.27	0.96	0.11
	-0.18	1.51	0.20		-0.25	1.23	0.13		-0.25	1	0.13
	-0.08	1.52	0.30		-0.17	1.24	0.21		-0.24	1	0.14
3	-0.19	1.23	0.19	3	-0.26	0.98	0.12	3	-0.28	0.74	0.10
	-0.14	1.25	0.24		-0.19	0.99	0.19		-0.24	0.75	0.14
	-0.18	1.27	0.20		-0.26	1.01	0.12		-0.31	0.77	0.07
	-0.2	1.28	0.18		-0.27	1.02	0.11		-0.31	0.79	0.07
	-0.05	1.3	0.33		-0.12	1.03	0.26		-0.19	0.8	0.19
4	-0.17	1.49	0.21	4	-0.23	1.22	0.15	4	-0.22	1.03	0.16
	-0.13	1.5	0.25		-0.2	1.23	0.18		-0.22	0.96	0.16
	-0.18	1.5	0.20		-0.23	1.22	0.15		-0.24	0.97	0.14
	-0.14	1.5	0.24		-0.24	1.23	0.14		-0.25	0.94	0.13
	-0.18	1.55	0.20		-0.24	1.26	0.14		-0.27	0.98	0.11
7	-0.14	1.43	0.24	7	-0.21	1.14	0.17	7	-0.21	0.9	0.17
	-0.2	1.43	0.18		-0.28	1.2	0.10		-0.25	0.96	0.13
	-0.09	1.43	0.29		-0.18	1.17	0.20		-0.18	0.95	0.20
	-0.09	1.43	0.29		-0.19	1.14	0.19		-0.21	0.9	0.17
	-0.1	1.46	0.28		-0.18	1.18	0.20		-0.21	0.95	0.17
10	0.04	1.35	0.42	10	-0.05	1.09	0.33	10	-0.11	0.86	0.27
	-0.14	1.37	0.24		-0.24	1.05	0.14		-0.26	0.84	0.12
	-0.18	1.3	0.20		-0.23	1.05	0.15		-0.26	0.78	0.12
	-0.05	1.36	0.33		-0.19	1.06	0.19		-0.23	0.83	0.15
	-0.13	1.38	0.25		-0.22	1.11	0.16		-0.26	0.88	0.12
11	-0.18	1.32	0.20	11	-0.26	1.09	0.12	11	-0.26	0.87	0.12
	-0.09	1.33	0.29		-0.14	1.06	0.24		-0.16	0.81	0.22
	-0.2	1.31	0.18		-0.23	1.04	0.15		-0.24	0.8	0.14
	-0.14	1.36	0.24		-0.23	1.06	0.15		-0.25	0.83	0.13
	-0.21	1.32	0.17		-0.26	1.07	0.12		-0.27	0.82	0.11
12	-0.03	1.26	0.35	12	-0.11	1.03	0.27	12	-0.22	0.86	0.16
	-0.17	1.27	0.21		-0.24	0.98	0.14		-0.27	0.75	0.11
	-0.1	1.28	0.28		-0.19	1	0.19		-0.22	0.78	0.16
	-0.16	1.27	0.22		-0.23	1.02	0.15		-0.25	0.82	0.13
	-0.22	1.25	0.16		-0.27	1.03	0.11		-0.18	1.03	0.20
16	-0.15	1.4	0.23	16	-0.23	1.13	0.15	16	-0.25	0.9	0.13
	-0.17	1.41	0.21		-0.25	1.15	0.13		-0.27	0.92	0.11
	-0.12	1.39	0.26		-0.23	1.12	0.15		-0.25	0.88	0.13
	-0.25	1.37	0.13		-0.28	1.11	0.10		-0.29	0.85	0.09
	-0.16	1.37	0.22		-0.27	1.15	0.11		-0.29	0.92	0.09
17	-0.08	1.35	0.30	17	-0.16	1.12	0.22	17	-0.22	0.94	0.16
	-0.17	1.32	0.21		-0.22	1.11	0.16		-0.21	0.95	0.17
	-0.16	1.32	0.22		-0.24	1.05	0.14		-0.28	0.82	0.10
	-0.14	1.34	0.24		-0.23	1.1	0.15		-0.25	0.89	0.13
	-0.25	1.31	0.13		-0.25	1.05	0.13		-0.26	0.84	0.12
20	-0.07	1.24	0.31	20	-0.12	1.01	0.26	20	-0.12	0.84	0.26
	-0.1	1.28	0.28		-0.15	1.05	0.23		-0.2	0.81	0.18
	-0.11	1.24	0.27		-0.22	1.03	0.16		-0.18	0.85	0.20
	-0.08	1.27	0.30		-0.16	1.05	0.22		-0.14	0.87	0.24
	-0.01	1.29	0.37		-0.08	1.06	0.30		-0.07	0.88	0.31

[2] ID refers to the pedestrian number that was assigned to the participants during the experiments.

Appendix 5: Group Experiments with 10 pedestrians: Opening of 0.85 m

Right Arm

Position and distance to edge of body joints for right arm relative to the centre of the opening (0.85 m)											
Right Wrist				Right Elbow				Right Shoulder			
ID[3]	X	Y	Distance to edge (m)	ID[3]	X	Y	Distance to edge (m)	ID[3]	X	Y	Distance to edge (m)
2	0.3	0.93	0.125	2	0.32	1.18	0.105	2	0.29	1.47	0.135
	0.28	0.92	0.145		0.31	1.24	0.115		0.17	1.5	0.255
	0.33	1.02	0.095		0.37	1.23	0.055		0.36	1.47	0.065
	-	-	-		-	-	-		-	-	-
	-	-	-		-	-	-		-	-	-
3	0.38	0.83	0.045	3	0.4	1.03	0.025	3	0.35	1.24	0.075
	0.36	0.8	0.065		0.33	0.99	0.095		0.25	1.24	0.175
	0.33	0.84	0.095		0.32	1.03	0.105		0.23	1.25	0.195
	0.4	0.81	0.025		0.41	1	0.015		0.41	1.23	0.015
	-	-	-		-	-	-		-	-	-
6	0.31	0.8	0.115	6	0.35	1.02	0.075	6	0.32	1.27	0.105
	0.26	0.8	0.165		0.23	1	0.195		0.21	1.27	0.215
	-	-	-		-	-	-		-	-	-
	-	-	-		-	-	-		-	-	-
	-	-	-		-	-	-		-	-	-
7	0.3	0.95	0.125	7	0.33	1.17	0.095	7	0.28	1.39	0.145
	0.33	0.9	0.095		0.37	1.14	0.055		0.32	1.4	0.105
	0.42	1	0.005		0.42	1.2	0.005		0.41	1.41	0.015
	0.42	1	0.005		0.42	1.2	0.005		0.41	1.41	0.015
	-	-	-		-	-	-		-	-	-
10	0.28	0.82	0.145	10	0.3	1.05	0.125	10	0.26	1.32	0.165
	0.02	0.94	0.405		0.19	1.08	0.235		0.13	1.34	0.295
	0.14	0.84	0.285		0.13	1.1	0.295		0.07	1.33	0.355
	0.26	0.84	0.165		0.25	1.06	0.175		0.19	1.33	0.235
	0.06	0.89	0.365		0.04	1.09	0.385		-0.01	1.4	0.435
11	0.18	0.94	0.245	11	0.22	1.11	0.205	11	0.2	1.33	0.225
	0.2	0.9	0.225		0.25	1.08	0.175		0.22	1.32	0.205
	0.37	0.77	0.055		0.35	0.99	0.075		0.32	1.3	0.105
	0.19	0.86	0.235		0.15	1.07	0.275		0.1	1.33	0.325
	0.3	0.83	0.125		0.31	1.07	0.115		0.36	1.32	0.065
12	0.19	0.76	0.235	12	0.12	1	0.305	12	0.05	1.28	0.375
	0.15	0.8	0.275		0.1	1.01	0.325		0.03	1.28	0.395
	0.39	0.79	0.035		0.29	0.98	0.135		0.22	1.24	0.205
	0.05	0.89	0.375		0.08	1.07	0.345		0.12	1.3	0.305
	-	-	-		-	-	-		-	-	-
13	0.22	0.86	0.205	13	0.19	1.12	0.235	13	0.13	1.34	0.295
	0.11	0.88	0.315		0.1	1.09	0.325		0.04	1.33	0.385
	0.25	0.82	0.175		0.22	1.02	0.205		0.16	1.29	0.265
	0.32	0.94	0.105		0.29	1.05	0.135		0.25	1.27	0.175
	-	-	-		-	-	-		-	-	-
16	0.1	0.89	0.325	16	0.22	1.09	0.205	16	0.2	1.36	0.225
	0.01	0.9	0.415		0.01	1.19	0.415		0	1.39	0.425
	0.1	0.93	0.325		0.08	1.17	0.345		0.06	1.39	0.365
	0.07	0.91	0.355		0.05	1.16	0.375		0.03	1.38	0.395
	0.09	0.87	0.335		0.04	1.04	0.385		0.01	1.31	0.415
17	0.21	0.87	0.215	17	0.18	1.11	0.245	17	0.18	1.32	0.245
	0.32	1.02	0.105		0.23	1.17	0.195		0.15	1.23	0.275
	0.12	1.17	0.305		0.03	1.03	0.395		0.03	1.28	0.395
	0.11	0.87	0.315		0.06	1.02	0.365		0.02	1.29	0.405

[3] ID refers to the pedestrian number that was assigned to the participants during the experiments.

Left Arm

Position and distance to edge of body joints for left arm relative to the centre of the opening (0.85 m)											
Left Wrist				**Left Elbow**				**Left Shoulder**			
ID[4]	X	Y	Distance to edge (m)	ID[4]	X	Y	Distance to edge (m)	ID[4]	X	Y	Distance to edge (m)
2	0	1.51	0.425	2	-0.18	1.3	0.245	2	-0.28	1.04	0.145
	-0.28	1.49	0.145		-0.32	1.21	0.105		-0.26	1.02	0.165
	0.04	1.53	0.465		0.03	1.32	0.455		-0.05	0.99	0.375
	-	-	-		-	-	-		-	-	-
	-	-	-		-	-	-		-	-	-
3	0.08	1.28	0.505	3	-0.02	1.07	0.405	3	-0.06	0.87	0.365
	-0.09	1.28	0.335		-0.16	1.02	0.265		-0.19	0.8	0.235
	-0.11	1.27	0.315		-0.18	1.01	0.245		-0.21	0.79	0.215
	0.16	1.25	0.585		0.14	1	0.565		0.11	0.82	0.535
	-	-	-		-	-	-		-	-	-
6	-0.02	1.31	0.405	6	-0.09	1.07	0.335	6	-0.1	0.83	0.325
	-0.27	1.29	0.155		-0.28	0.99	0.145		-0.31	0.81	0.115
	-	-	-		-	-	-		-	-	-
	-	-	-		-	-	-		-	-	-
	-	-	-		-	-	-		-	-	-
7	-0.06	1.47	0.365	7	-0.14	1.19	0.285	7	-0.17	0.95	0.255
	-0.02	1.45	0.405		-0.12	1.21	0.305		-0.14	0.97	0.285
	0.17	1.51	0.595		0.14	1.22	0.565		0.06	0.96	0.485
	0.17	1.51	0.595		0.14	1.22	0.565		0.06	0.96	0.485
	-	-	-		-	-	-		-	-	-
10	-0.11	1.36	0.315	10	-0.2	1.1	0.225	10	-0.22	0.87	0.205
	-0.19	1.36	0.235		-0.27	1.06	0.155		-0.25	0.84	0.175
	-0.24	1.35	0.185		-0.22	1.09	0.205		-0.13	0.97	0.295
	-0.15	1.34	0.275		-0.23	1.06	0.195		-0.27	0.83	0.155
	-0.29	1.38	0.135		-0.34	1.07	0.085		-0.27	0.86	0.155
11	-0.13	1.35	0.295	11	-0.19	1.17	0.235	11	-0.19	0.95	0.235
	-0.11	1.33	0.315		-0.17	1.1	0.255		-0.14	0.94	0.285
	-0.01	1.32	0.415		-0.08	1.05	0.345		-0.11	0.82	0.315
	-0.23	1.32	0.195		-0.26	1.06	0.165		-0.28	0.8	0.145
	-0.06	1.37	0.365		-0.12	1.09	0.305		-0.14	0.87	0.285
12	-0.26	1.28	0.165	12	-0.32	1.02	0.105	12	-0.31	0.78	0.115
	-0.27	1.27	0.155		-0.32	1	0.105		-0.27	0.8	0.155
	-0.1	1.28	0.325		-0.18	1.04	0.245		-0.16	0.87	0.265
	-0.23	1.3	0.195		-0.18	1.06	0.245		-0.05	0.93	0.375
	-	-	-		-	-	-		-	-	-
13	-0.19	1.33	0.235	13	-0.19	1.07	0.235	13	-0.25	0.85	0.175
	-0.27	1.34	0.155		-0.32	1.09	0.105		-0.33	0.85	0.095
	-0.17	1.3	0.255		-0.25	1.04	0.175		-0.3	0.82	0.125
	-0.09	1.3	0.335		-0.17	1.04	0.255		-0.21	0.83	0.215
	-	-	-		-	-	-		-	-	-
16	-0.14	1.38	0.285	16	-0.27	1.15	0.155	16	-0.25	0.96	0.175
	-0.31	1.39	0.115		-0.34	1.17	0.085		-0.3	0.98	0.125
	-0.27	1.46	0.155		-0.29	1.19	0.135		-0.3	0.87	0.125
	-0.26	1.42	0.165		-0.3	1.17	0.125		-0.32	0.98	0.105
	-0.3	1.32	0.125		-0.35	1.16	0.075		-0.35	0.9	0.075
17	-0.21	1.33	0.215	17	-0.21	1.09	0.215	17	-0.22	0.86	0.205
	-0.13	1.32	0.295		-0.2	1.1	0.225		-0.19	0.95	0.235
	-0.24	1.33	0.185		-0.3	1.08	0.125		-0.33	0.87	0.095
	-0.25	1.35	0.175		-0.3	1.05	0.125		-0.33	0.86	0.095

[4] ID refers to the pedestrian number that was assigned to the participants during the experiments.

Appendix 6: Group Experiments with 10 pedestrians: Opening of 1.05 m

Right Arm[5]

Position and distance to edge of body joints for right arm relative to the centre of the opening (1.05 m)												
Right Wrist				Right Elbow				Right Shoulder			
ID[6]	X	Y	Distance to edge (m)	ID[5]	X	Y	Distance to edge (m)	ID[5]	X	Y	Distance to edge (m)
2	0.02	0.97	0.505	2	-0.02	1.23	0.545	2	-0.07	1.48	0.595
	0.08	0.97	0.445		-0.04	1.24	0.565		-0.08	1.52	0.605
	-0.12	1.08	0.645		-0.13	1.32	0.655		-0.17	1.46	0.695
	0.4	1.03	0.125		0.41	1.27	0.115		0.35	1.49	0.175
3	-0.1	1.03	0.625	3	-0.09	1.04	0.615	3	-0.1	1.26	0.625
	0	1.02	0.525		-0.02	0.98	0.545		-0.06	1.25	0.585
	-0.01	0.82	0.535		-0.01	0.99	0.535		-0.05	1.26	0.575
	0	0.77	0.525		-0.03	0.99	0.555		-0.08	1.25	0.605
	0.39	0.78	0.135		0.43	0.97	0.095		0.42	1.25	0.105
4	-0.02	1.12	0.545	4	0.1	1.3	0.425	4	0.05	1.51	0.475
	0.2	0.99	0.325		0.19	1.22	0.335		0.13	1.49	0.395
	0.05	0.98	0.475		0.04	1.23	0.485		-0.03	1.48	0.555
	0	0.99	0.525		-0.03	1.22	0.555		-0.2	1.53	0.725
	0.09	1.09	0.435		0.04	1.29	0.485		-0.04	1.54	0.565
7	0.46	0.9	0.065	7	0.49	1.13	0.035	7	0.36	1.34	0.165
	0.36	0.88	0.165		0.34	1.15	0.185		0.33	1.33	0.195
	0.49	1	0.035		0.49	1.21	0.035		0.42	1.42	0.105
	0.27	1.02	0.255		0.39	1.27	0.135		0.33	1.45	0.195
	0.31	0.89	0.215		0.28	1.13	0.245		0.21	1.52	0.315
11	0.26	0.8	0.265	11	0.24	1.03	0.285	11	0.24	1.26	0.285
	0.12	0.87	0.405		0.08	1.06	0.445		0.05	1.36	0.475
	0.03	0.88	0.495		0	1.12	0.525		-0.07	1.29	0.595
12	0.25	1.06	0.275	12	0.37	1.03	0.155	12	0.36	1.21	0.165
	0.34	0.79	0.185		0.36	1.01	0.165		0.29	1.28	0.235
	0.41	0.8	0.115		0.42	1.01	0.105		0.35	1.28	0.175
	0.41	0.77	0.115		0.42	0.97	0.105		0.43	1.21	0.095
	0.09	0.77	0.435		0.06	0.99	0.465		-0.01	1.25	0.535
13	0.14	0.87	0.385	13	0.26	1.07	0.265	13	0.25	1.27	0.275
	0.27	0.82	0.255		0.29	1.04	0.235		0.24	1.27	0.285
	0.06	0.83	0.465		0.04	1.09	0.485		-0.01	1.33	0.535
	0.39	0.9	0.135		0.38	1.03	0.145		0.35	1.31	0.175
	0.46	0.85	0.065		0.45	0.9	0.075		0.44	1.29	0.085
16	-0.02	0.87	0.545	16	-0.03	1.13	0.555	16	-0.07	1.38	0.595
	-0.03	0.88	0.555		-0.03	1.13	0.555		-0.06	1.37	0.585
	0.37	0.91	0.155		0.37	1.17	0.155		0.34	1.37	0.185
	-0.11	0.98	0.635		-0.08	1.2	0.605		-0.13	1.39	0.655
17	-0.01	1.2	0.535	17	0.13	1.1	0.395	17	0.06	1.21	0.465
	0.19	1.13	0.335		0.33	1.15	0.195		0.26	1.27	0.265
	0.21	1.26	0.315		0.34	1.13	0.185		0.26	1.29	0.265
	0.15	1.23	0.375		0.31	1.12	0.215		0.31	1.34	0.215
	0.31	1.23	0.215		0.43	1.11	0.095		0.37	1.22	0.155
20	0.15	0.81	0.375	20	0.13	1.06	0.395	20	0.06	1.27	0.465
	0.06	0.8	0.465		0.05	1.02	0.475		0.09	1.28	0.435
	0.12	0.8	0.405		0	1.01	0.525		0.04	1.25	0.485
	0.3	0.83	0.225		0.23	0.97	0.295		0.16	1.17	0.365
	0.1	0.77	0.425		0.1	0.99	0.425		0.03	1.27	0.495

[5] Video feed was used to determine when two pedestrians crossed the opening at the same time generating two lanes.

[6] ID refers to the pedestrian number that was assigned to the participants during the experiments.

Left Arm[7]

Position and distance to edge of body joints for left arm relative to the centre of the opening (1.05 m)												
Right Wrist				**Right Elbow**				**Right Shoulder**			
ID[8]	X	Y	Distance to edge (m)	ID[8]	X	Y	Distance to edge (m)	ID[8]	X	Y	Distance to edge (m)
2	-0.37	1.51	0.155	2	-0.45	1.23	0.075	2	-0.43	0.99	0.095
	-0.37	1.5	0.155		-0.41	1.23	0.115		-0.41	0.94	0.115
	-0.41	1.5	0.115		-0.45	1.31	0.075		-0.47	1.11	0.055
	0.07	1.54	0.595		0.09	1.35	0.615		0.24	1.07	0.765
3	-0.4	1.26	0.125	3	-0.45	1.05	0.075	3	-0.27	1.01	0.255
	-0.37	1.27	0.155		-0.42	1.01	0.105		-0.32	0.94	0.205
	-0.38	1.28	0.145		-0.43	1	0.095		-0.46	0.77	0.065
	-0.41	1	0.115		-0.46	0.98	0.065		-0.48	0.73	0.045
	0.11	1.28	0.635		0.06	0.99	0.585		0.03	0.77	0.555
4	-0.31	1.54	0.215	4	-0.39	1.27	0.135	4	-0.42	1.02	0.105
	-0.22	1.51	0.305		-0.31	1.24	0.215		-0.26	1.01	0.265
	-0.39	1.49	0.135		-0.43	1.23	0.095		-0.45	1	0.075
	-0.39	1.51	0.135		-0.41	1.25	0.115		-0.29	0.97	0.235
	-0.4	1.53	0.125		-0.43	1.29	0.095		-0.39	1.08	0.135
7	0.08	1.41	0.605	7	-0.02	1.16	0.505	7	-0.01	0.93	0.515
	0.05	1.39	0.575		0.01	1.17	0.535		-0.02	0.91	0.505
	0.12	1.45	0.645		0.08	1.23	0.605		0.02	1.05	0.545
	0.09	1.47	0.615		0.05	1.27	0.575		0.03	1.45	0.555
	-0.13	1.45	0.395		-0.23	1.17	0.295		-0.24	0.92	0.285
11	-0.08	1.32	0.445	11	-0.19	1.1	0.335	11	-0.21	0.87	0.315
	-0.28	1.31	0.245		-0.34	1.06	0.185		-0.36	0.8	0.165
	-0.39	1.3	0.135		-0.4	1.07	0.125		-0.4	0.85	0.125
12	0.13	1.25	0.655	12	0.15	1.04	0.675	12	0.24	1.07	0.765
	0.01	1.27	0.535		-0.04	1.07	0.485		-0.05	0.81	0.475
	0.11	1.32	0.635		0.06	1.01	0.585		0.03	0.77	0.555
	0.16	1.27	0.685		0.07	1.02	0.595		0.06	0.82	0.585
	-0.34	1.27	0.185		-0.41	0.99	0.115		-0.44	0.8	0.085
13	-0.02	1.31	0.505	13	-0.07	1.07	0.455	13	-0.11	0.83	0.415
	-0.08	1.33	0.445		-0.17	1.06	0.355		-0.2	0.84	0.325
	-0.34	1.33	0.185		-0.4	1.07	0.125		-0.4	0.87	0.125
	0.03	1.32	0.555		-0.06	1.06	0.465		-0.09	0.84	0.435
	0.08	1.29	0.605		0.02	1.07	0.545		-0.04	0.87	0.485
16	-0.4	1.38	0.125	16	-0.44	1.12	0.085	16	-0.43	0.88	0.095
	-0.34	1.36	0.185		-0.44	1.13	0.085		-0.42	0.92	0.105
	0.01	1.39	0.535		-0.07	1.14	0.455		-0.07	0.94	0.455
	-0.41	1.4	0.115		-0.46	1.19	0.065		-0.48	0.95	0.045
17	-0.21	1.33	0.315	17	-0.27	1.13	0.255	17	-0.1	1.21	0.425
	0.04	1.33	0.565		-0.03	1.14	0.495		0.13	1.15	0.655
	0.01	1.36	0.535		-0.04	1.14	0.485		0.13	1.23	0.655
	-0.09	1.36	0.435		-0.09	1.15	0.435		0.1	1.15	0.625
	0.1	1.35	0.625		0.03	1.15	0.555		0.17	1.21	0.695
20	-0.22	1.28	0.305	20	-0.29	1.06	0.235	20	-0.3	0.86	0.225
	-0.18	1.29	0.345		-0.25	1.07	0.275		-0.23	0.87	0.295
	-0.24	1.26	0.285		-0.3	1.04	0.225		-0.28	0.84	0.245
	-0.03	1.24	0.495		-0.14	1	0.385		-0.15	0.78	0.375
	-0.25	1.29	0.275		-0.31	1.06	0.215		-0.3	0.85	0.225

[7] Video feed was used to determine when two pedestrians crossed the opening at the same time generating two lanes.

[8] ID refers to the pedestrian number that was assigned to the participants during the experiments.

Appendix 7: Group Experiments with 14 pedestrians: Opening of 0.75 m

Right Arm

Position and distance to edge of body joints for right arm relative to the centre of the opening (0.75 m)											
Right Wrist				Right Elbow				Right Shoulder			
ID[9]	X	Y	Distance to edge (m)	ID[9]	X	Y	Distance to edge (m)	ID[9]	X	Y	Distance to edge (m)
1	0.23	0.82	0.145	1	0.19	1.02	0.185	1	0.1	1.26	0.275
	0.19	0.81	0.185		0.15	0.99	0.225		0.08	1.25	0.295
	0.22	0.81	0.155		0.17	0.99	0.205		0.09	1.21	0.285
	0.21	0.82	0.165		0.18	1.04	0.195		0.1	1.26	0.275
2	0.2	0.86	0.175	2	0.26	1.23	0.115	2	0.16	1.51	0.215
	0.23	0.82	0.145		0.28	1.28	0.095		0.17	1.46	0.205
	0.24	0.84	0.135		0.28	1.28	0.095		0.22	1.47	0.155
	0.19	0.83	0.185		0.29	1.22	0.085		0.13	1.49	0.245
	0.29	0.82	0.085		0.27	1.25	0.105		0.13	1.48	0.245
3	0.33	0.84	0.045	3	0.27	1.01	0.105	3	0.19	1.27	0.185
	0.18	0.78	0.195		0.15	1.01	0.225		0.1	1.3	0.275
	0.22	0.82	0.155		0.22	1.03	0.155		0.11	1.28	0.265
4	0.3	1.03	0.075	4	0.2	1.21	0.175	4	0.2	1.53	0.175
	0.3	0.98	0.075		0.3	1.24	0.075		0.22	1.51	0.155
	0.25	1.06	0.125		0.23	1.3	0.145		0.14	1.57	0.235
6	0.15	0.81	0.225	6	0.13	1.03	0.245	6	0.1	1.29	0.275
	0.32	0.8	0.055		0.27	1.02	0.105		0.21	1.27	0.165
	0.24	0.86	0.135		0.25	0.99	0.125		0.2	1.31	0.175
7	0.21	0.97	0.165	7	0.29	1.21	0.085	7	0.27	1.45	0.105
	0.19	0.97	0.185		0.32	1.18	0.055		0.29	1.46	0.085
	0.34	0.98	0.035		0.34	1.21	0.035		0.31	1.43	0.065
10	0.3	0.85	0.075	10	0.29	1.08	0.085	10	0.25	1.36	0.125
	0.33	0.85	0.045		0.32	1.07	0.055		0.3	1.37	0.075
	0.32	0.87	0.055		0.31	1.07	0.065		0.29	1.37	0.085
11	0.27	0.87	0.105	11	0.24	1.11	0.135	11	0.2	1.37	0.175
	0.21	0.88	0.165		0.19	1.14	0.185		0.17	1.34	0.205
	0.24	0.84	0.135		0.25	1.08	0.125		0.26	1.35	0.115
	0.28	0.84	0.095		0.24	1.05	0.135		0.21	1.36	0.165
12	0.18	0.87	0.195	12	0.13	1.07	0.245	12	0.03	1.33	0.345
	0.2	0.88	0.175		0.12	1.09	0.255		0.04	1.32	0.335
	0.22	0.89	0.155		0.11	1.09	0.265		0.04	1.33	0.335
13	0.22	0.86	0.155	13	0.21	1.05	0.165	13	0.16	1.27	0.215
	0.17	0.87	0.205		0.16	1.06	0.215		0.1	1.3	0.275
	0.23	0.86	0.145		0.17	1.06	0.205		0.14	1.31	0.235
	0.22	0.81	0.155		0.21	1.06	0.165		0.17	1.33	0.205
	0.2	0.84	0.175		0.17	1.05	0.205		0.11	1.3	0.265
16	0.15	0.94	0.225	16	0.16	1.15	0.215	16	0.12	1.4	0.255
	0.11	0.91	0.265		0.13	1.14	0.245		0.11	1.4	0.265
	0.13	0.92	0.245		0.13	1.17	0.245		0.1	1.4	0.275
17	0.31	0.92	0.065	17	0.22	1.08	0.155	17	0.31	1.28	0.065
	0.14	0.84	0.235		0.11	1.07	0.265		0.04	1.3	0.335
	0.11	0.86	0.265		0.13	1.09	0.245		0.02	1.3	0.355
19	0.24	0.87	0.135	19	0.29	1.17	0.085	19	0.21	1.29	0.165
	0.13	0.87	0.245		0.11	1.13	0.265		0.06	1.22	0.315
	0.28	0.87	0.095		0.27	1.16	0.105		0.21	1.37	0.165
	0.15	0.98	0.225		0.23	1.12	0.145		0.22	1.33	0.155
20	0.17	0.88	0.205	20	0.13	1.07	0.245	20	0.09	1.31	0.285
	0.21	0.81	0.165		0.21	1.06	0.165		0.17	1.33	0.205
	0.16	0.85	0.215		0.12	1.07	0.255		0.06	1.31	0.315
	0.12	0.84	0.255		0.12	1.07	0.255		0.02	1.3	0.355

[9] ID refers to the pedestrian number that was assigned to the participants during the experiments.

Left Arm

Position and distance to edge of body joints for left arm relative to the centre of the opening (0.75 m)												
Left Wrist				Left Elbow				Left Shoulder			
ID[10]	X	Y	Distance to edge (m)	ID	X	Y	Distance to edge (m)	ID	X	Y	Distance to edge (m)
1	-0.17	1.27	0.205	1	-0.27	1.03	0.105	1	-0.28	0.81	0.095
	-0.18	1.27	0.195		-0.29	1.02	0.085		-0.27	0.84	0.105
	-0.17	1.24	0.205		-0.25	1.02	0.125		-0.26	0.8	0.115
	-0.17	1.28	0.205		-0.25	1.05	0.125		-0.27	0.85	0.105
2	-0.18	1.53	0.195	2	-0.25	1.26	0.125	2	-0.24	0.88	0.135
	-0.17	1.53	0.205		-0.2	1.24	0.175		-0.21	0.88	0.165
	-0.21	1.58	0.165		-0.22	1.29	0.155		-0.24	0.85	0.135
	-0.2	1.55	0.175		-0.28	1.26	0.095		-0.28	0.9	0.095
	-0.2	1.52	0.175		-0.22	1.25	0.155		-0.24	0.85	0.135
3	-0.13	1.31	0.245	3	-0.19	1.05	0.185	3	-0.26	0.82	0.115
	-0.24	1.3	0.135		-0.31	1.04	0.065		-0.31	0.81	0.065
	-0.2	1.31	0.175		-0.27	1.05	0.105		-0.29	0.82	0.085
4	-0.16	1.53	0.215	4	-0.21	1.25	0.165	4	-0.21	0.94	0.165
	-0.15	1.51	0.225		-0.22	1.25	0.155		-0.19	1.04	0.185
	-0.22	1.57	0.155		-0.28	1.29	0.095		-0.27	1.03	0.105
6	-0.19	1.29	0.185	6	-0.23	1.06	0.145	6	-0.16	0.87	0.215
	-0.13	1.31	0.245		-0.2	1.05	0.175		-0.21	0.83	0.165
	-0.1	1.31	0.275		-0.21	1.08	0.165		-0.24	0.86	0.135
7	-0.03	1.51	0.345	7	-0.1	1.26	0.275	7	-0.1	1.01	0.275
	-0.03	1.51	0.345		-0.1	1.27	0.275		-0.15	1.04	0.225
	-0.02	1.52	0.355		-0.08	1.27	0.295		-0.12	1.05	0.255
10	-0.09	1.41	0.285	10	-0.17	1.12	0.205	10	-0.19	0.88	0.185
	-0.04	1.33	0.335		-0.13	1.07	0.245		-0.17	0.86	0.205
	0	1.31	0.375		-0.12	1.1	0.255		-0.18	0.83	0.195
11	-0.13	1.36	0.245	11	-0.19	1.11	0.185	11	-0.2	0.87	0.175
	-0.19	1.33	0.185		-0.25	1.11	0.125		-0.24	0.9	0.135
	-0.1	1.37	0.275		-0.15	1.09	0.225		-0.16	0.86	0.215
	-0.15	1.36	0.225		-0.22	1.1	0.155		-0.21	0.9	0.165
12	-0.27	1.33	0.105	12	-0.3	1.05	0.075	12	-0.29	0.83	0.085
	-0.24	1.32	0.135		-0.28	1.06	0.095		-0.27	0.82	0.105
	-0.21	1.35	0.165		-0.27	1.1	0.105		-0.26	0.82	0.115
13	-0.16	1.34	0.215	13	-0.22	1.08	0.155	13	-0.25	0.83	0.125
	-0.23	1.32	0.145		-0.29	1.07	0.085		-0.29	0.84	0.085
	-0.19	1.33	0.185		-0.25	1.07	0.125		-0.28	0.87	0.095
	-0.16	1.33	0.215		-0.22	1.07	0.155		-0.24	0.85	0.135
	-0.22	1.31	0.155		-0.29	1.05	0.085		-0.31	0.83	0.065
16	-0.21	1.44	0.165	16	-0.28	1.16	0.095	16	-0.28	0.92	0.095
	-0.22	1.44	0.155		-0.27	1.18	0.105		-0.27	0.95	0.105
	-0.21	1.42	0.165		-0.25	1.19	0.125		-0.24	0.95	0.135
17	0.05	1.35	0.425	17	-0.04	1.11	0.335	17	-0.05	0.9	0.325
	-0.24	1.32	0.135		-0.27	1.05	0.105		-0.27	0.91	0.105
	-0.24	1.3	0.135		-0.25	1.06	0.125		-0.26	0.9	0.115
19	-0.15	1.29	0.225	19	-0.16	1.08	0.215	19	-0.18	0.86	0.195
	-0.19	1.37	0.185		-0.21	1.13	0.165		-0.23	0.91	0.145
	-0.05	1.34	0.325		-0.09	1.14	0.285		-0.12	0.89	0.255
	-0.07	1.35	0.305		-0.16	1.13	0.215		-0.18	0.89	0.195
20	-0.18	1.31	0.195	20	-0.25	1.05	0.125	20	-0.24	0.85	0.135
	-0.15	1.33	0.225		-0.21	1.06	0.165		-0.24	0.83	0.135
	-0.23	1.33	0.145		-0.28	1.1	0.095		-0.28	0.86	0.095
	-0.26	1.32	0.115		-0.27	1.1	0.105		-0.27	0.87	0.105

[10] ID refers to the pedestrian number that was assigned to the participants during the experiments.

Appendix 8: Group Experiments with 14 pedestrians: Opening of 0.85 m

Right Arm

Position and distance to edge of body joints for right arm relative to the centre of the opening (0.85 m)												
Right Wrist				Right Elbow				Right Shoulder			
ID[11]	X	Y	Distance(m)	ID[11]	X	Y	Distance(m)	ID[11]	X	Y	Distance(m)
1	0.2	0.79	0.225	1	0.13	1.03	0.295	1	0.04	1.23	0.385
	0.19	0.8	0.235		0.11	0.97	0.315		0.05	1.21	0.375
	0.15	0.9	0.275		0.11	1.06	0.315		0.05	1.24	0.375
	0.17	0.81	0.255		0.13	0.99	0.295		0.06	1.23	0.365
	0.29	0.8	0.135		0.23	0.98	0.195		0.11	1.22	0.315
2	0.15	1.05	0.275	2	0.13	1.33	0.295	2	0.06	1.53	0.365
	0.37	0.98	0.055		0.42	1.22	0.005		0.33	1.47	0.095
	0.27	0.93	0.155		0.24	1.18	0.185		0.15	1.49	0.275
3	0.05	0.85	0.375	3	0.05	1.14	0.375	3	0	1.39	0.425
	0.32	0.73	0.105		0.28	0.99	0.145		0.21	1.28	0.215
	0.26	0.85	0.165		0.24	1.09	0.185		0.17	1.36	0.255
4	0.03	1.02	0.395	4	-0.01	1.29	0.435	4	-0.04	1.5	0.465
	-0.12	1.06	0.545		-0.07	1.3	0.495		-0.02	1.54	0.445
	0.2	1.02	0.225		0.21	1.24	0.215		0.1	1.51	0.325
6	0.36	0.82	0.065	6	0.41	1.02	0.015	6	0.36	1.25	0.065
	0.12	0.79	0.305		0.1	1.08	0.325		0.03	1.28	0.395
	0.08	0.75	0.345		0.03	0.97	0.395		0.02	1.28	0.405
	0.13	0.99	0.295		0.08	1.06	0.345		0.01	1.26	0.415
	0.19	0.77	0.235		0.13	1.03	0.295		0.06	1.28	0.365
10	0.29	0.88	0.135	10	0.32	1.09	0.105	10	0.3	1.35	0.125
	0.35	0.88	0.075		0.39	1.09	0.035		0.36	1.33	0.065
	0.27	0.86	0.155		0.31	1.07	0.115		0.31	1.33	0.115
	0.26	0.86	0.165		0.3	1.08	0.125		0.28	1.34	0.145
	0.36	0.83	0.065		0.33	1.04	0.095		0.23	1.33	0.195
11	0.27	0.84	0.155	11	0.24	1.02	0.185	11	0.2	1.3	0.225
	0.18	0.87	0.245		0.14	1.07	0.285		0.11	1.32	0.315
	0.22	0.8	0.205		0.2	1.02	0.225		0.17	1.29	0.255
12	0.24	0.81	0.185	12	0.19	1.02	0.235	12	0.14	1.25	0.285
	0.17	0.78	0.255		0.12	1	0.305		0.06	1.28	0.365
	0.15	0.78	0.275		0.13	0.98	0.295		0.08	1.27	0.345
	0.15	0.77	0.275		0.11	1.01	0.315		0.05	1.25	0.375
	0.16	0.82	0.265		0.13	1	0.295		0.1	1.23	0.325
13	0.2	0.79	0.225	13	0.15	0.97	0.275	13	0.09	1.24	0.335
	0.03	0.87	0.395		0.17	1.02	0.255		0.12	1.28	0.305
	0.29	0.89	0.135		0.25	1.06	0.175		0.21	1.27	0.215
	0.3	0.79	0.125		0.29	1.01	0.135		0.22	1.28	0.205
16	0.05	0.89	0.375	16	0.05	1.16	0.375	16	0.02	1.39	0.405
	0.08	0.87	0.345		0.1	1.09	0.325		0.08	1.35	0.345
	0.04	0.91	0.385		0.06	1.13	0.365		0.04	1.38	0.385
	0.1	0.88	0.325		0.1	1.1	0.325		0.09	1.37	0.335
17	0.28	0.8	0.145	17	0.23	1.02	0.195	17	0.17	1.29	0.255
	0.24	0.8	0.185		0.19	1.02	0.235		0.15	1.29	0.275
	0.36	0.81	0.065		0.29	0.99	0.135		0.23	1.24	0.195
	0.18	0.86	0.245		0.14	1.07	0.285		0.06	1.33	0.365
19	0.4	0.85	0.025	19	0.36	1.1	0.065	19	0.35	1.35	0.075
	0.21	0.81	0.215		0.16	1.03	0.265		0.13	1.33	0.295
	0.24	0.89	0.185		0.32	1.09	0.105		0.25	1.23	0.175
	0.33	0.87	0.095		0.33	1	0.095		0.28	1.3	0.145
20	-0.08	0.85	0.505	20	0.02	1.09	0.405	20	-0.01	1.35	0.435
	0.33	0.87	0.095		0.21	1.05	0.215		0.25	1.26	0.175
	0.24	0.75	0.185		0.22	0.97	0.205		0.17	1.26	0.255

[11] ID refers to the pedestrian number that was assigned to the participants during the experiments.

Left Arm

Position and distance to edge of body joints for left arm relative to the centre of the opening (0.85 m)											
Left Wrist				**Left Elbow**				**Left Shoulder**			
ID[12]	X	Y	Distance to edge (m)	ID[12]	X	Y	Distance to edge (m)	ID[12]	X	Y	Distance to edge (m)
1	-0.23	1.25	0.195	1	-0.3	1.05	0.125	1	-0.3	0.81	0.125
	-0.2	1.22	0.225		-0.29	1.03	0.135		-0.32	0.78	0.105
	-0.23	1.26	0.195		-0.3	1.08	0.125		-0.33	0.88	0.095
	-0.21	1.25	0.215		-0.3	1.02	0.125		-0.31	0.83	0.115
	-0.15	1.25	0.275		-0.13	0.99	0.295		-0.21	0.79	0.215
2	-0.29	1.54	0.135	2	-0.34	1.26	0.085	2	-0.36	1.04	0.065
	0.04	1.52	0.465		0.02	1.25	0.445		-0.02	0.97	0.405
	-0.17	1.51	0.255		-0.22	1.2	0.205		-0.24	0.96	0.185
3	-0.33	1.39	0.095	3	-0.36	1.12	0.065	3	-0.35	0.87	0.075
	-0.11	1.29	0.315		-0.16	1.02	0.265		-0.16	0.77	0.265
	-0.17	1.37	0.255		-0.22	1.1	0.205		-0.19	0.88	0.235
4	-0.32	1.53	0.105	4	-0.33	1.27	0.095	4	-0.34	1.06	0.085
	-0.24	1.53	0.185		-0.28	1.36	0.145		-0.21	1	0.215
	-0.26	1.52	0.165		-0.3	1.24	0.125		-0.31	0.99	0.115
6	0.11	1.31	0.535	6	0.08	1.04	0.505	6	0.06	0.88	0.485
	-0.31	1.3	0.115		-0.33	1.14	0.095		-0.34	0.77	0.085
	-0.28	1.3	0.145		-0.26	1.07	0.165		-0.17	0.89	0.255
	-0.29	1.28	0.135		-0.17	1.14	0.255		-0.2	1.24	0.225
	-0.26	1.31	0.165		-0.33	1.09	0.095		-0.34	0.85	0.085
10	0.01	1.38	0.435	10	-0.05	1.26	0.375	10	-0.01	1.01	0.415
	0.06	1.38	0.485		-0.02	1.14	0.405		-0.06	0.96	0.365
	0	1.37	0.425		-0.07	1.08	0.355		-0.13	0.86	0.295
	-0.04	1.36	0.385		-0.1	1.07	0.325		-0.14	0.85	0.285
	-0.08	1.35	0.345		-0.19	1.07	0.235		-0.25	0.86	0.175
11	-0.12	1.3	0.305	11	-0.22	1.08	0.205	11	-0.25	0.84	0.175
	-0.22	1.33	0.205		-0.28	1.07	0.145		-0.32	0.83	0.105
	-0.15	1.3	0.275		-0.22	1.03	0.205		-0.24	0.79	0.185
12	-0.19	1.29	0.235	12	-0.29	0.99	0.135	12	-0.36	0.79	0.065
	-0.27	1.27	0.155		-0.34	0.99	0.085		-0.36	0.76	0.065
	-0.24	1.27	0.185		-0.32	1.01	0.105		-0.3	0.81	0.125
	-0.27	1.27	0.155		-0.33	1.04	0.095		-0.29	0.86	0.135
	-0.21	1.28	0.215		-0.31	1.01	0.115		-0.27	0.81	0.155
13	-0.24	1.31	0.185	13	-0.32	1.09	0.105	13	-0.27	0.87	0.155
	-0.19	1.3	0.235		-0.31	1.09	0.115		-0.33	0.89	0.095
	-0.11	1.32	0.315		-0.23	1.07	0.195		-0.28	0.85	0.145
	-0.11	1.29	0.315		-0.17	1.03	0.255		-0.21	0.81	0.215
16	-0.29	1.38	0.135	16	-0.34	1.14	0.085	16	-0.28	0.91	0.145
	-0.25	1.37	0.175		-0.34	1.11	0.085		-0.32	0.9	0.105
	-0.29	1.41	0.135		-0.33	1.16	0.095		-0.34	0.92	0.085
	-0.25	1.4	0.175		-0.32	1.13	0.105		-0.31	0.89	0.115
17	-0.09	1.36	0.335	17	-0.16	1.1	0.265	17	-0.18	0.89	0.245
	-0.13	1.35	0.295		-0.2	1.07	0.225		-0.26	0.86	0.165
	-0.05	1.33	0.375		-0.13	1.07	0.295		-0.21	0.85	0.215
	-0.23	1.36	0.195		-0.26	1.11	0.165		-0.26	0.88	0.165
19	0.03	1.34	0.455	19	-0.04	1.11	0.385	19	-0.12	0.87	0.305
	-0.14	1.36	0.285		-0.21	1.11	0.215		-0.22	0.91	0.205
	-0.01	1.32	0.415		-0.07	1.12	0.355		-0.12	0.91	0.305
	-0.02	1.33	0.405		-0.08	1.06	0.345		-0.13	0.84	0.295
20	-0.31	1.35	0.115	20	-0.41	1.11	0.015	20	-0.38	0.88	0.045
	-0.02	1.27	0.405		-0.09	1.04	0.335		-0.08	0.82	0.345
	-0.17	1.26	0.255		-0.21	0.99	0.215		-0.27	0.76	0.155

[12] ID refers to the pedestrian number that was assigned to the participants during the experiments.

Appendix 9: Group Experiments with 14 pedestrians: Opening of 1.05 m

Right Arm[13]

Position and distance to edge of body joints for right arm relative to the centre of the opening (1.05 m)												
Right Wrist				Right Elbow				Right Shoulder			
ID[14]	X	Y	Distance (m)	ID[14]	X	Y	Distance(m)	ID[14]	X	Y	Distance(m)
1	0.41	0.79	0.115	1	0.37	0.97	0.155	1	0.27	1.23	0.255
	0.37	0.77	0.155		0.33	0.97	0.195		0.18	1.27	0.345
	0.12	0.77	0.405		0.08	0.97	0.445		-0.01	1.21	0.535
	0.09	0.72	0.435		0.04	0.93	0.485		-0.05	1.19	0.575
	0.1	0.77	0.425		0.05	0.98	0.475		-0.03	1.22	0.555
2	0.02	1	0.505	2	0.04	1.22	0.485	2	0.05	1.51	0.475
	0.15	1.02	0.375		0.17	1.22	0.355		0.16	1.47	0.365
	0.09	0.98	0.435		0.14	1.24	0.385		0.13	1.52	0.395
	0.34	0.98	0.185		0.34	1.21	0.185		0.3	1.49	0.225
	0.14	1.17	0.385		0.22	1.22	0.305		0.22	1.5	0.305
3	0.48	0.71	0.045	3	0.42	0.94	0.105	3	0.39	1.24	0.135
	0.36	0.82	0.165		0.42	0.99	0.105		0.39	1.23	0.135
	0.27	1.14	0.255		0.42	1.06	0.105		0.26	1.2	0.265
	0.31	1.22	0.215		0.43	1.47	0.095		0.43	1.21	0.095
4	0.28	1.03	0.245	4	0.29	1.22	0.235	4	0.21	1.47	0.315
	-0.08	0.97	0.605		-0.06	1.21	0.585		-0.02	1.51	0.545
	-0.07	1.01	0.595		-0.1	1.29	0.625		-0.06	1.5	0.585
	-0.04	0.99	0.565		-0.04	1.27	0.565		-0.05	1.53	0.575
	0.15	0.94	0.375		0.07	1.16	0.455		-0.02	1.48	0.545
6	0.39	0.87	0.135	6	0.32	1.05	0.205	6	0.31	1.26	0.215
	0.51	0.87	0.015		0.41	1.02	0.115		0.27	1.26	0.255
	0.11	0.86	0.415		-0.01	1.03	0.535		0.02	1.27	0.505
	0.45	0.8	0.075		0.41	1	0.115		0.3	1.25	0.225
	0.41	0.77	0.115		0.45	0.99	0.075		0.42	1.23	0.105
7	0.02	1.13	0.505	7	0.02	1.29	0.505	7	-0.03	1.46	0.555
	0.17	0.98	0.355		0.24	1.23	0.285		0.19	1.42	0.335
	0.17	0.99	0.355		0.27	1.21	0.255		0.19	1.41	0.335
	0.18	0.72	0.345		0.27	1.15	0.255		0.3	1.41	0.225
	0.16	0.98	0.365		0.28	1.23	0.245		0.21	1.42	0.315
10	0.28	0.86	0.245	10	0.3	1.05	0.225	10	0.26	1.32	0.265
	0.34	0.83	0.185		0.32	1.05	0.205		0.27	1.33	0.255
	0.16	0.87	0.365		0.15	1.09	0.375		0.1	1.34	0.425
	0.25	0.89	0.275		0.25	1.06	0.275		0.19	1.31	0.335
	0.06	0.83	0.465		0.03	1.02	0.495		0.01	1.32	0.515
11	0.28	0.85	0.245	11	0.26	1.06	0.265	11	0.22	1.32	0.305
	0.25	0.75	0.275		0.3	1.01	0.225		0.26	1.3	0.265
	0.43	0.73	0.095		0.4	0.97	0.125		0.35	1.29	0.175
	0.43	0.81	0.095		0.42	1.01	0.105		0.4	1.31	0.125
	0.36	0.92	0.165		0.36	1.02	0.165		0.38	1.33	0.145
12	0.35	0.71	0.175	12	0.3	0.94	0.225	12	0.21	1.25	0.315
	0.39	0.82	0.135		0.34	1.03	0.185		0.27	1.25	0.255
	0.2	1.06	0.325		0.37	1.04	0.155		0.37	1.26	0.155
	0.25	1.07	0.275		0.42	1.05	0.105		0.42	1.23	0.105
	0.44	1.05	0.085		0.42	1.01	0.105		0.36	1.26	0.165
13	0.47	0.87	0.055	13	0.48	1.07	0.045	13	0.41	1.29	0.115
	0.22	0.85	0.305		0.19	1.04	0.335		0.16	1.31	0.365
	0.13	0.89	0.395		0.1	1.06	0.425		0.06	1.32	0.465
	0.06	0.86	0.465		0.03	1.07	0.495		-0.03	1.33	0.555
	0.05	0.88	0.475		0.04	1.09	0.485		-0.01	1.32	0.535

[13] Video feed was used to determine when two pedestrians crossed the opening at the same time generating two lanes.

[14] ID refers to the pedestrian number that was assigned to the participants during the experiments.

16	-0.14	0.91	0.665	16	-0.13	1.12	0.655	16	-0.15	1.37	0.675
	-0.06	0.9	0.585		-0.05	1.11	0.575		-0.06	1.36	0.585
	0.04	0.91	0.485		-0.14	1.14	0.665		-0.13	1.38	0.655
	-0.02	0.88	0.545		-0.03	1.12	0.555		-0.08	1.38	0.605
	-0.08	0.89	0.605		-0.07	1.11	0.595		-0.1	1.36	0.625
17	0.28	0.89	0.245	17	0.19	1.06	0.335	17	0.11	1.27	0.415
	0.46	0.91	0.065		0.42	1.08	0.105		0.35	1.3	0.175
	0.41	0.79	0.115		0.43	1	0.095		0.39	1.3	0.135
	0.39	0.9	0.135		0.36	1.08	0.165		0.29	1.32	0.235
	0.1	1.25	0.425		0.06	1.04	0.465		0.14	1.2	0.385
19	0.19	0.8	0.335	19	0.26	1.06	0.265	19	0.21	1.31	0.315
	0.21	0.77	0.315		0.24	1.03	0.285		0.26	1.31	0.265
	0.22	1.19	0.305		0.43	1.09	0.095		0.42	1.31	0.105
20	0.25	0.86	0.275	20	0.09	1.03	0.435	20	0.17	1.27	0.355
	-0.06	0.82	0.585		-0.07	1.02	0.595		-0.14	1.27	0.665
	-0.01	0.85	0.535		-0.06	1.09	0.585		-0.12	1.28	0.645
	0	0.87	0.525		-0.02	1.06	0.545		-0.08	1.27	0.605
	0.25	0.85	0.275		0.09	1.05	0.435		0.1	1.27	0.425

Left Arm[15]

Position and distance to edge of body joints for left arm relative to the centre of the opening (1.05 m)											
Left Wrist				Left Elbow				Left Shoulder			
ID[16]	X	Y	Distance(m)	ID[16]	X	Y	Distance(m)	ID[16]	X	Y	Distance(m)
1	0	1.24	0.525	1	-0.08	1.02	0.445	1	-0.09	0.8	0.435
	-0.01	1.27	0.515		-0.13	1	0.395		-0.18	0.78	0.345
	-0.27	1.25	0.255		-0.36	0.99	0.165		-0.38	0.78	0.145
	-0.31	1.22	0.215		-0.41	0.97	0.115		-0.41	0.79	0.115
	-0.3	1.24	0.225		-0.39	0.99	0.135		-0.42	0.77	0.105
2	-0.27	1.53	0.255	2	-0.36	1.28	0.165	2	-0.35	1.02	0.175
	-0.15	1.5	0.375		-0.25	1.26	0.275		-0.22	1.05	0.305
	-0.2	1.53	0.325		-0.3	1.27	0.225		-0.3	1.05	0.225
	-0.04	1.49	0.485		-0.11	1.27	0.415		0.09	1.27	0.615
	-0.11	1.52	0.415		-0.18	1.25	0.345		-0.23	0.99	0.295
3	0.07	1.27	0.595	3	0	1.04	0.525	3	0	0.79	0.525
	0.09	1.28	0.615		0.09	1.06	0.615		-0.04	0.85	0.485
	0.06	1.25	0.585		-0.03	1.05	0.495		0.11	1.17	0.635
	0.14	1.28	0.665		0.11	1.06	0.635		0.19	1.16	0.715
4	-0.14	1.5	0.385	4	-0.2	1.22	0.325	4	-0.21	0.94	0.315
	-0.34	1.51	0.185		-0.39	1.25	0.135		-0.41	1.01	0.115
	-0.37	1.49	0.155		-0.42	1.23	0.105		-0.36	1.02	0.165
	-0.4	1.52	0.125		-0.44	1.25	0.085		-0.45	0.98	0.075
	-0.39	1.48	0.135		-0.44	1.21	0.085		-0.4	0.99	0.125
6	-0.01	1.31	0.515	6	-0.11	1.07	0.415	6	-0.12	0.85	0.405
	0	1.28	0.525		-0.11	1.02	0.415		-0.11	0.78	0.415
	-0.29	1.3	0.235		-0.37	1.07	0.155		-0.37	0.84	0.155
	-0.02	1.28	0.505		-0.11	1.07	0.415		-0.04	0.89	0.485
	0.11	1.3	0.635		0.03	1.07	0.555		0.03	0.88	0.555
7	-0.37	1.48	0.155	7	-0.44	1.27	0.085	7	-0.47	1.1	0.055
	-0.19	1.46	0.335		-0.27	1.22	0.255		-0.26	1.02	0.265
	-0.17	1.43	0.355		-0.25	1.21	0.275		-0.25	1.01	0.275
	-0.04	1.44	0.485		-0.14	1.21	0.385		-0.14	1.01	0.385
	-0.16	1.47	0.365		-0.24	1.23	0.285		-0.23	1.03	0.295

[15] Video feed was used to determine when two pedestrians crossed the opening at the same time generating two lanes. ID

[16] ID refers to the pedestrian number that was assigned to the participants during the experiments.

10	-0.09	1.36	0.435	10	-0.21	1.09	0.315	10	-0.25	0.87	0.275
	-0.07	1.36	0.455		-0.19	1.09	0.335		-0.27	0.87	0.255
	-0.23	1.35	0.295		-0.28	1.09	0.245		-0.28	0.88	0.245
	-0.16	1.34	0.365		-0.29	1.18	0.235		-0.09	1.34	0.435
	-0.35	1.36	0.175		-0.43	1.07	0.095		-0.46	0.84	0.065
11	-0.1	1.32	0.425	11	-0.16	1.05	0.365	11	-0.2	0.8	0.325
	-0.06	1.31	0.465		-0.13	1.06	0.395		-0.17	0.83	0.355
	0.03	1.31	0.555		-0.02	1.05	0.505		-0.06	0.83	0.465
	0.07	1.31	0.595		0.04	1.04	0.565		0.01	0.81	0.535
	0.06	1.34	0.585		0.04	1.02	0.565		0.04	0.93	0.565
12	-0.1	1.26	0.425	12	-0.22	1.01	0.305	12	-0.3	0.81	0.225
	-0.03	1.28	0.495		-0.23	1.08	0.295		-0.17	0.86	0.355
	0.07	1.3	0.595		0.01	1.11	0.535		0.07	1.03	0.595
	0.11	1.27	0.635		0.04	1.06	0.565		0.08	1.07	0.605
	-0.07	1.26	0.455		-0.02	1.04	0.505		0.01	1.07	0.535
13	0.08	1.28	0.605	13	0.05	1.02	0.575	13	0.04	0.8	0.565
	-0.17	1.33	0.355		-0.27	1.08	0.255		-0.29	0.86	0.235
	-0.28	1.34	0.245		-0.37	1.08	0.155		-0.4	0.86	0.125
	-0.35	1.32	0.175		-0.41	1.09	0.115		-0.42	0.88	0.105
	-0.34	1.32	0.185		-0.4	1.08	0.125		-0.4	0.88	0.125
16	-0.43	1.39	0.095	16	-0.44	1.16	0.085	16	-0.38	0.89	0.145
	-0.39	1.39	0.135		-0.45	1.13	0.075		-0.44	0.91	0.085
	-0.41	1.4	0.115		-0.46	1.16	0.065		-0.42	0.94	0.105
	-0.41	1.38	0.115		-0.45	1.12	0.075		-0.43	0.89	0.095
	-0.4	1.37	0.125		-0.45	1.12	0.075		-0.44	0.9	0.085
17	-0.15	1.29	0.375	17	-0.21	1.08	0.315	17	-0.11	0.87	0.415
	0.07	1.35	0.595		-0.01	1.16	0.515		0.14	1.07	0.665
	0.11	1.34	0.635		0.08	1.11	0.605		0.09	1.14	0.615
	0	1.37	0.525		-0.07	1.1	0.455		-0.1	0.88	0.425
	-0.1	1.36	0.425		-0.21	1.16	0.315		-0.08	1.22	0.445
19	-0.1	1.33	0.425	19	-0.18	1.07	0.345	19	-0.22	0.85	0.305
	0.02	1.29	0.545		-0.12	1.06	0.405		-0.15	0.86	0.375
	0.15	1.32	0.675		0.15	1.03	0.675		0.24	1.2	0.765
20	-0.12	1.28	0.405	20	-0.22	1.06	0.305	20	-0.25	0.84	0.275
	-0.43	1.28	0.095		-0.46	1.05	0.065		-0.46	0.83	0.065
	-0.38	1.31	0.145		-0.44	1.09	0.085		-0.44	0.91	0.085
	-0.36	1.3	0.165		-0.43	1.07	0.095		-0.44	0.85	0.085
	-0.15	1.3	0.375		-0.23	1.08	0.295		-0.22	0.89	0.305